

Biological roles of DExH RNA helicase, RHAU

INAUGURALDISSERTATION

zur

Erlangung der Würde eines Doktors der Philosophie
Vorgelegt der
Philosophisch-Naturwissenschaftlichen Fakultät
der Universität Basel

von
Fumiko Iwamoto
aus Fukuoka, Japan

Dissertationsleiter: Dr. Yoshikuni Nagamine
Friedrich Miescher Institute for Biomedical Research

Basel 2007

Genehmigt von der Philosophisch-Naturwissenschaftlichen Fakultät
auf Antrag von

Prof. Frederick Meins, Dr. Yoshikuni Nagamine, Prof. Christoph
Moroni, Dr. Witold Filipowicz, und Prof. Nancy Hynes.

Basel, den 13. Dezember 2007

Prof. Dr. Hans-Peter Hauri
Dekan der Philosophisch-
Naturwissenschaftlichen Fakultät

Basel, den 20. November 2007

Ich erkläre hiermit, dass ich die Dissertation

Biological roles of DExH RNA helicase, RHAU

nur mit der darin angegebenen Hilfe verfasst und bei keiner anderen Fakultät eingereicht habe.

Fumiko Iwamoto

TABLE OF CONTENTS

THESIS SUMMARY	7
SECTION 1 - INTRODUCTION	9
1.01. Regulation of gene expression at different steps	9
1.02. Regulation of mRNA stability.....	10
1.02.01. Regulation of mRNA stability contributes to changes of gene expression.....	10
1.02.02. mRNA degradation machinery.....	11
1.02.03. cis-element	12
1.03. AU-rich element-mediated mRNA decay (AMD).....	12
1.03.01. AU-rich element.....	12
1.03.02. Degradation machinery and AUBPs.....	13
1.04. RHAU : RNA helicase-associated with AU-rich element	14
1.04.01. RHAU as a destabilizing factor of ARE-RNA.	14
1.04.02. RHAU as a G4 DNA resolvase.	15
1.04.03. Affinity to other molecules - protein and RNA	15
1.04.04. Evolutional conservation and expression pattern.....	16
1.04.05. Intracellular localization.	16
1.05. RNA helicases	17
1.05.01. Structure.	17
1.05.02. helicase and RNPase.	18
1.05.03. Various functions of RNA helicases.	19
1.06. Spatial controls of RNA and proteins involved in RNA metabolisms.....	21
AIMS	23
SECTION 2 - MATERIALS AND METHODS	25
2.01. Plasmids.....	25
2.02. Cell culture and transfection.....	25
2.03. Antibodies	26
2.04. Protein extraction and Western blotting.....	26
2.05. Immunoprecipitation.....	27
2.06. in situ extraction	27
2.07. Immunocytochemistry and image processing.....	28
2.08. Luciferase reporter assay	28
2.09. GeneChip microarrays and the analysis of RNA half-lives.....	28
2.10. Cell growth and viability.....	30
2.11. Nuclear run-on assay	30
2.12. Real time PCR	30
2.13. Tumor generation in nude mice.....	31
2.14. GST-RHAU pull-down assay	31

SECTION 3 - RESULTS	33
3.01. Possible roles of RHAU in the nucleus.....	33
3.01.01. RHAU is mainly localized in the nucleus and tightly associated with RNA.....	33
3.01.02. Nuclear speckles and nucleolar cap-localization induced by transcriptional arrest.....	35
3.01.03 Transcription-dependent localization of RHAU in the nucleolar caps with DEAD-box helicases p68 and p72.....	37
3.01.04 Interaction of RHAU with regulators of transcription.....	38
3.01.05 N-terminal domain of RHAU is responsible for the nuclear and nucleolar caps localization.....	39
3.02. Microarray analysis using RHAU knockdown cells.....	41
3.02.01. Inducible RHAU-knockdown HeLa cell-line.....	41
3.02.02. DNA microarray to measure steady-state mRNA and mRNA half-life.....	42
3.02.03. Differences in steady-state levels after RHAU knockdown are not correlated to their half-lives.....	44
3.02.04. Influence of RHAU on mRNA half-life.....	48
3.02.05. Change in mRNA level in RHAU-knockdown cells can be rescued by exogenous RHAU expression.....	50
3.03. RHAU on stress-response.....	52
3.03.01. Influence of RHAU depletion on cell growth.....	52
3.03.02. Microarray analysis using cells under serum-starvation.....	53
SECTION 4 - DISCUSSIONS	55
4.01. RHAU is a nuclear-enriched protein.....	55
4.02. ATPase activity and localization.....	57
4.03. Transcriptional arrest-dependent localization of RHAU to nucleolar caps.....	57
4.04. Microarray to determine the RHAU target gene and RNA.....	58
4.05. RHAU changes gene expression through a mechanism not involved in mRNA degradation.....	59
4.06. Involvement of RHAU in mRNA degradation.....	60
4.07. Relationship of regulations by transcription and mRNA stability.....	61
4.08. RHAU in tumor cell growth.....	61
4.09. RHAU as a multi-functional RNA helicase.....	62
PERSPECTIVES	65
ACKNOWLEDGEMENTS	67
APPENDIX - I : Oligonucleotides used in this study.....	68
APPENDIX - II : RHAU-target mRNAs (on steady-state mRNA level).....	70
APPENDIX - III : RHAU-target mRNAs (on mRNA stability).....	72
APPENDIX - IV : Starvation-sensitive genes.....	75
REFERENCES	77
FIGURE INDEX	85
CURRICULUM VITAE	87

THESIS SUMMARY

In this thesis, I have described the work carried out on a single protein called RHAU, dealing with aspects of protein localization in cells, the regulation of global gene expression by different mechanisms, and cellular stress-responses. RHAU, *RNA helicase associated with AU-rich element*, was originally identified from the results of RNA affinity chromatography using the AU-rich element of uPA messenger RNA. RHAU was characterized as a factor accelerating AU-rich element-mediated mRNA degradation.

The aim of this present study was to investigate possible role(s) of RHAU in mammalian cells. In the first part of the study, dealing with the cellular localization of RHAU using biochemical fractionation and microscopic analysis, I found that RHAU is predominantly localized in the nucleus, despite the fact that mRNA degradation occurs in the cytoplasm. In HeLa cells, RHAU is localized throughout the nucleoplasm with some concentration in nuclear speckles in a manner dependent on ATPase activity. Furthermore, it has been shown that transcriptional arrest changes RHAU localization to nucleolar caps, where it is co-localized with other RNA helicases, p68 and p72. This suggests that RHAU is involved in transcription-related RNA metabolism in the nucleus.

The discovery that RHAU is localized mainly in the nucleus prompted me to consider the nuclear functions of RHAU, which led to a second project using RHAU-knockdown. To see whether RHAU affects global gene expression either transcriptionally or posttranscriptionally, microarray analysis using total RNA prepared from RHAU-depleted HeLa cell lines was performed to measure both the steady-state mRNA level and mRNA half-life by actinomycinD-chase. Most transcripts whose steady-state levels were affected by RHAU knockdown showed no change in half-life, suggesting that these transcripts were the subject of transcriptional regulation.

In cells depleted of RHAU using shRNA, retardation of growth was observed, especially when cells were stressed, for example, by serum-starvation. RHAU indeed affected more genes in starved conditions, suggesting the involvement of RHAU in cellular stress responses in mammalian cells.

Overall, the results suggest that each RNA helicase is involved in various cellular processes. RHAU has dual functions, being involved in both the synthesis and degradation of mRNA in different subcellular compartments. Thus, my work presents a novel view of RNA helicases as proteins with multiple functions in different cellular contexts.

SECTION 1 - INTRODUCTION

1.01. Regulation of gene expression at different steps

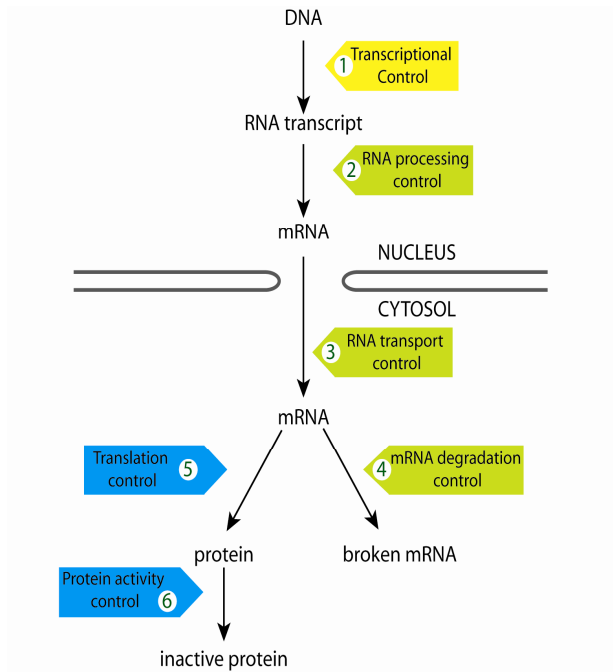


Figure 1. Six steps at which eukaryotic gene expression can be controlled.

Control of gene expression in eukaryotes is a complex process involving numerous steps, from the binding of transcription factors to their target sequence to the post-translational modification of proteins. Specific factors, either proteins or functional RNAs, are involved at each step to maintain cellular homeostasis in changing environments. Figure 1 illustrates six steps important for the control of gene expression in eukaryotic cells. In principle, all steps leading from DNA to protein can be regulated and will influence total protein activity. The initial transcriptional control is of paramount importance to the expression of most genes because only this step can result in “on” or “off” of RNA synthesis, which dramatically changes protein levels. The subsequent steps 2-4 are regulatory steps acting on mRNA. Many mammalian mRNAs require pre-mRNA splicing and some are processed or edited. These steps, including alternative splicing, contribute to variation in mRNA. Since maturation of mRNAs is required for nuclear export and mRNA stability, malfunction of these mechanisms is coupled to abnormal states of gene expression. The third step of mRNA transport is important for maintaining RNA quality because it ensures that all nuclear metabolic events of mRNAs are completed prior to export from the nucleus. Thus, this step is intimately connected to other steps in RNA-metabolism. Some mRNAs must be transported to specific locations in the cytoplasm, resulting in localized protein synthesis (St Johnston 2005). The fourth step of mRNA degradation changes cytoplasmic concentrations of mRNA more directly. This is a highly regulated step responsible for determining mRNA amount and turnover. Gene silencing mediated by small RNAs like micro RNAs (miRNAs) is also based on mRNA degradation as well as the suppression of

Control of gene expression in eukaryotes is a complex process involving numerous steps, from the binding of transcription factors to their target sequence to the post-translational modification of proteins. Specific factors, either proteins or functional RNAs, are involved at each step to maintain cellular homeostasis in changing environments. Figure 1 illustrates six steps important for the control of gene expression in eukaryotic cells. In principle, all steps leading from DNA to protein can be regulated and will influence total protein activity. The initial transcriptional control is of paramount importance to the expression of most genes because only this step can result in “on” or “off” of RNA synthesis, which dramatically changes protein levels. The subsequent steps 2-4

translation, both of which have a large impact on total protein. The rate of translation is also regulated and varies depending on cellular conditions. Finally, post-translational modifications, such as phosphorylation, methylation and acetylation, regulate protein activities, and protein degradation, e.g. by ubiquitin-dependent proteolysis, is also highly regulated depending on the cellular status.

It is, therefore, important to consider the regulation of these different steps when investigating control of gene expression. Referring to total mRNA, at least the two different parameters of synthesis and degradation must be considered. As discussed in the next section, not only the rate of transcription but also the regulation of mRNA degradation can greatly affect fine-tuning of gene expression in eukaryotic cells. Importantly, there is evidence for cross-talk between these different steps (Reed 2003). For example, factors of the general transcription machinery, such as the C-terminal domain of RNA polymerase II (CTD) and the transcription elongation factor TAT-SF1, associate with components of the splicing pathway (Abovich and Rosbash 1997; Morris and Greenleaf 2000; Fong and Zhou 2001). mRNA export is also physically and functionally linked to transcription and splicing: export factors are loaded on to synthesized mRNAs co-transcriptionally (Strasser et al. 2002; Vinciguerra and Stutz 2004; Kohler and Hurt 2007). The coupling of cellular pathways requires the interaction of molecules involved in the different pathways and this is achieved by regulated intracellular transport of molecules by energy-dependent mechanisms. In this thesis, I report on the investigation of one particular protein that associates with RNA and various proteins at different cellular locations. The study was initiated with the single question of why this molecule is actively translocated into different cellular compartments. The results I report here do not fully answer the question but suffice to put forward the hypothesis that the protein is transported to fulfil different functions in different intracellular locations and also that it mediates between different steps of RNA metabolism through its association with various molecules.

1.02. Regulation of mRNA stability

1.02.01. Regulation of mRNA stability contributes to changes of gene expression.

Regulation of gene expression at the level of mRNA stability is an important and highly regulated process. Half-lives vary considerably between mRNA species. In yeast, mRNA half-lives range from 1 min to more than 100 min (Gouka et al. 1996) and in mammalian cells from less than 20 min to over 50 h (Stolle and Benz 1988). For a given mRNA molecule, stability changes in response to extracellular stimuli. T cell activation, for example, dramatically stabilizes lymphokine mRNAs, such as IL2, GM-CSF, INF- γ , and TNF- α , contributing to increases in total mRNA (Lindstein et al. 1989). Global gene expression analyses using microarrays have revealed that regulation of mRNA stability accounts for about 50% of all changes in response to cellular signals (Fan et al. 2002; Cheadle

et al. 2005). These data all clearly suggest the existence of a mechanism to maintain and regulate mRNA stability in cells.

The rapid induction as well as reversal of gene expression allows prompt changes in mRNA steady-state levels in response to changing environmental conditions. Transiently expressed genes, early response genes, are induced by various cellular stimuli, with transcript levels increasing as much as 50-fold in a short time. Change in mRNA stability is especially critical for the rapid reduction of mRNA following induction, as a reduction of transcription rate alone is not sufficient to quickly reduce cellular mRNA levels. Microarray analysis has shown that 74% of mRNAs that declined in response to stress did so not by inactivation of transcription but by mRNA destabilization (Fan et al. 2002). Computational models also predict that the best strategy to reduce cellular mRNA concentration is a decrease in half-life. Conversely, induction of transcription rather than stabilization of mRNAs seems to be effective for increasing mRNA concentration in a short time (Perez-Ortin et al. 2007).

1.02.02. mRNA degradation machinery

Most mRNAs in eukaryotes are 5'-capped and 3'-polyadenylated. These mRNA modifications occur shortly after initiation of transcription and are both important in the protection of mRNAs from exonucleolytic degradation. Poly(A) tail shortening is often the initial and rate-limiting step of mRNA degradation in yeast and mammalian cells. Three independent complexes possessing poly(A)-specific 3'-exoribonuclease activities exist in most eukaryotic cells but yeast and *Drosophila* contain only two, CCR4-CAF1 and PAN2-PAN3. In mammalian cells, these two complexes represent the major cytoplasmic deadenylation activity (Yamashita et al. 2005). Decay of both stable and nonsense-codon-containing unstable β -globin mRNAs is first initiated by the PAN2-PAN3 complex and then by CCR4-CAF1 in the second phase of deadenylation, which is followed by degradation of the mRNA body (Yamashita et al. 2005). In contrast, higher eukaryote-specific poly(A) exoribonuclease, PARN, seems to deadenylate specific sets of mRNAs, such as those containing AU-rich elements (ARE). It has been shown that PARN catalyses ARE-dependent deadenylation *in vitro* (Lai et al. 2003).

As soon as poly(A) is removed, mRNA is destined for rapid exonucleolytic decay, either from the 5' or 3' end. The 5'-to-3' decay pathway starts by removal of the cap by decapping protein 2 (DCP2) together with the other activators DCP1, LSM1-7 complex and Pat1. Following decapping, 5'-to-3' exoribonuclease XRN1 digests the mRNA body (Wilusz et al. 2001; Meyer et al. 2004). In the other pathway, deadenylation is followed by 3'-to-5' decay of the RNA body mediated by the exosome. The exosome consists of 9-11 subunits of 3'-to-5' exonucleases

forming a donut-like structure that progressively phosphorylates the mRNA body from 3' ends (Liu et al. 2006).

Although deadenylation-dependent exonucleolytic decay is the major mRNA degradation pathway in eukaryotes, mRNAs such as for insulin-like growth factor 2 (IGF2), *c-myc*, and transferrin receptor are degraded by endonucleolytic activities independent of deadenylation (Bernstein et al. 1992; Binder et al. 1994; Scheper et al. 1995; Scheper et al. 1996). This process is mediated by specific endonucleases and particular sets of mRNAs, often in response to extracellular stimuli. Endoribonuclease RNaseL, for example, plays an important role in viral infection and the interferon response (Silverman 1994; Li et al. 1998; Li et al. 2000).

1.02.03. *cis*-element

mRNA stability is controlled by regulatory *cis*-acting elements on transcripts and their *trans*-acting binding proteins (Ross 1995; Guhaniyogi and Brewer 2001). *Cis*-acting elements are frequently found in 3'-untranslated regions (UTR), for example, of AU-rich elements (ARE; a destabilizing element) (Chen and Shyu 1995), iron-response elements (IRE; an iron-regulatory element also found in 5'UTR) (Thomson et al. 1999), constitutive decay elements (CDE, a destabilizing element) (Stoecklin et al. 2003), pyrimidine-rich elements (stabilizing elements of α -globin, β -globin, and α -collagen) (Kiledjian et al. 1995; Yu and Russell 2001; Lindquist et al. 2004) and others (Guhaniyogi and Brewer 2001). Regulatory elements are also found in the 5'UTR and even in protein-coding regions such as the *c-jun* response element in the 5'UTR of IL-2 mRNA (Chen et al. 1998) and coding elements of *c-myc* mRNA, which destabilize the message (Yeilding and Lee 1997). Each element associates with specific binding partners that can recruit or avoid associating mRNAs to/from degradation complexes, depending on the cellular conditions, thus regulating mRNA stability.

1.03. AU-rich element-mediated mRNA decay (AMD)

1.03.01. AU-rich element

By far the best-studied *cis*-element is ARE, located in the 3'UTR of many transcripts encoding, for example, cytokines, proto-oncogenes and transcription factors (Khabar 2005). In 1986, a conserved sequence enriched with adenylate and uridylate was found in the 3'UTR of mRNAs encoding inflammatory mediators (Caput et al. 1986). This sequence was shown later to be responsible for the instability of granulocyte macrophage-colony stimulating factor (GM-CSF) message since it elicited the rapid decay of otherwise stable β -globin reporter

mRNA (Shaw and Kamen 1986). Subsequently, the ARE has been characterized as an instability regulatory element for numerous mRNAs encoding proteins with diverse cellular functions. A database of ARE-containing mRNAs predicts that 5-8 % of human genes encode transcripts containing AREs (Bakheet et al. 2006). AREs vary in sequence and length but most contain one or more copies of the octamer UUAUUUAU, the AUUUA core sequence of which is essential for the mRNA destabilization elicited by AREs. According to the classification by Chen and Shyu (Chen and Shyu 1995), class I AREs contain 1-3 non-tandem copies of the pentanucleotide AUUUA embedded within a U-rich region. Class II AREs contain two or more reiterated copies of this motif and class III ARE, exemplified by that found in c-jun mRNA, are U-rich sequences lacking AUUUA motifs (Peng et al. 1996).

1.03.02. Degradation machinery and AUBPs

To elicit rapid degradation, ARE must be recognized by the mRNA degradation machinery. ARE-RNA itself can interact with the exosome component Pmscl-75 (Mukherjee et al. 2002) and the *in vitro* reconstituted exosome drives efficient degradation of AU-containing RNA but not the generic RNA without ARE (Liu et al. 2006). This suggests that ARE-RNA has a higher affinity for the exosome than other stable mRNAs. However, the *in vitro* reconstituted exosome does not degrade poly(A)-tailed mRNA efficiently (Liu et al. 2006), whereas the immunopurified exosome from HeLa cells can degrade ARE-RNA with poly(A) tails (Chen et al. 2001), suggesting that further factors in addition to the exosome are required for efficient deadenylation and decay of ARE-RNA. A group of proteins termed ARE-binding proteins (AUBPs) with affinity for ARE has been shown to mediate AMD. Three AUBPs, 37-kDa isoforms of AUF1, KSRP, and tristetraprolin (TTP), have affinity for the exosome and the latter two factors are required for exosome-mediated AMD. TTP and its binding partner BRF1 are also involved in the 5'-to-3' decay pathway, since they interact with a decapping complex (Kedersha et al. 2005; Lykke-Andersen and Wagner 2005). It has been shown that ARE stimulates decapping activity in HeLa cells (Gao et al. 2001). Furthermore, ARE-RNA is detected in cytoplasmic processing bodies (P-bodies), colocalizing with TTP, BRF1, and DCP1. P-bodies are cytoplasmic foci containing many components of 5'-to-3' decay pathways, including XRN1, DCP1, and the LSM complex but not the exosome (Franks and Lykke-Andersen 2007), which suggests that ARE-RNA is degraded in P-bodies by the 5'-to-3' decay machinery. However, Lin *et al* reported that ARE-RNA is also present in distinct cytoplasmic granules containing the exosome (Lin et al. 2007). Furthermore, a significant but diffuse amount of ARE-RNA is found in the cytosol, suggesting that P-bodies may not be the only site of AMD (Lin et al. 2007).

It is currently unclear which pathways of exonucleolysis, either from the 5' or 3' end, contribute to AMD in mammalian cells. In siRNA approaches to

downregulate individual decay factors in HeLa cells, two groups (Stoecklin et al. 2006; Lin et al. 2007) showed that knockdown of the 5'-to-3' pathway components XRN1 and LSM1 as well as the exosome components Pms1-75 and Rps46 impaired AMD. Downregulation of two factors, one involved in 5'-to-3' and another in 3'-to-5' decay, produced the largest impairment of AMD, implying that both pathways are active in AMD and that some are not redundant. In addition to these two distinct pathways, miRNA-mediated gene silencing has also been implicated in AMD in *Drosophila* and HeLa cells. RISC complexes, required for miRNA and siRNA-mediated gene silencing, are directed to ARE-RNA by imperfect base pairing between miR-16 and AREs, which eventually facilitates degradation of ARE-RNA (Jing et al. 2005). Most recently, ARE has been implicated in upregulation of translation by fragile-X mental-retardation-related protein 1 (FXR1) and an essential miRNA-loading factor, Argonaute2 (Vasudevan and Steitz 2007). A relationship between ARE and translational regulation has also been described in another pathway, in which HuR (an AUBP) suppresses miRNA-mediated translational repression (Bhattacharyya et al. 2006). Although the direction of ARE-mediated translational regulation may vary and the mechanism itself is not yet fully understood, these reports suggest that ARE is a mediator of mRNA degradation and translation. Interestingly, not only ARE-RNAs are localized in P-bodies but also miRNAs and miRNA-regulatory factors (Liu et al. 2005; Eulalio et al. 2007). ARE-RNA may affect gene expression in various ways in specific cytoplasmic locations.

1.04. RHAU : RNA helicase-associated with AU-rich element

RHAU (alias: DHX36) is a putative RNA helicase identified by RNA-affinity chromatography using ARE of uPA mRNA and human HeLa nuclear extracts (Tran et al. 2004). It was termed RHAU for "RNA helicase-associated with AU-rich elements" since it contains DExH-conserved motifs giving rise to the putative RNA helicase activity.

1.04.01. RHAU as a destabilizing factor of ARE-RNA.

As RHAU has a specific affinity for the ARE sequence of mRNA, the effect of RHAU on AMD was studied first. In HeLa cells, overexpression of RHAU caused destabilization of reporter ARE (β -globin mRNA harbouring uPA-ARE) as well as endogenous uPA mRNA. Examination of the *in vitro* mRNA decay system also showed that recombinant RHAU protein accelerates deadenylation and decay of β -globin-ARE^{uPA}. In contrast, downregulation of RHAU by siRNA in HeLa cells stabilized the reporter ARE. It was concluded that RHAU is a factor promoting degradation of ARE-containing mRNAs. RHAU requires ATPase activity, since the mutant E335A, which is unable to hydrolyze ATP, has no effect on the decay of ARE^{uPA} either *in vivo* or *in vitro*. In this study, a destabilizing effect of RHAU was found for uPA-ARE but not other types of mRNA, e.g. for the uPA receptor,

which contains a different class of ARE. This suggests that RHAU has a specific role in AMD (Tran et al. 2004).

1.04.02. RHAU as a G4 DNA resolvase.

In 2005, Akman's group isolated RHAU as the major source of guanine quadruplex (G4) DNA-resolving activity in HeLa cell lysates (Vaughn et al. 2005). G4 DNA is a highly stable DNA structure composed of several layers of a guanine tetrad in which four guanine residues from the same or different strands are linked by Hoogsteen-type hydrogen bonding (Maizels 2006). G4 structures are expected to occur in guanine-rich regions such as telomeres, ribosomal DNA, and immunoglobulin class switch regions, as well as in the promoter regions of several proto-oncogenes such as *c-myc* and *c-kit*, the transcriptional activity of which is repressed by this structure (Siddiqui-Jain et al. 2002; Maizels 2006; Shirude et al. 2007). Therefore, G4-resolving activity is expected to activate the transcription of genes containing G4 in the promoters. However, the biological functions of G4-DNA and G4-resolving enzymes (G4-resolvase) *in vivo* are largely unknown and the physiological significance of RHAU G4 resolvase activity has also not been defined.

1.04.03. Affinity to other molecules - protein and RNA

Several RNA-related proteins have been found to interact with RHAU either via RNA or not. Examples of mRNA degradation factors include the exosome components, PM/Scp100 and hRrp40p, and poly(A) ribonuclease PARN, which interact with RHAU even in the absence of RNA (Tran et al. 2004). It was suggested, therefore, that RHAU first promotes deadenylation of ARE-RNA, and then recruits it into the exosome for rapid degradation. RHAU also interacts with further AUBPs, namely NF90 and HuR, that were co-precipitated in the initial RNA-affinity chromatography by which RHAU was isolated. These AUBPs both interact with RHAU in a manner dependent on RNA. In the case of NF90, strong interaction was observed in the presence of uPA-ARE but not IL2-ARE or mutated uPA-ARE. Downregulation of NF90 stabilized uPA-ARE. Thus, it is likely that both proteins have very specific roles in promoting decay of uPA-mRNA (Akimitsu, unpublished data).

RHAU was first isolated from HeLa nuclei with uPA-ARE oligonucleotides (Tran et al. 2004). However, *in vitro* RNA electrophoretic mobility shift assays (REMSA) using recombinant RHAU protein and ARE-uPA showed that RHAU by itself has little interaction with ARE. The interaction was observed more clearly when protein and RNA were crosslinked, suggesting that RHAU interacts with RNA only transiently (Akimitsu and Lattmann, unpublished data). It seems that additional proteins are required for a more stable association of RHAU with RNA. One such protein is NF90. The intensity of the interaction of RHAU with uPA-

ARE was increased 2.7-fold by addition of recombinant NF90. Unlike RHAU, NF90 itself has strong affinity for uPA-ARE and, thus, NF90 may promote the interaction between RHAU and ARE that is required to stimulate mRNA degradation (Akimitsu, unpublished data).

1.04.04. Evolutional conservation and expression pattern.

According to sequence alignment data, RHAU is found in every clade in the Metazoa except for the phylum Nematode. The yeast DEAH-box protein YLR419w shows similarity to five human DExH proteins, including RHAU. Thus YLR419w is probably a common ancestor of these proteins (see Figure 2). YLR419w is dispensable in yeast and has not been characterized so far (Colley et al. 2000). RHAU is highly conserved, especially in vertebrates, through the central helicase core motifs and the C-terminal extremity but not the N-terminus, suggesting that the N-terminal domain is involved in its specific function in higher eukaryotes (Lattmann, unpublished data).

In humans, RHAU is moderately expressed in most tissue and cell types but is especially highly expressed in lymphocytes such as T-, B-, and NK cells, as well as in their precursors (Human GeneAtlas GNF1H, <http://symatlas.gnf.org/SymAtlas/>). Northern blot analyses of various mouse tissues showed highest expression of RHAU in thymus, also suggesting a possible role for RHAU in the immune system (Akimitsu, unpublished data). Bone marrow and blood were not tested. Many mRNAs encoding cytokines in immune cells contain ARE sequences and their expression is tightly controlled by mRNA degradation. RHAU may be involved in such regulation in lymphocytes.

1.04.05. Intracellular localization.

RHAU was originally identified in HeLa nuclear extracts. Ectopically expressed HA-RHAU was predominantly localized in the nuclei of HeLa cells (Tran et al. 2004). This localization pattern raised the possibility that RHAU has other functions in the nucleus, since mature mRNA degradation occurs in the cytoplasm or in cytoplasmic bodies. This hypothesis will be discussed further.

1.05. RNA helicases

1.05.01. Structure.

RNA helicases are ATP-hydrolytic enzymes found in virus, bacteria, archaea and eukaryotes, where they are the largest protein family involved in RNA metabolism (Anantharaman et al. 2002). All currently known RNA helicases belong to the helicase superfamilies 1-4, which include both DNA and RNA helicases. They share a highly conserved helicase domain consisting of several motifs (Tanner and Linder 2001; Linder 2006). A few RNA helicases belong to helicase superfamily 1 (SF1), including Upf1, an enzyme required for nonsense-mediated decay (NMD), but most RNA helicases belong to helicase superfamily 2 (SF2). RNA helicases in SF2 are further classified into three groups, DEAD-box, DEAH-box and DExH-box, based on the amino acid sequence of motif II in the helicase domain. In humans, DEAD-box proteins have the gene symbol of DDX-, whereas DEAH and DExH-box proteins are designated as DHX- (Abdelhaleem et al. 2003). RHAU belongs to the DExH-box protein family and, therefore, has the gene symbol of DHX36.

DExH/D proteins contain at least eight conserved motifs (I, Ia, Ib, and II-VI) in the helicase core domain. These motifs have been characterized by biochemical approaches as they have ATP-binding and hydrolytic activity (I, II, VI), bind to nucleic acids (Ia, Ib, IV), or coordinate polynucleotide binding and ATPase activity (III and V) (Tanner and Linder 2001). Furthermore, recent studies of protein structure have provided more information on the helicase domain structure. Up to now, structures of two DEAD-box proteins, eIF4AIII (Andersen et al. 2006; Bono et al. 2006) and Vasa (Sengoku et al. 2006), and one viral DExH-box protein, HCV NS3 (Kim et al. 1998; Mackintosh et al. 2006), have been determined in the presence of nucleic acids. The helicase domain is formed by two domains connected via a flexible linker region. Without ATP or nucleic acids, the two domains are relatively open, especially in DEAD-box proteins. ATP and/or nucleic acid binding bring the two domains into a more defined arrangement (Jankowsky and Fairman 2007). Thus, it is possible that binding to nucleic acid promotes ATP binding and hydrolysis and *vice versa*. Many DEAD-box proteins are in fact unable to bind or hydrolyze ATP without RNA (Lorsch and Herschlag 1998; Iost et al. 1999; Polach and Uhlenbeck 2002; Talavera and De La Cruz 2005). DExH proteins, in contrast, show ATP hydrolysis without RNA, although RNA can still stimulate ATP hydrolysis (Shuman 1992; Tanaka and Schwer 2005; Tanaka and Schwer 2006). The DExH protein HCV NS3 indeed shows less dramatic movements upon binding to ATP and nucleic acid (Kim et al. 1998; Jankowsky and Fairman 2007). Whether RNA-dependent or not, changes in conformation caused by binding to ATP seem to be an important feature of RNA helicases when acting as ATP-driven switches at specific points of RNA metabolism.

1.05.02. helicase and RNPase.

DExH/D proteins are characterized as ATP-dependent RNA helicases since some of the proteins, but not all, exhibit unwinding activity on duplex RNA molecules *in vitro*. The unwinding activity of viral DExH protein HCV NS3 has been monitored at the single-molecule level using a 60-bp RNA hairpin, which supported the model that DExH proteins first load onto the single-strand region of RNA and then translocate along one of the strands in a unidirectional and progressive fashion (Dumont et al. 2006). In contrast to the viral DExH proteins that can unwind several dozen base pairs, DEAD-box proteins are normally unable to unwind long duplexes but only a few base pairs, in a manner different to that of DExH proteins (Jankowsky et al. 2000; Cordin et al. 2006). DEAD-box protein Ded1 directly loads onto the duplex region and spontaneously initiates strand dissociation from the loading region. Single-strand regions increase the efficiency of duplex unwinding but this facilitates the loading of enzymes rather than loading onto the single-strand region itself (Yang and Jankowsky 2006). The physiological importance of duplex RNA unwinding activity has been less characterized than the biochemical unwinding experiments. For some RNA helicases, helicase activity is clearly required for the biological role. Dbp4p dissociates duplexes of U14 snoRNA and pre-rRNA, and thus duplex-unwinding activity is required for release of U14 from pre-ribosomes, an essential step in the pre-rRNA processing pathway (Kos and Tollervey 2005). However, the actual substrates of many other RNA helicases are unknown and, thus, the relevance of their unwinding activity for their biological function has not been clarified, even though they unwind duplexes *in vitro* (Tanner and Linder 2001; Cordin et al. 2006; Linder 2006).

The results of recent studies suggested that the activity of RNA helicases is not restricted to rearrangement of RNA secondary structure, but that it includes the modification of protein-RNA interactions (Jankowsky and Bowers 2006). Two proteins, viral DExH NPH-II and yeast DEAD-box protein DED1, have been shown to dissociate proteins from RNA in an ATP-dependent fashion with four different substrate RNPs *in vitro* (Jankowsky et al. 2001; Fairman et al. 2004; Bowers et al. 2006). Although the dissociation rate constant depends on various helicases and substrates, both proteins are able to displace exon junction complex (EJC), a protein complex bound upstream of exon-exon junctions, from the single-stranded spliced mRNAs, indicating that unwinding activity is not required for this activity (Jankowsky et al. 2001; Fairman et al. 2004; Bowers et al. 2006). These authors have proposed a novel feature of RNA helicases as a remodeler of RNPs. Since RNAs are invariably complexed with various proteins, the rearrangement of RNA-protein interactions by an RNA helicase is likely to be a feature of every step of the RNA metabolic pathway.

1.05.03. Various functions of RNA helicases.

RNA helicases are involved in all aspects of RNA metabolism. In yeast, almost all RNA helicases are essential for cell viability and there are orthologs for most of these proteins in mammals (de la Cruz et al. 1999). In humans, 38 DEAD-box helicases and 14 DExH-box helicases have been identified so far (Abdelhaleem et al. 2003; Linder 2006) and functions have been assigned in various steps of RNA metabolism. Four DExH helicases are involved in pre-mRNA splicing and one in ribosomal RNA processing; all of these are essential in yeast. Although YLR490w, an ancestor of five human DExH proteins including RHAU, is not essential for yeast viability, DHX9, which is also known as RNA helicase A (RHA) or NDH II and shares the same yeast ancestor, is required for mouse embryonic development (Lee et al. 1998). This suggests that RHA has gained additional functions during evolution.

Whilst it looks as though a unique RNA helicase is engaged in each RNA metabolic step, many authors have reported that a single RNA helicase harbours multiple functions acting at different steps from transcription, splicing, and RNA export to mRNA stability (Fuller-Pace 2006). RHA is one such protein, playing many roles in the regulation of gene expression. In the nucleus, RHA interacts with RNA polymerase II and transcriptional regulators such as CBP/p300 (Nakajima et al. 1997), BRCA1 (Anderson et al. 1998) and NF- κ B (Tetsuka et al. 2004), as well as promoters of the p16INK4a and MDR1 genes (Myohanen and Baylin 2001; Zhong and Safa 2004) and activates their transcription. RHA is also involved in RNA export mediated by the constitutive transport element (CTE) (Tang et al. 1997; Tang et al. 1999), in RNA splicing by interacting with SMN (survival motor neuron complex), and in the translation of selected mRNAs (Hartman et al. 2006; Bolinger et al. 2007). Most recently, RHA has been identified also in the RNA-induced silencing complex (RISC) in HeLa cells, functioning as an siRNA-loading factor (Robb and Rana 2007).

In another case, DEAD box proteins p68 (DDX5) and p72 (DDX17) have been shown also to regulate transcription via interaction with various transcription regulators, such as β -catenin (Yang et al. 2006), MyoD (Caretta et al. 2006), Smads (Warner et al. 2004), HDAC1 (Wilson et al. 2004), and p53 (Bates et al. 2005). They, thus, play a role in epithelial mesenchymal transition, myogenesis, regulation of apoptosis, general transcriptional repression, and tumorigenesis, respectively. Furthermore, it has also been suggested that they are required for pre-mRNA splicing (Liu 2002; Lin et al. 2005) and alternative splicing (Guil et al. 2003) as well as the processing of rRNA and miRNAs (Fukuda et al. 2007). These observations indicate that a single RNA helicase plays many different roles, depending on interactions with various molecules in different cellular environments.

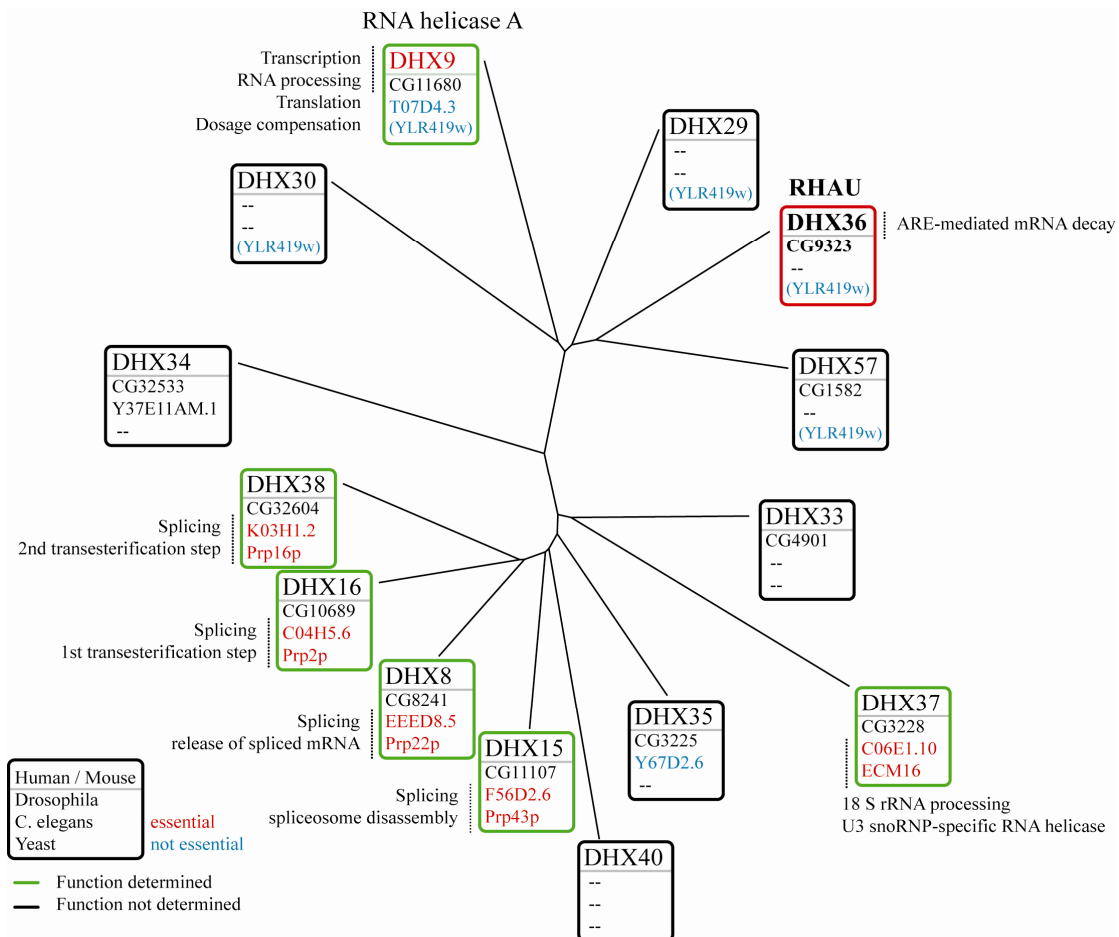


Figure 2. Human DExH proteins. Amino acid sequences of fourteen human DExH proteins were aligned by an online program, MAFFT ver.6 (<http://align.bmr.kyushu-u.ac.jp/mafft/online/server/>). Graphic tree was made based on the sequence distances between each protein using Tree View 1.6.6. Essential (in red): lethal phenotype described in knockout organisms. Not essential (in blue): knockout organisms are not lethal. *Lattmann, unpublished data.*

1.06. Spatial controls of RNA and proteins involved in RNA metabolisms.

Compartmentalization is one of the most important features of cells. Eukaryotic cells are themselves surrounded by a plasma membrane that fulfils specific roles but they also include many different compartments, like organelles, each of which contains a characteristic set of enzymes and other molecules active in its specialized role. The nucleus, for example, stores compacted DNA and enzymes to synthesize mRNAs. The nuclear membrane separates the sites of RNA synthesis and protein synthesis, thus avoiding the translation of premature mRNAs to proteins. Further subdomains have been characterized inside organelles or in the cytosol. These cellular “bodies” are not surrounded by membranes but by a local accumulation of selected molecules that can be visualized by specific markers. The cytosol contains P-bodies as well as stress granules formed in response to stress. Both bodies contain mRNA and specific RNA-binding proteins and function as sites of mRNA degradation (P-body), mRNA storage (stress granule), and suppression of translation (both of these organelles) (Anderson and Kedersha 2002; Kedersha et al. 2005; Eulalio et al. 2007; Parker and Sheth 2007). The nucleus is more complex than the cytoplasm, fulfilling many different roles in a small space, such as storage of genomic DNA, synthesis, processing, and export of RNA, as well as the degradation of premature and incorrectly processed RNAs. Therefore, it has been suggested that the nucleus has a very precise layout that ensures the efficiency of assorted nuclear activities. Many nuclear bodies have been characterized, such as nuclear speckles involved in the storage, assembly, and modification of pre-mRNA splicing factors, PML bodies playing a role in transcriptional regulation of specific genes, cajal bodies involved in snRNP and snoRNP biogenesis and posttranscriptional modification of newly assembled spliceosomal snRNAs, and polycomb bodies containing silencing proteins, etc. The numbers and sizes of these nuclear bodies vary depending on cell type and conditions, which suggest that they are involved in regulatory steps of cellular metabolism (Matera 1999; Lamond and Sleeman 2003; Matera and Shpargel 2006).

AIMS

To understand biological role(s) of RHAU in mammalian cells.

To determine subcellular localization of RHAU and its regulations.

To determine RHAU target genes and mRNAs.

To determine the effect of RHAU-depletion in mammalian cells.

SECTION 2 - MATERIALS AND METHODS

2.01. Plasmids

Oligonucleotides used in this work are presented in Appendix I. Plasmid pTER was kindly provided by Hans Clevers (van de Wetering et al. 2003). To construct pTER-shRHAU1 and pTER-shRHAU2, annealed oligonucleotides of shRHAU1-s, shRHAU2-s and shRHAU1-as, shRHAU2 were inserted into *BglII/HindIII* sites of the pTER vector to target RHAU mRNA at the site 1344-1364 nt and 2570-2590 nt, respectively. pTER-shLuc was kindly provided by A. Hergovich and B.A. Hemmings (Hergovich et al. 2007). To derive the N-terminal fusion plasmid pEGFP-RHAU, full-length RHAU was cut out from pcDNA3-HA-RHAU (Tran et al. 2004) using *BamHI/XhoI* and inserted into the *BglII/SaI* sites of pEGFP-C1 (Clontech laboratories, Inc., Mountain View, CA). To introduce the ATPase-deficient mutation, pEGFP-RHAU-E335A was made using site-directed mutagenesis with oligonucleotides (E335A-s and E335A-as) that mutate the Glu335 of RHAU to Ala. To derive RHAU truncated mutants with N-terminal EGFP-tags, truncated forms of RHAU cDNAs were amplified by PCR using specific primers containing restriction sites and inserted into the *BglII/EcoRI* sites of pEGFP-C1. To derive the C-terminal fusion plasmids pRHAU-EGFP and pRHAU-E335A-EGFP, full-length RHAU was amplified by PCR using the primers RHAU 2 fw BamHI and RHAU1008 rv EcoRI with the plasmids pcDNA3-HA-RHAU and EGFP-RHAU-E335A, respectively, and inserted into the *BamHI/EcoRI* sites of pEGFP-N1 (Clontech). pcDNA3-Flag-RHAUsm was made by replacing the HA tag of pcDNA3-HA-RHAU in *HindIII/BamHI* sites with annealed oligonucleotides coding the Flag sequence. To introduce silent mutations in the RHAU expression vector at the shRHAU-targeting site, we did site-directed mutagenesis using oligonucleotides RHAUsm-s and RHAUsm-as to amplify, using PCR, a mutated vector that contained two point mutations, G1350A and A1353G. To derive pGEX-RHAU(1-200aa), truncated RHAU was amplified by PCR using the primers RHAU 2 fw BamHI and RHAU 200 rv EcoRI with the plasmid pcDNA3-HA-RHAU and inserted into *BamHI/EcoRI* sites of pGEX-2T (GE health care life sciences). To derive pcDNA3-HA-p68 and pcDNA3-HA-p72, full-length cDNA of p68 and p72 were amplified using the primers p68-fw/p68-rv and p72-fw/p72-rv, respectively, using cDNA derived by reverse transcription of purified HeLa total RNA, and inserted into *BamHI/XhoI* sites of the pcDNA3.1(+)-HA vector. pcDNA3.1(+)-HA was made by inserting the annealed oligonucleotide fragment coding the HA sequence into the *HindIII/BamHI* sites of the pcDNA3.1(+) vector (Invitrogen Corporation, Carlsbad, CA). pcDNA3.1-HDAC1^{FLAG} and pcDNA3.1-HDAC3^{FLAG} were kindly from P. Matthias (FMI). The sequences of all plasmids made by PCR-cloning were confirmed.

2.02. Cell culture and transfection

HeLa cells and COS7 cells were maintained in Dulbecco's Modified Eagle's Medium (DMEM), supplemented with 10% fetal calf serum at 37°C in the

presence of 5% CO₂. T-RExTM-HeLa cells (Invitrogen) were maintained as above with the additional supplement of 3 µg/ml blasticidine (Invitrogen). T-RExTM-HeLa cells were stably transfected with pTER-shRHAU or pTER-shLuc vectors using FuGENE6 (Roche Applied Science, Rotkreuz, Switzerland) and selected with zeocin (InvivoGen, San Diego, CA) at a final concentration of 450 µg/ml. Zeocin-resistant colonies were picked up as independent clones. The independent clones from same transfections were pooled in some experiments. To induce shRNA expression, cells were treated with doxycycline (Sigma-Aldrich Co.) at a final concentration of 1 µg/ml. HeLa-shRHAU1 cells, stably transfected with pTER-shRHAU1, were used in all experiments except Figure 22. They are indicated as HeLa-shRHAU cells in these figures. In Figure 22, two different cell lines targeting different region of RHAU mRNA, HeLa-shRHAU1 (same cell line as HeLa-shRHAU in the other figures) and HeLa-shRHAU2 that were stably transfected with pTER-shRHAU1 and pTER-shRHAU2, respectively, were used. Transient transfection of plasmid DNA using FuGENE6 was performed according to instructions provided by the manufacturer. We used 1 µg plasmid DNA and 3 µl FuGENE6 per 35-mm dish.

2.03. Antibodies

Mouse anti-RHAU monoclonal antibody was generated against a peptide sequence which corresponds to the C terminal of RHAU, aa991-1007, and which has previously been reported (Vaughn et al. 2005). Rabbit anti-H3-K9 trimethylation and rabbit anti-NDH II (RNA helicase A) antibodies were kindly provided by A.H. Peters (Peters et al. 2003) and S. Zhang (Zhang et al. 1995), respectively. Commercially obtained antibodies were: mouse anti-DRBP76 (for detecting NF90) and mouse anti-Cleaved PARP (Asp214) from BD Biosciences (San Jose, CA), mouse anti-TRF2 (4A794) from Novus Biologicals, Inc. (Littleton, CO), rabbit Cleaved Caspase-3 (Asp175) from Cell Signaling Technology, Inc. (Danvers, MA), mouse anti-HDAC1 (2E10) from Millipore Corporation (Billerica, MA), rabbit anti-Histone H3 from Abcam plc. (Cambridge, UK), mouse anti-Ku (p80) (Ab-2, Clone111) from Lab vision Corp. (Fremont, CA), rabbit anti-BTF antibody (BL2521) from Bethyl Laboratories, Inc. (Montgomery, TX), mouse anti-β-tubulin, mouse anti-SC35, and mouse anti-FLAG[®] M2 from Sigma-Aldrich Co. (St. Louis, MO), and mouse anti-GAPDH (6C5), goat anti-ERK1 (C-16)-G, rabbit anti-CRM1 (H-300), mouse anti-Oct1 (E-8), rabbit anti-hnRNP C1/C2 (H-105), rabbit anti-HA (Y-11), and mouse anti-GFP (B-2) from Santa Cruz Biotechnology, Inc. (Santa Cruz, CA). Mouse antibodies were all monoclonal antibodies.

2.04. Protein extraction and Western blotting

To prepare total cell lysates, cells were lysed with NP40 buffer (50 mM Tris-HCl, pH 7.4, 120 mM NaCl, 1% NP-40, 1 mM EDTA, 5 mM Na₃VO₄, 5 mM NaF, 0.5 µg/ml aprotinin, 1 µg/ml leupeptin) on ice for 30 min and centrifuged at 11,000 × *g* for 5 min at 4°C to remove cell debris. Typically, 20 µg of the total cell lysate were loaded for Western blotting. Nuclear fractionation was followed by Fey's

protocol as previously described (Fey et al. 1986). HeLa cells were collected using PBS and subsequently lysed with CSK buffer (10 mM PIPES, pH 6.8, 50 mM NaCl, 300 mM sucrose, 3 mM MgCl₂, 1 mM EGTA, 0.5 % Triton-X100) with Complete® (EDTA-free) (Roche Applied Science) for 3 min on ice and centrifuged at 650 × *g* for 5 min. The pellet was dissolved in the nuclear extraction buffer (10 mM PIPES, pH 6.8, 300 mM sucrose, 3 mM MgCl₂, 1 mM EGTA, 0.5 % Triton-X100, 0.25 M (NH₄)₂SO₄) with Complete®, left for 5 min on ice and then centrifuged at 1000 × *g* to obtain soluble (supernatant) and chromatin-rich (pellet) fractions. Each fraction was mixed with SDS-PAGE loading buffer and sonicated briefly before loading into the SDS-PAGE for the Western blotting. To visualize the bands, we used either the direct infrared fluorescence detection method or the chemiluminescence method. For the fluorescent blots, IR dye 800CW-conjugated secondary antibodies were used at a dilution of 1:10,000 and quantified using an Odyssey infrared imager (LI-COR Biosciences UK Ltd., Cambridge, UK). For the chemiluminescent blots, we used horseradish peroxidase (HRP)-conjugated secondary antibodies at a dilution of 1:4,000 and ECL™ western blotting detection reagents (Amersham Biosciences, Piscataway, NJ). The membranes were exposed to Kodak X-Omat LS films.

2.05. Immunoprecipitation

8×10⁵ HeLa cells were seeded in 10 cm dishes and transfected the next day with total 6 µg of plasmids using 18 µl of FuGENE6. After 48 h of transfection, cells were collected and lysed with IP buffer (20 mM HEPES pH 7.5, 3 mM MgCl₂, 150 mM NaCl, 0.3% CHAPS) and briefly sonicated. To the lysates, 400U/ml RNasin (Promega Co., Madison, Wis.) or 10 µg/ml RNaseA plus 100 U/ml RNaseT1 was added. The lysate was suspended with anti-FLAG M2 affinity gel (Sigma-Aldrich Co.), rotated for 2 h at 4°C, and then washed with the IP buffer. The precipitates were redissolved and loaded into SDS-PAGE for the Western blotting using anti-FLAG and anti-HA antibodies.

2.06. *in situ* extraction

HeLa cells (8×10⁴ cells per well) were seeded in 12-well plates with coverslips and transfected the next day with 500 ng of plasmids using FuGENE6. After 48 h of transfection, cells were washed with ice-cold PBS once and added 0.1 % Triton-X100 in PBS for 5 min on ice to permeabilize plasma membranes. Permeabilized cells were further treated with DNase or RNase by adding 100 U/ml DNase I plus 400 U/ml RNasin in CSK buffer or 20 µg/ml RNase A plus 100 U/ml RNase T1 in CSK buffer, respectively, and incubated at room temperature for 20 min. Cells were washed twice with PBS and fixed with 3.8 % paraformaldehyde in PBS for 10 min at room temperature. Cells were further double stained using anti-BTF (transcription factor, (Haraguchi et al. 2004)) antibody to stain nucleus both in DNase- and RNase-treated cells as well as DAPI to confirm breakdown of DNA in DNase-treated cells. Images taken by confocal microscope were analyzed to obtain numbers of EGFP-positive cells out of about 200 cells visualized by the BTF-staining.

2.07. Immunocytochemistry and image processing

HeLa cells (8×10^4 cells per well) were seeded in 12-well plates with coverslips and transfected the next day with 500 ng of plasmids using FuGENE6. For inhibition of transcription, Actinomycin D (ActD: AppliChem GmbH, Darmstadt, Germany) or dichlororibofuranosyl benzimidazole (DRB: Sigma-Aldrich Co) was added 2 h before fixation to a final concentration of 5 $\mu\text{g/ml}$ or 25 $\mu\text{g/ml}$, respectively. Cells were fixed with 3.8% paraformaldehyde in PBS 48 h after transfection, permeabilized with 0.5% Triton-X100 in PBS and blocked with 5% horse serum in PHEM buffer (25 mM HEPES, 10 mM EGTA, 60 mM PIPES, 2 mM MgCl_2 , pH 6.9). Cells were incubated with primary antibodies in the same buffer at 4°C over night. Mouse anti-SC35, rabbit anti-H3 K9 trimethylation, rabbit anti-HA, rabbit anti-BTF, and mouse anti-TRF2 antibodies were used at dilutions of 1:4,000, 1:500, 1:200, 1:400, and 1:500, respectively. We used Cy2™, Cy3™, or Cy5™ - conjugated donkey secondary antibodies (Jackson ImmunoResearch Laboratories, Inc., West Grove, PA) at a dilution of 1:2,000 with 2.5% horse serum in PHEM buffer at room temperature for 40 min. Cells were then incubated with 500 ng/ml DAPI (Santa Cruz Biotechnology, Inc.) to identify the nuclei. ProLong® Gold antifade reagent (Invitrogen) was used for mounting. Images were acquired on a confocal microscope (LSM 510 META, Carl Zeiss GmbH, Jena, Germany) with a Plan-NeoFluar $\times 40/1.3$ oil DIC objective (optical section $\sim 1 \mu\text{m}$). To avoid cross-talk, DAPI, EGFP, Cy3, and Cy5 fluorescence was detected sequentially using the 405 nm laser in combination with the BP420-480 nm filter, the 488 nm laser with the BP505-550 nm filter, the 543 nm laser with the BP561-646 nm filter, and the 633 nm laser with the BP646-732 nm filter, respectively.

2.08. Luciferase reporter assay

HeLa-shLuc or HeLa-shRHAU cells, pool of four different clones, were seeded in 12-well plates (1×10^5 cells per well) with or without doxycycline (1 $\mu\text{g/ml}$). 24 h later, cells were transfected with 250 ng of pGL2-promoter (Promega Co., Madison, WI), a firefly luciferase-expressing plasmid, together with 1 ng of pRL-TK (for renilla luciferase expression as internal control) using FuGENE6. 48 h after transfection, cell lysates were prepared and luciferase expression was measured according to the given protocol (Dual-Luciferase Reporter Assay System, Promega). Firefly luciferase activity was normalized by renilla luciferase activity. Fold activation was derived from the normalization with dox- samples.

2.09. GeneChip microarrays and the analysis of RNA half-lives

HeLa-shLuc and HeLa-shRHAU cells were treated with doxycycline (1 $\mu\text{g/ml}$) for 6 days. On the 4th day of dox-treatment, four clones of each cell line were pooled and a total of 2×10^6 cells were reseeded in 10 cm dishes. For the starvation experiment, the medium was replaced with serum-free DMEM on the 5th day, 24 h before the collection of RNA. The ActD-chase experiment was done on the 6th day of doxycycline treatment. 5 $\mu\text{g/ml}$ ActD was added to the medium, and total

RNA was collected at 0, 30, 60, 90, and 120 min after the addition of ActD. Samples for time 0, representing the total amount of RNA collected from cells cultured in FCS-containing or starvation conditions were analyzed in triplicate, whereas ActD-treated samples for the mRNA decay study were analyzed in duplicate. Total RNA was isolated using the RNeasy kit from QIAGEN (Hombrechtikon, Switzerland).

Total RNA (5 µg) from each replicate was reverse transcribed and labeled using the Affymetrix 1-cycle labeling kit according to manufacturer's instructions. Biotinylated cRNA (20 µg) was fragmented by heating with magnesium (as per Affymetrix's instructions) and 15 µg of this fragmented cRNA was hybridized to Human U133 plus 2.0 GeneChips™ (Affymetrix, Santa Clara, CA). GC-RMA expression values and detection P-values were estimated using Refiner 4.0 from Genedata AG (Basel, Switzerland). Data analysis was performed using Analyst 4.0 from Genedata AG. The chip distributions were standardized by quantile normalization and they were scaled to make the median expression value, of genes with a detection P-value < 0.04, equal to 500. For the analysis of steady-state RNA levels, genes were required to have a detection P-value of less than 0.04 (Affymetrix default) in at least two replicates of at least one condition. The objective was to exclude genes that are not expressed in any condition. They were then subjected to a student *t*-test (P<0.05) and have a median fold change of 1.5 or 2 greater between samples dox+ and dox- or with and without starvation. Multiple testing errors were dealt with using a Benjamini and Hochberg false discovery correction.

To obtain mRNA half-lives, we used expression levels from the Affymetrix expression arrays at the start of the experiment (three biological replicates, "time 0") and at four successive timepoints (30, 60, 90, and 120 minutes, two biological replicates each). First, mRNAs with long half-lives were identified, defined by expression levels that decreased less than 13% ($= 1 - 2^{(-120/600)}$) in the course of 120 minutes, corresponding to half-lives of 600 minutes or more. Half-lives and the corresponding standard errors of the remaining mRNAs were estimated by fitting the time-course expression data to an exponential decay function $N(t) = N_0 \times 2^{(-t/t_{1/2})}$, where $N(t)$ and N_0 correspond to the expression levels at timepoints t and zero, respectively, and $t_{1/2}$ to the half-life, using the nonlinear least squares method as implemented in the R statistical program (www.r-project.org). Differences in half-lives were identified based on estimated half-lives and standard errors using the method described by Payton *et al.* (Payton *et al.* 2003). Half-lives with non-overlapping 88% confidence intervals were considered significantly different at a P value of 0.05.

For the general data analysis, the significance of the overlap between two sets of genes was calculated using the hypergeometric distribution as implemented in the R statistical program, which was also used to generate density plots of half-lives.

To find ARE-containing mRNAs, we used the human AU-rich element-containing mRNA database ARED (<http://rc.kfshrc.edu.sa/ARED/>). For the analysis of genes containing G4 structure in the promoter, the human promoters (defined as a sequence of 1000 nucleotides upstream of annotated transcripts that overlap

Affymetrix probesets) were obtained from Ensembl (www.ensembl.org, release 44) using a Perl script and the Ensembl Perl API (Curwen et al. 2004). Sequences were then scanned for the presence of G4 sequence using quadparser (Huppert and Balasubramanian 2005) with standard parameters.

The entire set of microarray data is in GEO (Gene Expression Omnibus) with accession number GSE8192. The list of RHAU-regulated probe sets at steady-state mRNA level, by mRNA stability, and the list of starvation-sensitive genes are shown in Appendix II, III, and IV, respectively.

2.10. Cell growth and viability

HeLa-shLuc or HeLa-shRHAU cells, pool of four different clones, were cultured with or without doxycycline for 5 days. For the growth analysis in FCS-containing condition, 1.5×10^5 cells per well were seeded in 12-well plates and viable cell numbers were obtained every 24 h using the automated cell counter ViCell™ (Beckman Coulter, Inc., Fullerton, CA). For the starvation experiment, 3×10^5 cells per well were seeded in 12-well plates. 24 h later, the medium was replaced with serum-free medium and viable cell numbers and cell viability values were obtained every 24 h using ViCell™. Microscopic images showing cell morphology were captured by a phase contrast microscope. To count apoptotic cells, AnnexinV-positive cells were detected by FACS using anti-AnnexinV-APC antibody, according to a manufacturer's instruction (BD Biosciences Pharmingen). To detect apoptotic marker proteins, starved cells were collected for Western blotting and stained by anti-cleaved caspase3 and anti-cleaved PARP antibodies.

2.11. Nuclear run-on assay

HeLa-shRHAU cells (clone 25) were treated for 6 days with doxycycline and then nuclear fractions were prepared as described (Medcalf et al. 1988). *In vitro* transcription was performed in 200 μ l of run-on reaction buffer (5 mM Tris-HCl, pH 8.0, 2.5 mM MgCl₂, 150 mM KCl) containing cold ATP, CTP, GTP (5 mM each) and [γ -³²P] UTP (100 μ Ci) and incubated at 30°C for 30 min. RNA was purified and hybridized with specific cDNA (1 μ g) immobilized on a positively charged nylon membrane for 3 days at 42°C. Hybridization signals were visualized and quantified using a Phosphoimager, and analyzed using Molecular Dynamics (version 5.2).

2.12. Real time PCR

First-strand cDNA was synthesized from total RNA (1 μ g) isolated from HeLa-shRHAU cells transfected with Flag-RHAUsm or empty vector (pBR-322), using the QuantiTect Reverse Transcription kit (QIAGEN) according to the manufacturer's instructions. 1 μ l of ten-times diluted RT reaction mixture was used to perform PCR with specific primer pairs (shown in APPENDIX I) corresponding to a particular gene of interest. Real-time PCR was performed using the QuantiTect SYBR Green PCR kit (QIAGEN) and the ABI PRISM 7000 sequence detector (Applied Biosystems, Foster City, CA) according to the

manufacturers' instructions. We used NDUFA12 (NADH dehydrogenase (ubiquinone) 1 alpha subcomplex, 12) for the normalization since expression of this gene was not altered in any samples analyzed by the microarray.

2.13. Tumor generation in nude mice

HeLa-TR-shRHAU1 or HeLa-TR-shRHAU2 cells were cultured with 1 µg/ml doxycycline for two days. Viable cells were counted and suspended in PBS (2×10^7 cells/ml). CD1 female nude mice (Charles River Laboratories, Inc., Sulzfeld Germany) were fed with water containing or not containing doxycycline (1mg/ml) two days prior to injection. HeLa cells in PBS (two million cells per injection) were subcutaneously injected into the right and left flanks of the nude mice. Once a tumor was detected, transcutaneous caliper measurements were used to measure the long and short dimensions of the tumor. Tumor volume was calculated on the assumption of an ellipsoidal volume, which was observed to be the predominant shape of the tumors. The tumor volume in milliliters was calculated according to the following formula, $V = 4/3 \pi ab^2$, where V represents volume and a and b represent the semiaxial dimensions.

2.14. GST-RHAU pull-down assay

Plasmids, pGEX-RHAU(1-200aa) or pGEX-2T, were transformed into *Escherichia coli* BL21 cells. Glutathion S-transferase (GST) fusion proteins were produced in the transformed BL21 cells and purified using glutathione sepharose 4B beads (GE healthcare). About 40 µg of purified GST proteins were incubated with 4 mg of HeLa nuclear or cytoplasmic S100 extracts in Buffer D (10 mM Hepes-KOH, pH 7.9, 3 mM MgOAc, 10% glycerol, 0.1 mM EDTA, 0.1 mM PMSF and 0.5 mM DTT) for two hours at 4 °C. Unbound proteins were removed by washing with Buffer D. Beads were boiled for 5 min in SDS-PAGE sample buffer and eluted proteins were analyzed in 10 % SDS-PAGE. Gels were stained with Coomassie blue. Proteins specifically interacting with GST-RHAU N-ter were identified by LC-MSMS.

SECTION 3 - RESULTS

3.01. Possible roles of RHAU in the nucleus.

3.01.01. RHAU is mainly localized in the nucleus and tightly associated with RNA.

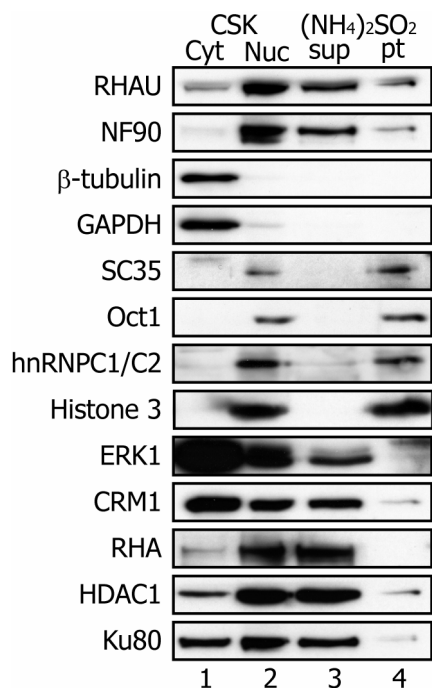


Figure 3. Cell fractionation using HeLa cells. Total HeLa cells were fractionated using CSK buffer to separate cytoplasmic (Cyt) and nuclear (Nuc) fractions. Nuclear fractions were further fractionated using an ammonium sulfate buffer to separate nuclear soluble (sup) and insoluble (pt) fractions. Each fraction corresponding to the equivalent cell numbers was analyzed by Western blotting using the antibodies indicated.

Previous studies have shown that exogenously expressed HA-RHAU is predominantly localized in the nucleus in HeLa cells (Tran et al. 2004). To investigate endogenous RHAU distribution, we performed cellular fractionation followed by Western blotting. Cells were first treated with detergent (0.5% Triton-X100) in CSK buffer, which permeabilized the plasma membranes. This buffer extracts cytoplasmic proteins from the cell and the supernatant, thus, contains cytoplasmic proteins such as β -tubulin and GAPDH, and the pellet contains nuclear proteins such as hnRNP1/C2 and histone 3, as well as the transcription factor Oct1 and the splicing factor SC35 (Figure 3, lanes 1 and 2). RHAU was found in both the cytoplasmic and nuclear fractions, being more abundant in the latter. Nuclear

fractions thus obtained were further fractionated using 0.25 M ammonium sulfate buffer to extract soluble proteins such as protein kinase ERK1 and nuclear export factor CRM1, leaving insoluble fractions that have strong interactions with nuclear structures, such as chromatin and ribonuclear proteins (RNPs) represented by histone3, hnRNP1/C2, Oct1, and SC35 (Fey et al. 1986). A small but significant portion of endogenous RHAU was present in the nuclear insoluble fractions, with a distribution pattern similar to NF90, a dsRNA and ARE-binding protein. In contrast, large amounts of nuclear histone deacetylase 1 (HDAC1), telomere-binding protein Ku80, and RHA were extracted with ammonium sulfate buffer (compare lanes 2, 3, and 4 in Figure 3). These results indicate that RHAU is a nuclear protein associated with nuclear structure with a similar or stronger affinity than other RNA-/ DNA-binding proteins.

In parallel, a similar analysis was done using the exogenously expressed EGFP-tagged RHAU. While mouse monoclonal and rabbit polyclonal antibodies against RHAU used in this work efficiently detected RHAU protein by Western blotting, they were unsuitable for detecting endogenous RHAU by immunocytochemistry. Therefore, to further investigate the cellular localization of RHAU, EGFP-tagged RHAU expression vectors were prepared and transiently transfected into HeLa cells. If EGFP-RHAU is tightly associated with nuclear structures, it should remain there even when nuclear membrane is permeabilized. To see if this was the case, cells were treated with 0.1% Triton X-100, washed out, then fixed with paraformaldehyde. Soluble nuclear protein such as EGFP was completely released from the nucleus in this condition (Figure 4B, EGFP, compare lanes fix and Triton). In contrast, significant level of fluorescence was still detected in the cells transfected with EGFP-RHAU albeit that the intensity was decreased (Figure 4A). In greater than 200 cells counted, 37.2 % of transfected cells showed detectable EGFP-signal after the Triton-permeabilization (17.7% cells out of 47.6% transfected cells). Further DNase treatment to the permeabilized cells did not change proportion of EGFP-RHAU-positive cells, whereas almost no cells showed the signal after the RNase treatment (Figure 4, compare Triton-permeabilized and DNase, RNase). The results of biochemical fractionation and the *in situ* extraction suggested that RHAU tightly associated with higher nuclear structures via RNA.

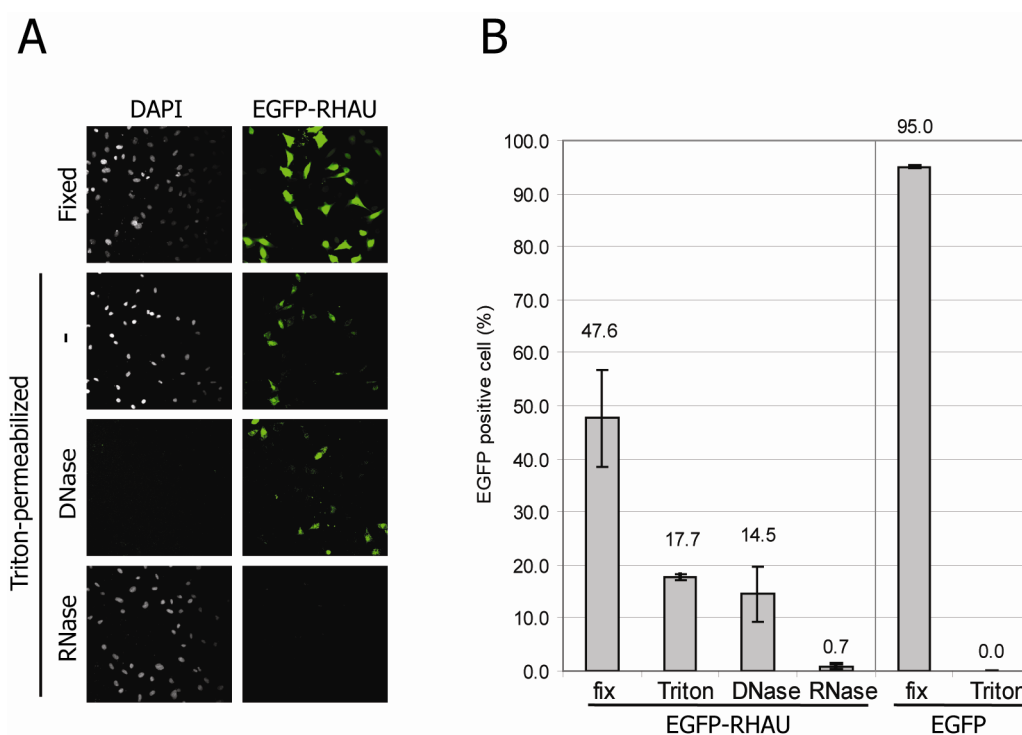


Figure 4. *In situ* extraction of EGFP-RHAU. (A) EGFP fluorescence images of cells transfected with EGFP-RHAU. Cells were transiently transfected with EGFP-RHAU and either fixed or permeabilized with 0.1 % Triton-X100. The permeabilized cells were further treated with DNase I (100 U/ml) with RNasin or mixture of RNase A (20 μ g/ml) and RNase T1 (100 U/ml), then fixed. (B) Cells showing significant EGFP-fluorescence were counted in greater than 200 cells in images taken from microscope. Average of two independent experiments is shown. Error bar, SEM.

3.01.02. Nuclear speckles and nucleolar cap-localization induced by transcriptional arrest.

The distribution of nuclear RHAU was further examined using EGFP-RHAU constructs. To avoid an artifact caused by terminal attachment of EGFP to RHAU, EGFP was tagged at either the N-terminal (EGFP-RHAU) or the C-terminal (RHAU-EGFP). Although the expression levels of differently tagged RHAU was about threefold different (Western blotting, Figure 5A, compare lanes 3 and 4), both proteins showed very similar distribution patterns. They were localized mainly in the nucleus excluding the nucleoli, with much lower expression in the cytoplasm. We found that RHAU was concentrated in nuclear speckles enriched with splicing factors and mRNAs (marked with splicing factor SC35) (Lamond and Spector 2003; Hall et al. 2006) but less abundant in heterochromatin (marked with H3-K9 trimethylation), supporting the idea that RHAU is closely associated with RNA but not compacted DNA (Figure 5B-a, b).

Therefore, we have examined whether RNA synthesis is linked to the specific nuclear localization of RHAU. Cells were treated with ActD, which intercalates into DNA and inhibits transcription by all types of RNA polymerase. In this condition, RHAU was no longer enriched in the nuclear speckles but formed prominent structures around the nucleoli. This structure was located close to but completely excluded from heterochromatin, as visualized by the antibody against H3-K9 trimethylation (Figure 5B-c, d). Time-course analysis showed that RHAU-containing cap-like structures became visible 1 h after the addition of ActD and enlarged subsequently. After 5 h, they completely occupied the nucleoli, but by then most cells were undergoing apoptosis (Figure 6). Treatment with DRB, an RNA polymerase II-specific inhibitor, exhibited a similar but milder effect on RHAU localization than ActD treatment; less RHAU was found around nucleoli and a significant amount was still concentrated in nuclear speckles (see Figure 7).

An ATPase-deficient mutant was also examined to see whether RHAU ATPase activity influences its cellular localization. EGFP-RHAU-E335A has an amino acid replacement at motif II of the conserved helicase domain from DEIH to DAIH and this mutation has been shown to cause a complete loss of RHAU ATPase activity *in vitro* (Tran et al. 2004). The ATPase-deficient mutant was localized only in the cytoplasm and its distribution was not altered by inhibition of transcription, suggesting that ATPase activity is necessary for the nuclear localization of RHAU (Figure 5C). As a control, EGFP alone was expressed and was seen to be distributed uniformly in the nucleoplasm under normal conditions. EGFP did not form cap-like structures upon treatment with any transcriptional inhibitors (Figure 5D).

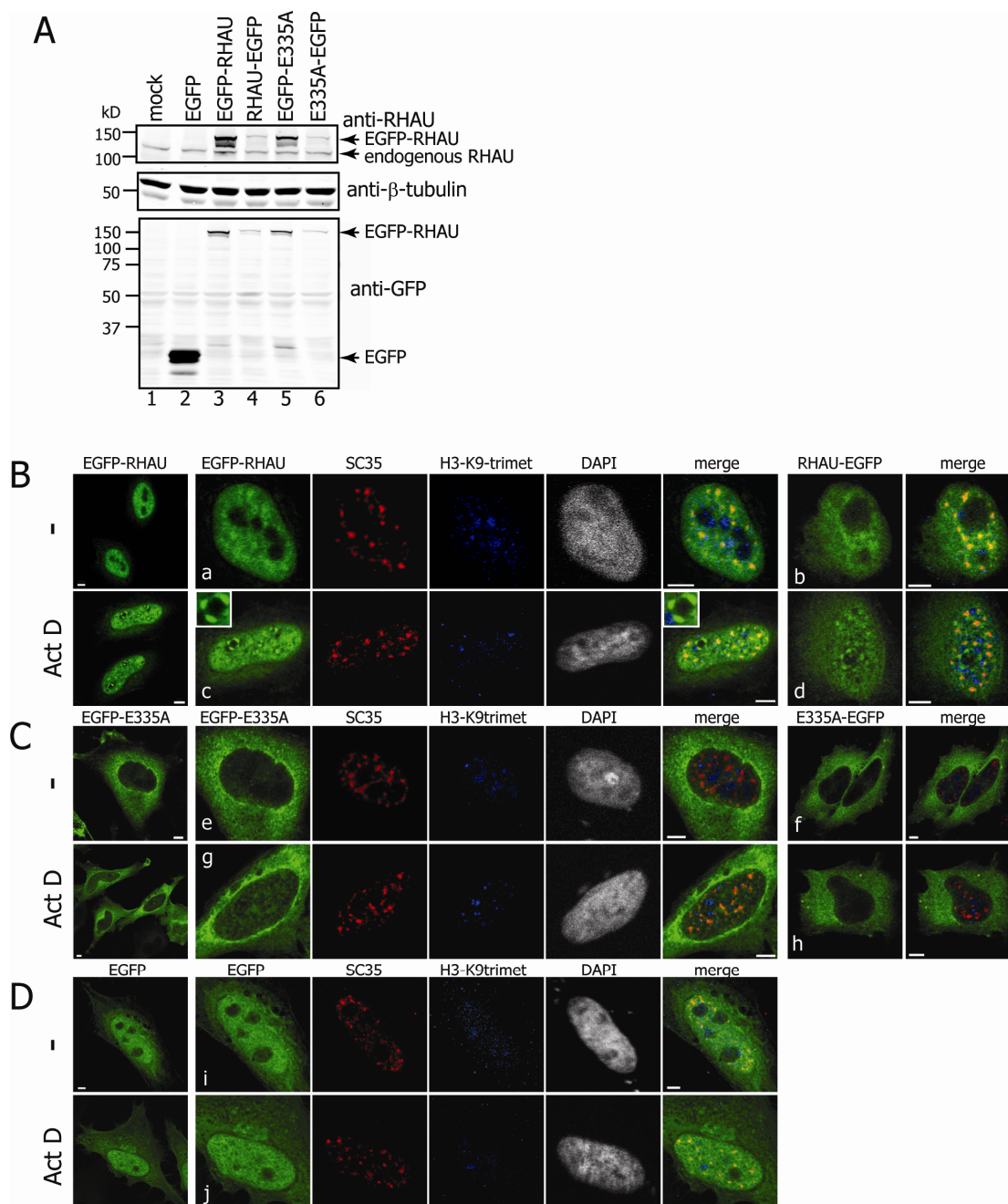


Figure 5. RHAU is enriched in the nucleus. (A) Western blotting showing EGFP-tagged RHAU. HeLa cells were transfected with EGFP-tagged RHAU (EGFP-RHAU or RHAU-EGFP), ATPase-deficient RHAU mutants (EGFP-E335A or E335A-EGFP) or EGFP. Total cell lysates were analyzed by Western blotting using the antibodies indicated. (B) Immunofluorescence images of EGFP-expressing cells. HeLa cells were transiently transfected with vectors expressing EGFP-tagged proteins. For ActD treatment, the drug (5 μg/ml) was added to the culture 2 h prior to fixation. Cells were multiply stained with anti-SC35 antibody (nuclear speckles; in red), anti-H3 K9-trimethylation antibody (heterochromatin; in blue), and DAPI (DNA; in white). The merging of three colors for EGFP, SC35, and H3-K9triMet is shown. For cells transfected with RHAU-EGFP and E335A-EGFP, only merged images are shown. Scale bar: 5 μm.

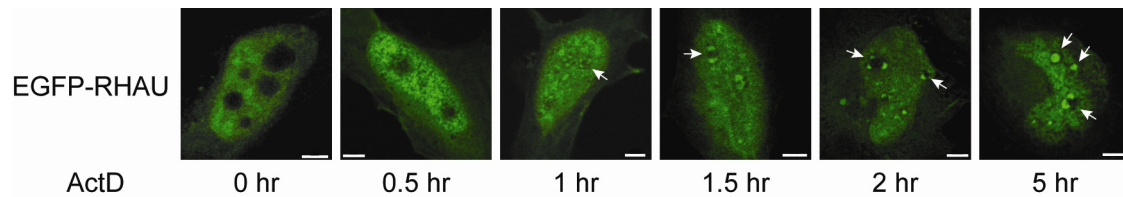


Figure 6. Nucleolar cap formation of EGFP-RHAU upon ActD treatment. HeLa cells were transiently transfected with EGFP-RHAU and treated with ActD (5 $\mu\text{g}/\text{ml}$) for the indicated time (0 - 5hr) prior to fixation. Nucleolar caps are indicated by arrow heads. Scale bar: 5 μm .

3.01.03 Transcription-dependent localization of RHAU in the nucleolar caps with DEAD-box helicases p68 and p72.

The ActD-induced structures of RHAU around nucleoli resembled previously reported nucleolar caps around nucleoli in mammalian cells upon transcriptional arrest (Shav-Tal et al. 2005). In this report, DEAD-box RNA helicase p68 was found to be localized in nucleolar caps when cells were treated with ActD. To test whether RHAU is co-localized with p68 and its dimer partner, p72, in the nucleolar caps, HA-tagged p68 or p72 were co-transfected with EGFP-RHAU and cells were stained with anti-HA and anti-SC35 antibodies. Under normal culture conditions, HA-p68 and HA-p72 were both concentrated in nuclear speckles as reported previously (Saitoh et al. 2004; Erukashvily et al. 2005), where EGFP-RHAU was also present (Figure 7 a, d: Co-localization of the three proteins appears as white areas in merged pictures resulting from a mix of red, blue, and green.). In transcription-arrested cells, p68 formed nucleolar caps and this was more marked with DRB than ActD (Figure 7 b, c). In contrast, p72 was more sensitive to ActD, forming a ring structure around nucleoli. In this situation of p72 overexpression, the localization of RHAU changed to a ring structure within p72 and no nucleoplasmic distribution was observed (Figure 7 e, f). Since single transfection of EGFP-RHAU or co-transfection with HA-p68 did not show such a remarkable structure, it seems that p72 recruited RHAU into such a structure around the nucleoli. In either case, RHAU was co-localized with p68 and p72 at the periphery of nucleolar caps, indicating that the structure formed by EGFP-RHAU was a part of the previously characterized nucleolar caps.

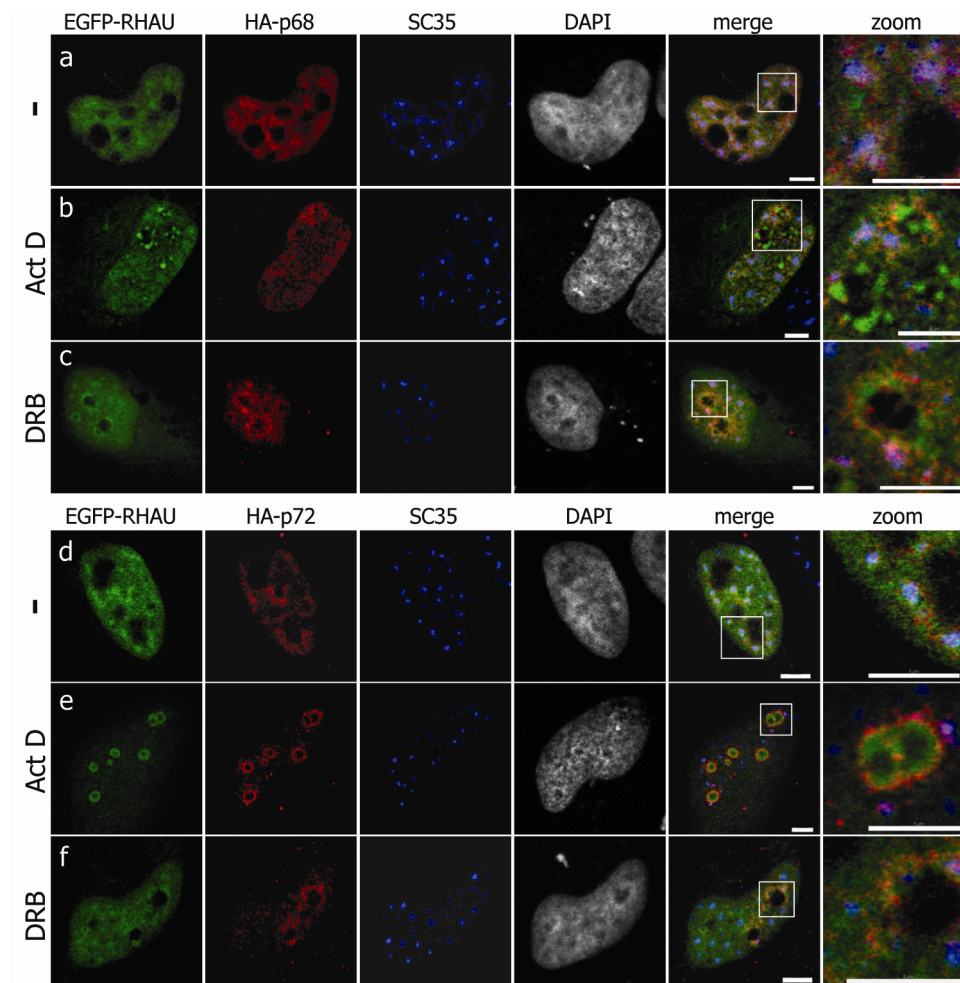


Figure 7. RHAU is co-localized with p68 and p72 in nucleolar caps upon transcriptional inhibition. (A) Immunofluorescence images of EGFP-expressing cells. ActD (5 µg/ml) or DRB (25 µg/ml) was added to the culture 2 h prior to fixation. Cells were stained with anti-HA antibody (in red), anti-SC35 antibody (in blue), and DAPI (in white). The merging of three colors for EGFP, HA, and SC35 is shown. Scale bar: 5 µm.

3.01.04 Interaction of RHAU with regulators of transcription.

To see whether RHAU interacts with p68 and p72, we transiently transfected Flag-RHAU together with HA-p68 or HA-p72 into HeLa cells and performed immunoprecipitation using anti-Flag antibody. HA-p68 and HA-p72 were co-precipitated with Flag-RHAU, indicating that RHAU interacts with p68 and p72 in cells (Figure 8A). Since p68 and p72 have been characterized as regulators of transcription, interaction between RHAU and these proteins suggest possible involvement of RHAU in transcriptional regulation. To see whether RHAU interacts with other known transcription regulators, the immunoprecipitation was performed with HDAC1 and 3. Histone deacetylases (HDACs) are general

transcription repressors and it has been reported that p68 and p72 associates with HDAC1, showing that these helicases repress transcription in some contexts (Wilson et al. 2004). We could detect the co-precipitation of RHAU when HDAC1 and HDAC3 were immunoprecipitated, suggesting that RHAU could be a part of transcriptional repression complex (Figure 8B). Since the addition of RNases into lysates abolished any of these interaction, RHAU likely associates with them via RNA.

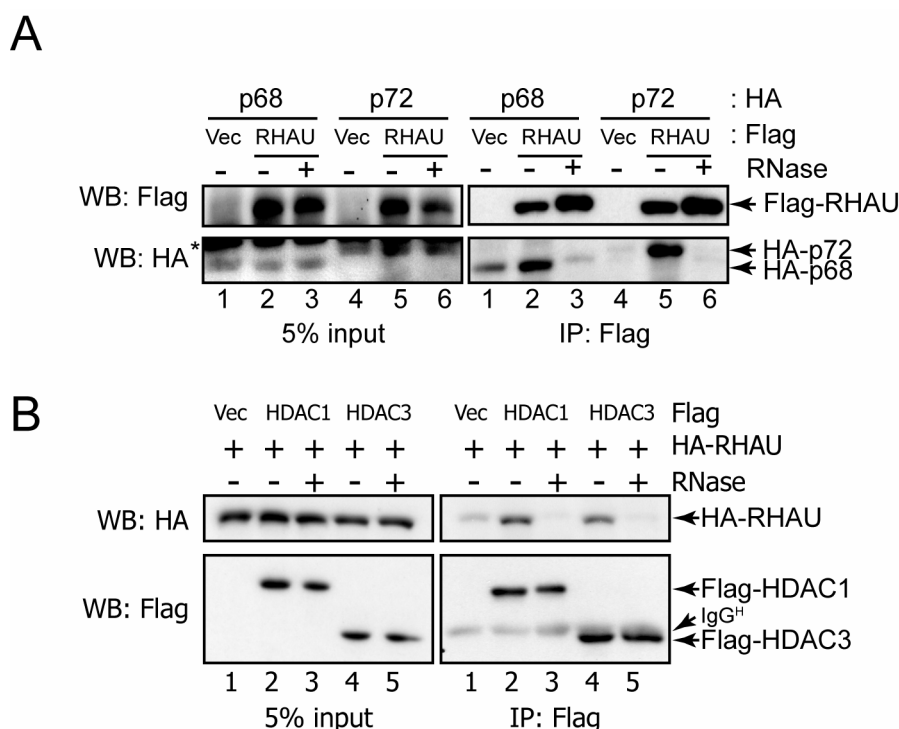


Figure 8. Interactions between RHAU and p68, p72, HDACs. (A) pcDNA3-Flag (Vec) or Flag-RHAU was co-transfected with either HA-p68 or HA-p72 into HeLa cells. Flag-RHAU was immunoprecipitated with anti-Flag and co-precipitated HA-p68 or HA-p72 proteins were visualized by Western blottings using anti-HA antibody. *, non-specific band. (B) pcDNA3-Flag (Vec), Flag-HDAC1, or Flag-HDAC3 was co-transfected with HA-RHAU into HeLa cells. Flag-HDAC was immunoprecipitated with anti-Flag and co-precipitated HA-RHAU was visualized by Western blottings using anti-HA antibody. 5% of input is also shown.

3.01.05 N-terminal domain of RHAU is responsible for the nuclear and nucleolar caps localization.

RHAU consists of a central helicase core region and N-terminal and C-terminal extended domains (Figure 9A). The beginning of the N-terminus contains a glycine-rich motif and the end of the helicase core region possesses a putative nuclear export signal that is enriched with leucine. We made truncated mutants of RHAU in each domain to characterize essential domains of RHAU for the nuclear location. Deletion mutants of RHAU tagged with EGFP showed that the

200 N-terminal amino acids were required for the nuclear localization because the deletion of those residues showed complete cytoplasmic localization of RHAU (Figure 9B-d, e, f). In contrast, the N-terminal domain was sufficient for localization in the nucleus, and it was concentrated in the nuclear speckles (Figure 9B-a). Upon inhibition of transcription by ActD, all truncated mutants which would normally go to the nucleus showed nucleolar caps (Figure 9B-g, h, i), indicating that import to the nucleus is sufficient for the formation of these caps.

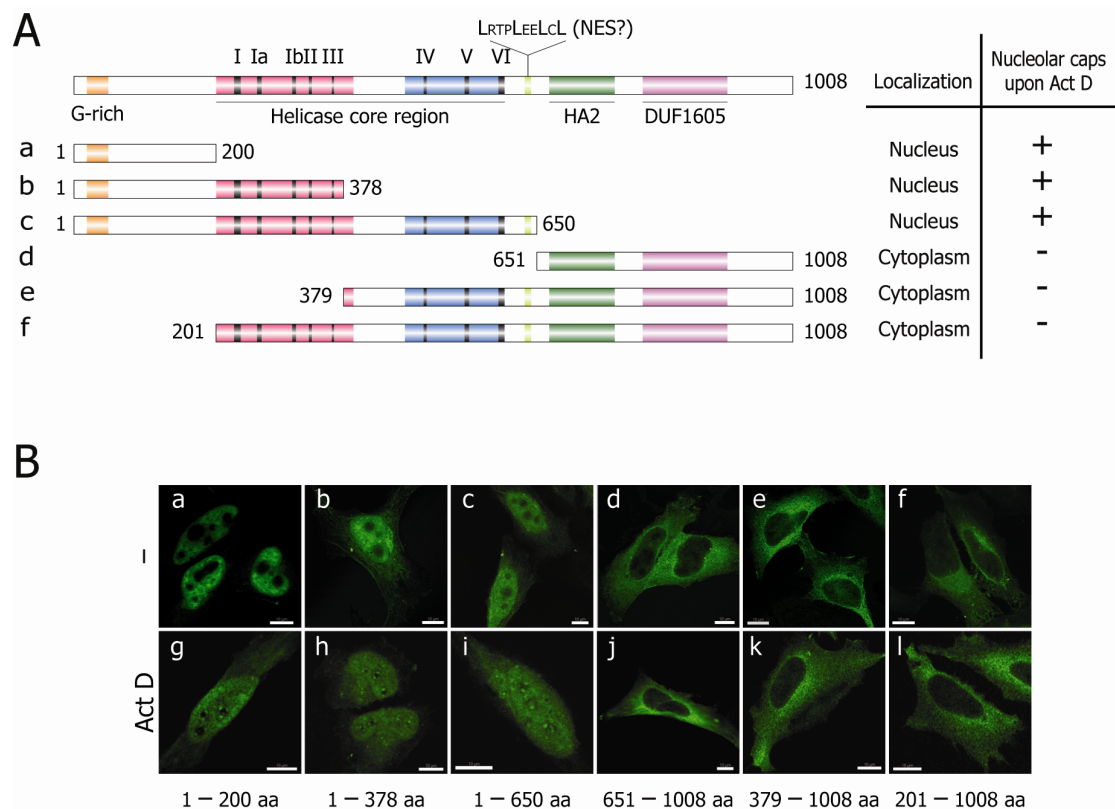


Figure 9. N-terminal domain of RHAU is responsible for the nuclear and nucleolar caps localization.

Differently truncated forms of RHAU were fused with EGFP at their N-termini. Each construct was transfected into HeLa cells. ActD (5 $\mu\text{g}/\text{ml}$) was added 2 h prior to fixation. EGFP-fluorescence was captured and is shown in white. (A) A schematic representation of various EGFP-RHAU constructs with the summary of results of their cellular localization. (B) Fluorescent images of cells transfected with the above-shown EGFP-RHAU constructs before and after ActD treatment. Scale bar: 5 μm .

3.02. Microarray analysis using RHAU knockdown cells.

The intracellular localization studies have shown that: [1] RHAU is much more abundant in the nucleus than in cytoplasm; [2] in the nucleus, RHAU is concentrated in RNA-rich nuclear speckles; [3] RNA-synthesis influences the distribution pattern of RHAU in the nucleus. These results prompted us to consider the possibility that RHAU influences some RNA metabolic pathways in the nucleus and, therefore, it may affect global gene expression either directly or indirectly. To test this hypothesis and to identify the possible genes affected, we performed Affymetrix microarray analysis using RHAU-depleted cells.

3.02.01. Inducible RHAU-knockdown HeLa cell-line.

To establish HeLa-T-REx-derived cell lines in which RHAU-specific hairpin RNA (shRNA) could be induced by doxycycline (van de Wetering et al. 2003), plasmids expressing shRNAs to target RHAU (shRHAU) and luciferase (shLuc) as a control under the control of the Tet repressor were stably transfected and zeocin-resistant clones were picked. To reduce clone-specific effects, we pooled four independent clones from each shRNA-transfection. Such a pool was then treated as one experimental replicate in the analysis. Western blots showed that RHAU was reduced in all the clones down to 30% of that found in the controls after 6 days of doxycycline treatment (Figure 10A). In time-course experiments, maximal downregulation was observed after a 6-day doxycycline treatment and, therefore, a 6-day treatment was used in all subsequent experiments. Expression of shLuc in control cells was confirmed from the downregulation of luciferase activity by transient transfection assays (Figure 10B).

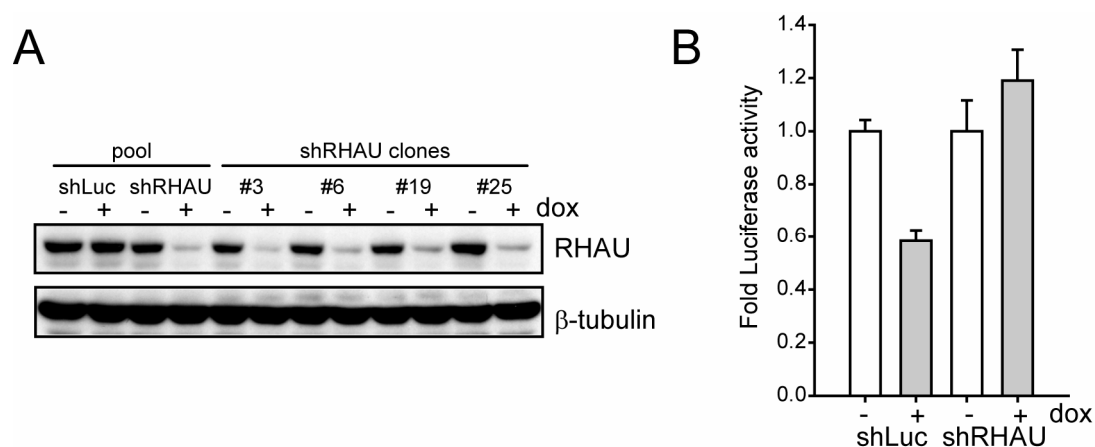


Figure 10. RHAU knockdown in HeLa cells by RHAU-specific shRNA expression. (A) Four independent clones derived from HeLa-shLuc or HeLa-shRHAU cells were pooled and treated or not treated with doxycycline (1 μ g/ml) to induce shRNA for 6 days. RHAU knockdown in pooled and four individual HeLa-shRHAU clones was assessed by Western blotting using anti-RHAU antibody. Pool, pool of four individual clones; shRHAU clones, individual clones (B) HeLa-shLuc or HeLa-shRHAU cells were transiently transfected with firefly luciferase-expressing vector (pGL2-promoter) with or without co-treatment with doxycycline (1 μ g/ml). Cells were collected 48 h after transfection. Firefly luciferase activity was normalized by renilla luciferase that was co-transfected as an internal control. Error bar, SEM of three replicates.

3.02.02. DNA microarray to measure steady-state mRNA and mRNA half-life.

RHAU was originally characterized as a destabilizer of uPA mRNA. As the steady-state level of mRNA reflects both its *de novo* synthesis and its degradation, we examined both steady-state levels of mRNAs and their half-lives by the microarray using RHAU knockdown cell lines. After complete knockdown of RHAU, cellular transcription was inhibited by ActD and total RNAs were collected every 30 min up to 120 min to determine the half-lives (see experimental procedure in Figure 11). The data from our microarrays showed that the expression of RHAU itself was successfully reduced to about 20% in doxycycline-treated (dox+) cells (Figure 11A). Acceleration of RHAU mRNA decay by shRNA-mediated mRNA degradation was also confirmed with a significant change in its half-life (Figure 11B). Thus, it was shown that microarray experiments could successfully detect changes in mRNA stability.

Materials

- | HeLa-shLuc dox-
- | HeLa-shLuc dox+
- | HeLa-shRHAU dox-
- | HeLa-shRHAU dox+

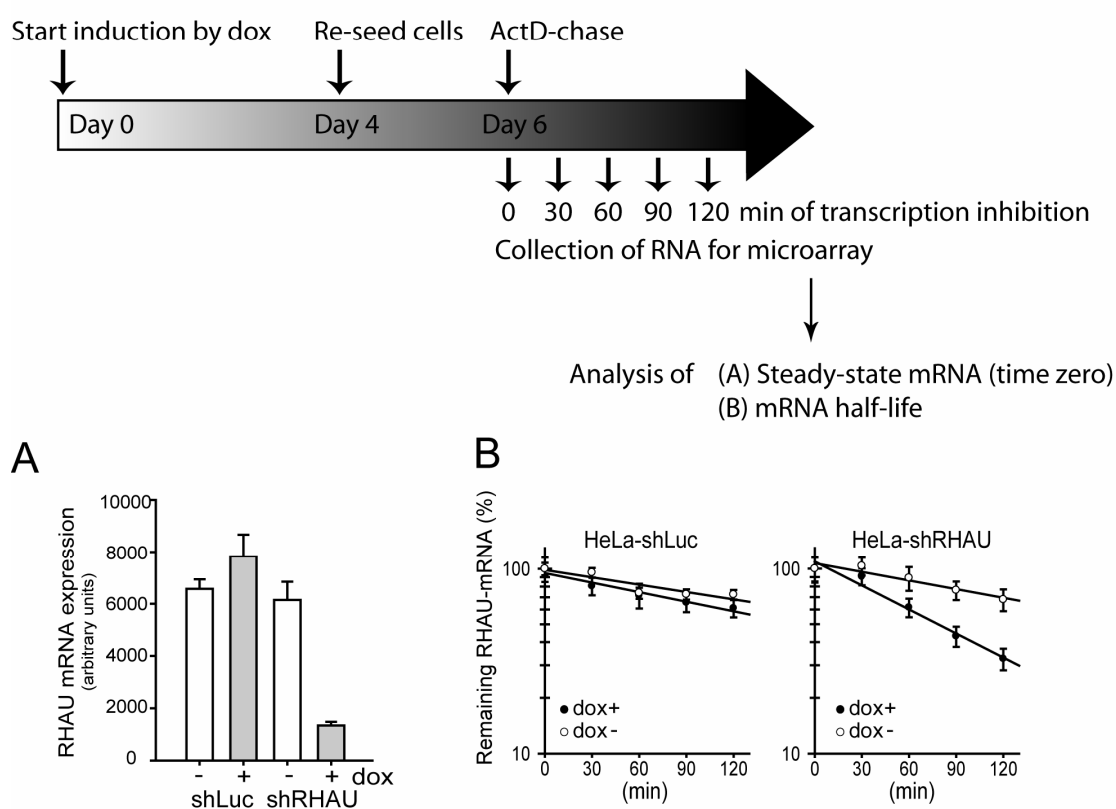


Figure 11. Microarray to measure both steady-state mRNA level and mRNA half-life. The scheme of microarray experiment is described. (A, B) Expression data of RHAU (Affymetrix name 223138_s_at) obtained from microarray analysis was plotted. Error bar, SEM of three or two replicates from microarray. (A) Steady-state mRNA level. (B) Decay of RHAU mRNA, which was accelerated by shRNA-mediated mRNA degradation.

Half-lives and the corresponding standard errors of every mRNA was estimated by fitting the time-course expression data of five time points to an exponential decay function using the nonlinear least squares method (See detail analysis in Material and Methods). We could confirm that ActD suppressed general transcription in our experiment since global decrease of mRNA levels in the ActD chase was detected by the microarray (Figure 12).

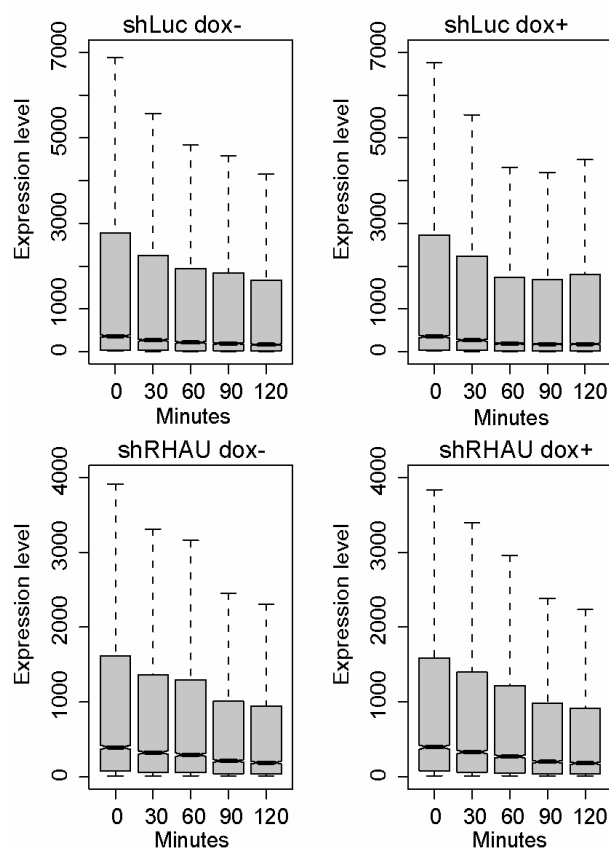


Figure 12. Box plots of mRNA levels at five time points. For each time point, a box plot of the observed expression levels is shown. The black line indicates the median, lower and upper box limits the first and third quartiles, respectively, and the whiskers show the total spread. Values further away than 1.5 times the interquartile range from the box were omitted as outliers. The difference of medians is significantly different at $P \leq 0.05$ if the notches around the medians of two box plots do not overlap.

3.02.03. Differences in steady-state levels after RHAU knockdown are not correlated to their half-lives.

To analyze microarray data, we first picked mRNAs showing significant differences in steady-state levels (time 0 of ActD treatment) in HeLa-shRHAU cells between doxycycline non-treated (dox⁻) and treated (dox⁺) conditions. As summarized in Table 1, 125 mRNAs showed more than a two-fold up- or down-regulation in RHAU-knockdown cells (dox⁺) compared with dox⁻ cells. In contrast, only two mRNAs showed a twofold difference in expression after doxycycline treatment in control HeLa-shLuc cells, indicating little effect of doxycycline on global gene expression (See gene lists in Appendix II).

TABLE 1. Comparison of probe sets with significantly altered steady-state levels in HeLa-shRHAU cells and other specific probe sets

		^A Steady-state	^B ARE	^C G4	^D mRNA half-life	
					decrease	increase
>1.5 fold	up	428	***109	n.s 142	***73	n.s 0
	down	474	**52	**191	n.s 6	**17
> two-folds	up	58	**13	n.s 22	**13	n.s 0
	down	67	n.s 5	n.s 28	n.s 2	n.s 2

Number of common probe sets between the sets that significantly increase or decrease their expression values in HeLa-shRHAU cells between dox⁻ and dox⁺ (defined by $P < 0.05$ and a minimal fold change, see Materials and Methods) and sets defined by additional characteristics are shown. The significance of the overlap is indicated as n.s.; not significant, *; $P < 0.01$, **; $P < 0.001$, ***; $P < 2e-16$, calculated using the hypergeometric distribution, with n corresponding to the total number of genes in the column-set and N indicating the total number of genes analyzed in both column- and row-sets. (A) Fold difference of total mRNA amount in HeLa-shRHAU cells between dox⁻ and dox⁺ ($P < 0.05$). $N=30,599$. Up, up-regulated in dox⁺; down, down-regulated in dox⁺. (B) Number of ARE-containing probe sets found in ARED (<http://rc.kfshrc.edu.sa/ARED/>). $N=30,599$, $n=1,530$; n was estimated under the assumption that the fraction of ARE-containing genes in the published screen (5%, (Bakheet et al. 2006)) is the same as the fraction of ARE-containing genes of all genes represented on the Affymetrix microarray. (C) Number of putative G4-sequence containing probe sets in the promoters (in 1 kb upstream from transcription starting sites) found by quadparser (Huppert and Balasubramanian 2005) with standard parameters. $N=30,599$, $n=13,066$; n was estimated under the assumption that the fraction of genes with G4-containing promoters in the published screen (42.7%, (Huppert and Balasubramanian 2005)) is the same as the fraction of genes with G4-containing promoters of all genes represented on the Affymetrix microarray. (D) Number of probe sets showing different half-lives ($P < 0.05$) between dox⁻ and dox⁺ samples. Decrease or Increase, decreased or increased half-life in dox⁺. $N=6,973$, $n^{decrease}=203$, $n^{increase}=99$.

Correlation between the steady-state differences and their half-lives were then examined. Based on the half-life profiles, up- or down-regulated mRNAs in RHAU-knockdown were assigned to three groups (Figure 13). The major group (Group 1) includes those mRNAs whose steady-state levels were altered without changes in half-life, as represented by DAPK1 and CLUAP1 mRNAs (Figure 14). Group 2 shows opposing correlation between steady-state level and mRNA decay, namely up-regulated steady-state levels with decreased half-lives or down-regulated steady-state levels with increased half-life (represented by SPRED1, Figure 14). Group 3 contains mRNAs whose steady-state levels were correlated with the mRNA decay rate as represented by CDKN1C, which showed decreased steady-state level and decreased mRNA half-life (Figure 14). Except for Group 3, involvement of the mRNA decay mechanism is unlikely, since changes in mRNA half-lives did not reflect steady-state mRNA levels. This is true for 99% of mRNAs whose steady state levels were affected by RHAU knockdown. These results suggest that the influence of RHAU on global gene expression is in general not through mRNA decay but rather through steps in the nucleus including transcription.

Among the mRNAs whose stability was up-regulated by RHAU knockdown, we collected a significant number of ARE-containing mRNAs that were found in the ARE-database, ARED (Bakheet et al. 2006) (Table 1B, see also Appendix II). However, the existence of ARE was not necessarily correlated to the misregulation of their half-lives, since the half-lives of the majority of ARE-containing mRNAs did not change in RHAU knockdown (5 out of 18 mRNAs showed changes of half-lives). This indicated that the effect of RHAU on steady-state mRNA level was not restricted to the ARE-mediated mRNA decay. We also analyzed whether those RHAU-regulated genes contained one or more G4 DNA structures in their promoters. According to bioinformatics analysis, about 40% of human promoters contain putative G4 sequences (Huppert and Balasubramanian 2005). In the down-regulated genes in RHAU knockdown, but not in the up-regulated mRNAs, we saw a slight enrichment of G4 sequences (53.5%) in their promoters, which was statistically significant ($P < 0.001$) (Table 1C). Thus, they are candidate target genes of the G4-resolvase RHAU, as RHAU resolves G4 DNA in their promoters, which activates transcription. However, the effect of RHAU knockdown on the abundance of G4 DNA in promoters was mild, and in fact no significant enrichment of G4 sequences was seen in 2-fold down-regulated mRNAs, suggesting that there could be another mechanism affecting mRNA steady-state levels in RHAU knockdown cells.

	Steady-state mRNA vs mRNA decay	Influence of mRNA decay rate on steady-state level	Change in transcription	Steady-state mRNA	t _{1/2}
Group 1	No change in mRNA decay	No	Yes	up or down	no change
Group 2	Opposite correlation	No	Yes	up down	decrease increase
Group 3	Correlation	Yes	Yes or No	down	decrease

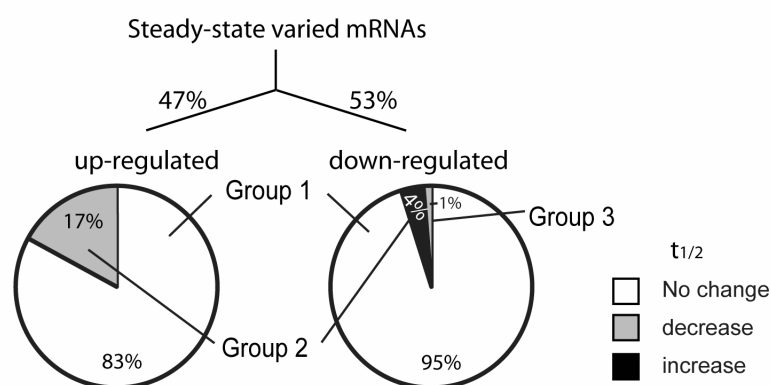


Figure 13. The relationship of steady-state difference and mRNA half-lives in RHAU-knock down cells. Three groups of steady-state different mRNAs and percentage of those mRNAs in up- or down- regulation is shown.

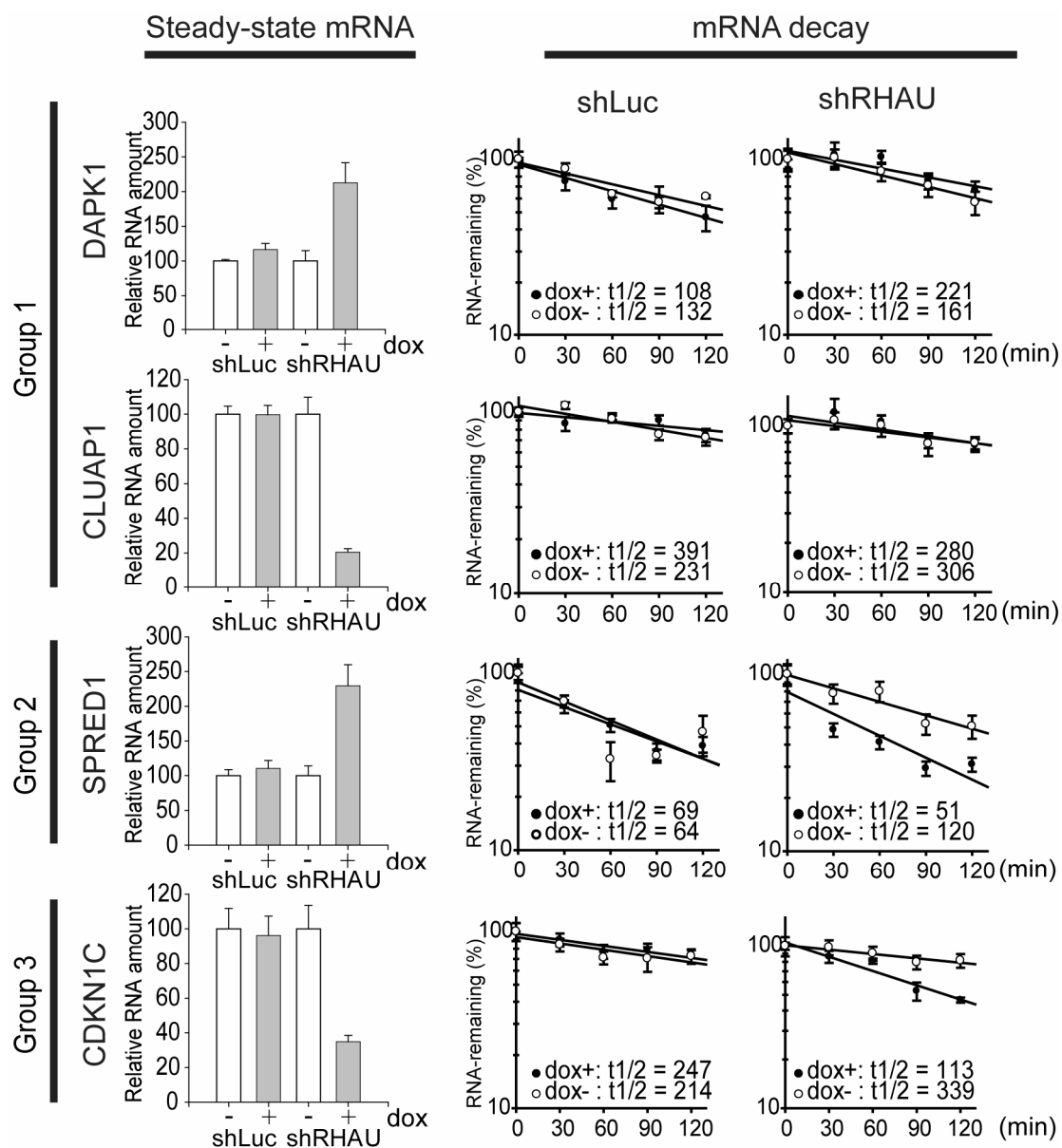


Figure 14. mRNAs regulated by RHAU. Expression values were obtained from microarray analysis. mRNAs whose expression levels were significantly affected after RHAU knockdown induced by doxycycline were selected and are represented here by six different mRNAs: DAPK1 (Affymetrix probe name: 203139_at), SPRED1 (226837_at), CLUAP1 (204576_s_at), CDKN1C (213348_at). The left panel shows steady-state levels of mRNAs normalized over the sample of dox⁻ in cells. The right panel shows the mRNA decay curve. mRNA expression was normalized over time 0 as 100%.

3.02.04. Influence of RHAU on mRNA half-life.

In the analysis of the mRNA decay rate, we found 99 mRNAs were significantly stabilized and 200 mRNAs were destabilized in knockdown although, surprisingly, the steady-state levels of the majority of these mRNAs were not significantly affected (Table 2, see also gene lists in Appendix III). The density plot of their half-lives is shown in Figure 15A. The y-axis shows the density of genes in each half-life shown on the x-axis. In contrast to control shLuc cells which showed almost no difference between dox⁻ and dox⁺, shRHAU cells showed a greater difference as overall distribution was shifted towards longer half-life in dox⁺, suggesting that RHAU tends to destabilize mRNAs as it was previously characterized. However, when we looked individual mRNAs, there were significantly more numbers of mRNAs showing decreased half-life in RHAU knockdown, suggesting that RHAU also stabilizes other mRNAs (Table 2). When we look at half-lives of mRNAs showing significant differences on steady-state levels, mRNAs whose steady-state levels were down-regulated did not show any significant half-life differences following RHAU knockdown. In contrast, half-lives in up-regulated mRNAs became significantly shorter after RHAU knockdown (in red, compare dox⁺ and dox⁻). Although this tendency indicates that up-regulation of those mRNAs was attributable not to the increase in their half-lives but rather to enhanced transcription, it suggests that regulation of mRNA stability also exists at the same time, perhaps to compensate the increased transcription rate.

TABLE 2. Number of probe sets with significantly altered mRNA half-life in HeLa-shRHAU or HeLa-shLuc cells treated with dox.

	sig. decrease			sig. increase		
	^A P<0.02	^B P<0.05	^C Steady-state	^A P<0.02	^B P<0.05	^C Steady-state
shRHAU ^a	93	203	15	24	99	2
shLuc ^b	3	18	1	5	28	0

(A and B) Number of probe sets showing statistically significant (P<0.02 or P<0.05) decrease or increase on their half-life between dox⁻ and dox⁺ in HeLa-shRHAU or HeLa-shLuc cells. (C) Number of common probe sets between the sets of half-life differences (p<0.05, the number showed by B) and the sets that show significantly different steady-state level between dox⁻ and dox⁺ (defined by P<0.05 and a minimal two-fold difference). a, n=5613; b, n=17221.

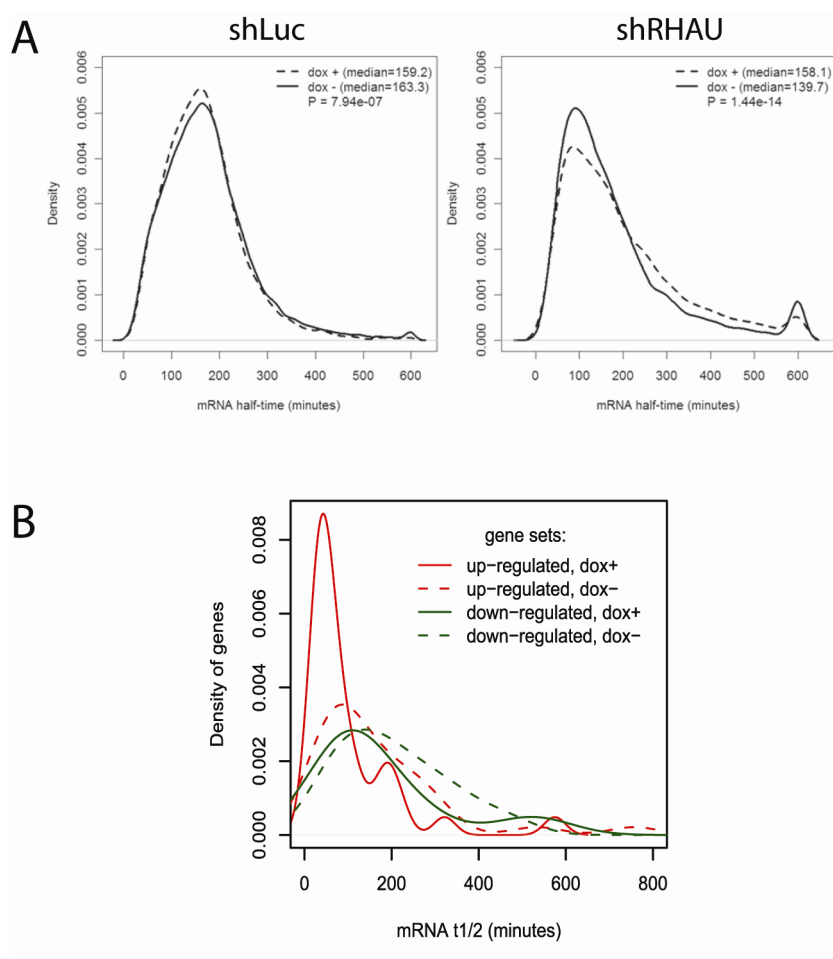


Figure 15. Distribution of RHAU-regulated mRNA half-lives. (A) Density plot of mRNA half-lives in shLuc cells (n=17221) or in shRHAU cells (n=5613). (B) Density plot of mRNA half-lives for gene sets whose steady-state levels were upregulated (red, n=58) or down-regulated (green, n=67) by RHAU knockdown in shRHAU cells.

3.02.05. Change in mRNA level in RHAU-knockdown cells can be rescued by exogenous RHAU expression.

To validate the microarray data, expression of several mRNAs was assessed by real-time PCR. We also examined whether the effect of RHAU knockdown can be reversed by exogenous expression of Flag-tagged RHAU_{sm}. This expression vector harbored a silent mutation at the target site of shRNA (Flag-RHAU_{sm}) allowing it to escape siRNA-mediated downregulation. Western blot analysis showed that exogenous Flag-RHAU_{sm} was expressed at a level similar to endogenous RHAU, indicating that Flag-RHAU_{sm} expression can restore RHAU in doxycycline-treated cells (Figure 16A). As shown in Figure 16B, real-time PCR is in agreement with the microarray analysis (compare dox⁻ and dox⁺; lanes 1 and 2) and expression of Flag-RHAU_{sm} rescued the effect of RHAU knockdown on many target mRNAs (dox⁺ with exogenous expression, in lane 3). Failure to reverse the effect of RHAU knockdown on some mRNAs suggests that these mRNAs are not direct targets of RHAU.

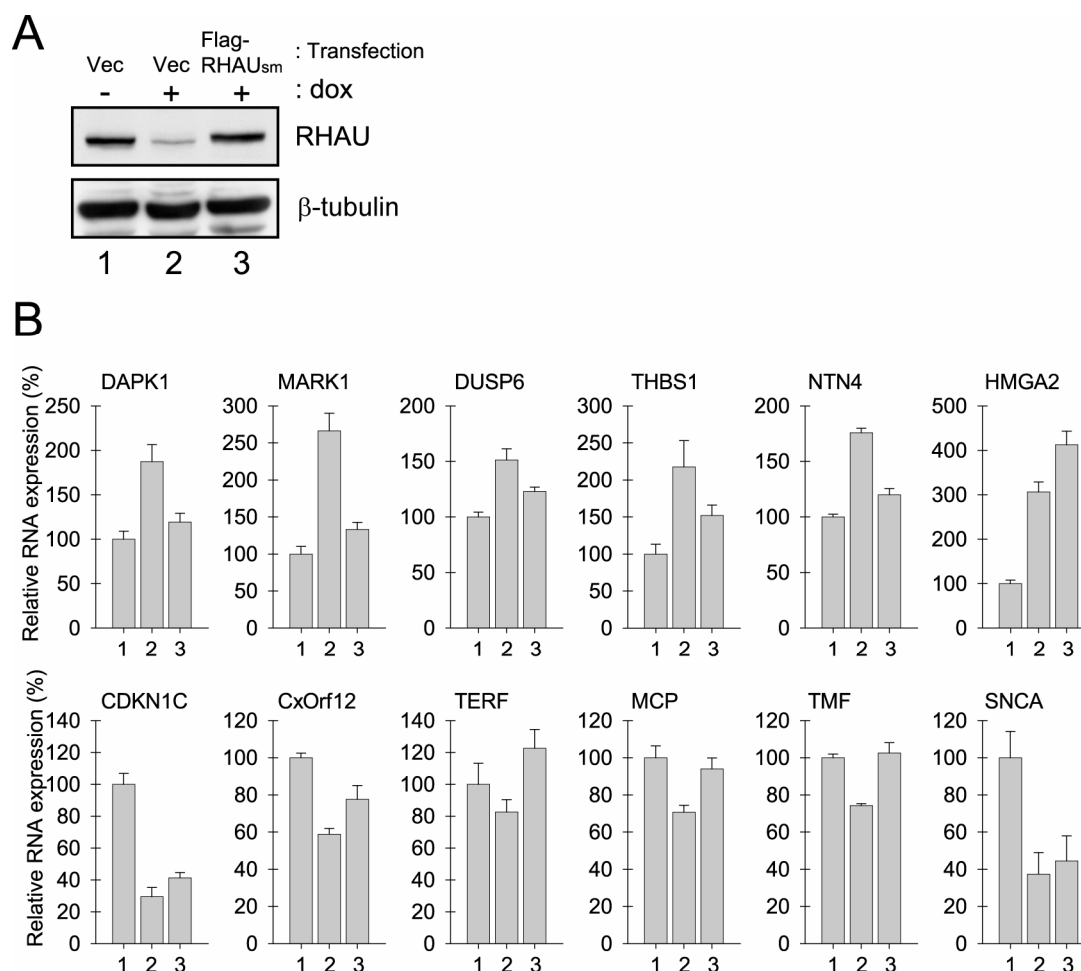


Figure 16. Rescue expression of RHAU by transient transfection of the silent RHAU mutant. The empty vector (pBR-322) or Flag-RHAU_{sm} (silent mutation) was transiently transfected in HeLa-shRHAU cells pre-treated with doxycycline (1 μ g/ml) for 5 days. 24 h after transfection, the cell lysate and total RNA were prepared. (A) Western blot of total cell lysate of transfected cells. Endogenous or exogenous RHAU was detected using the anti-RHAU monoclonal antibody. (B) Real-time PCR using the collected RNAs (1-3) with various primer sets as indicated. 1: dox⁻ with empty vector, 2: dox⁺ with empty vector, 3: dox⁺ with the expression of Flag-RHAU_{sm}.

Finally, transcriptional activity was tested for RHAU candidate targets picked from the microarray. Nuclear run-on assay using isolated nuclei from HeLa-shRHAU cells showed an increase in transcriptional activity of one of the upregulated genes (DAPK1) in RHAU knockdown cells (Figure 17). Taken together, these results indicate that RHAU influences gene expression at different steps including transcription and mRNA decay, depending on the type of the gene.

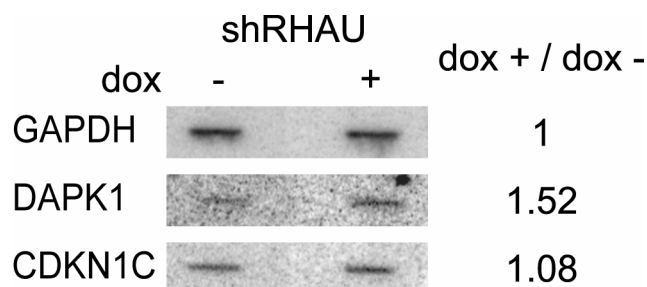


Figure 17. Nuclear run-on assay using HeLa-shRHAU cells. Nuclei were isolated from doxycycline-treated or non-treated cells, and cell-free transcription was performed as described in the Materials and Methods section using radio-labeled UTP. Isolated radio-labeled RNA was hybridized with the indicated DNA probes cross-linked on the nylon membrane. The signal intensity of each probe was normalized by GAPDH.

3.03. RHAU on stress-response.

3.03.01. Influence of RHAU depletion on cell growth.

We have observed mild growth retardation of RHAU knockdown cells in normal culture condition, although they could continue proliferation for more than two weeks (Figure 18A). In contrast to the normal culturing condition, RHAU knockdown caused severer growth defect as a result of decreased viability when cells were serum-starved, despite doxycycline non-treated HeLa-shRHAU cells and control HeLa-shLuc cells (with or without doxycycline pre-treatment) were able to grow in starved medium (Figure 18B, C). To support it, more numbers of apoptotic annexinV-positive cells were detected in RHAU knockdown cells than controls in starvation and when treated with other apoptosis inducer, staurosporine (Figure 18D). Furthermore, Western blottings detecting apoptotic markers such as cleaved-caspase3 and cleaved-PARP showed that RHAU knockdown cells underwent apoptosis significantly faster than control cells in starvation medium (Figure 18E). These observations suggest that RHAU have anti-apoptotic effect in stressed culture conditions.

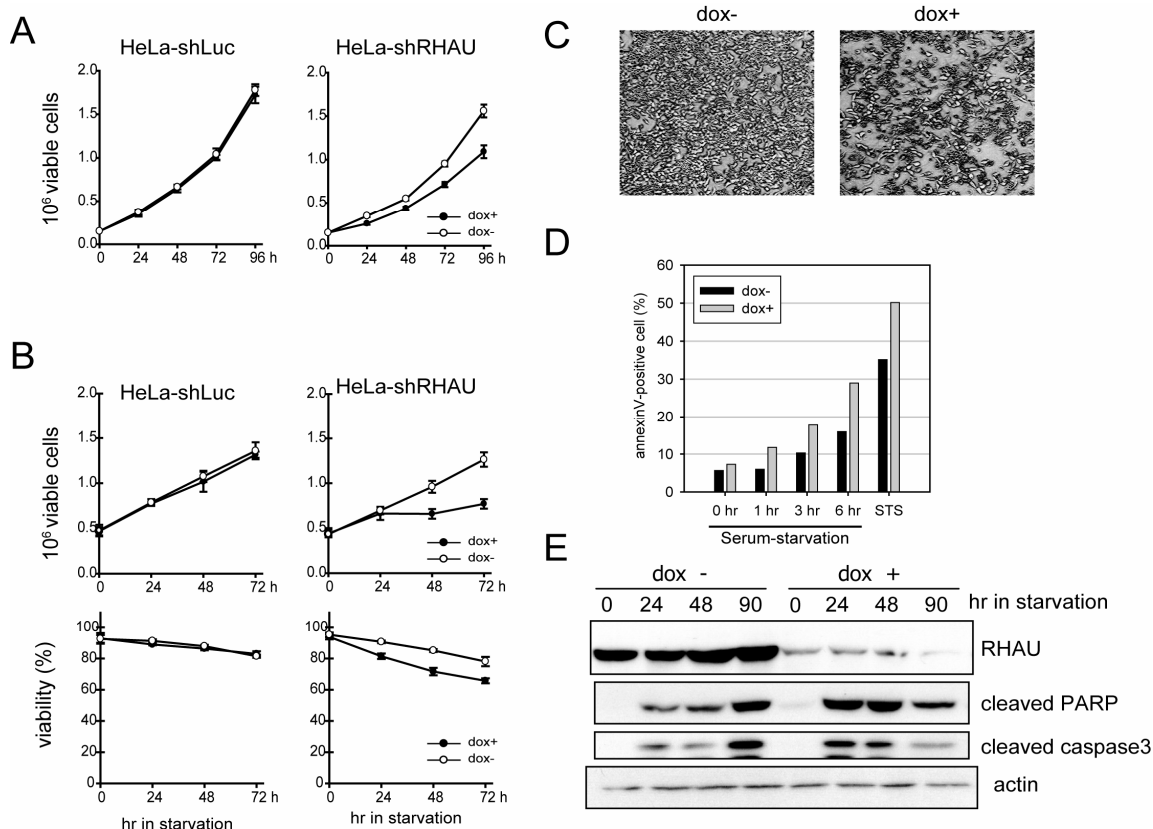


Figure 18. RHAU-knockdown cells undergo apoptosis upon serum-starvation. HeLa-shLuc or HeLa-shRHAU cells were treated or not treated with doxycycline for 5 days. Then cells were seeded in 12-well plates at 1.5×10^5 cells/well (A) or 3.0×10^5 cells/well (B) with or without doxycycline. (A) Viable cells were counted every 24 h by ViCell. (B) Culture medium was replaced with serum-free medium 24 h after cell seeding. Viable cell numbers and viability of cells were counted every 24 h using ViCell. Error bar, SD of four replicates. (C) Phase-contrast images taken for 24hr-starved HeLa-shRHAU cells either cultured with or without doxycycline. (D) HeLa-shRHAU cells cultured with serum-free medium for indicated hours or treated with $1 \mu\text{M}$ staurosporine (STS), protein kinase inhibitor that induces apoptosis, for 4 hours were collected to be analyzed by FACS to detect annexinV-positive cells. (E) HeLa-shRHAU cells were cultured in serum-free medium for indicated hours and collected for Western blotting. Same amount of whole cell lysates were loaded and analyzed using the antibodies indicated.

3.03.02. Microarray analysis using cells under serum-starvation.

We, therefore, attempted to identify target mRNAs of RHAU under stressed condition. HeLa-shRHAU cells were first treated with doxycycline for 5 days and then the medium was replaced with a serum-minus medium for 24 h prior to microarray analysis. In this analysis, we could first pick up as starvation-sensitive genes which showed different expression levels in starved conditions compared to serum-containing conditions irrespective of doxycycline pre-treatment (See gene lists in Appendix IV). The starvation-sensitive genes common in both HeLa-shLuc and HeLa-shRHAU cell line (in dox-) included the MAP-kinase inhibitor DUSP6 (14-fold up-regulation), the apoptosis-inducer TRAIL (13-fold up-regulation), and transgelin (20-fold down-regulation) which is involved in cytoskeleton reorganization; these may collectively contribute to the observed decrease in cell growth. We found that RHAU-regulated mRNAs were significantly enriched with these starvation-sensitive genes (Table 3B), indicating a close relationship between cellular responses induced by RHAU knockdown and serum starvation. In fact, most mRNAs that were up- or down-regulated in RHAU knockdown in the serum-containing condition showed the same changes under the serum-starvation condition (Table 3C). In addition, the effect of RHAU knockdown during serum-starvation was more pronounced for the down-regulated mRNAs, suggesting that RHAU is involved in the activation of gene expression in serum-starved conditions.

TABLE 3. Comparison of probe sets with significantly altered steady-state levels in HeLa-shRHAU cells and starvation-sensitive genes.

		^A Steady-state	^B STV-sensitive	^C RHAU-KD in STV	
				>1.5 fold	> two-folds
>1.5 fold	up	428	***45	***75	***25
	down	474	***63	***346	***129
> two-folds	up	58	**12	***18	***12
	down	67	***18	***55	***47

Number of common probe sets between the sets that significantly increase or decrease their expression values in HeLa-shRHAU cells between dox- and dox+ (defined by $P < 0.05$ and a minimal fold change, see Materials and Methods) and sets defined by additional characteristics are shown. The significance of the overlap is indicated as n.s.; not significant, *, $P < 0.01$, **, $P < 0.001$, ***, $P < 2e-16$, calculated using the hypergeometric distribution, with n corresponding to the total number of genes in the column-set and N indicating the total number of genes analyzed in both column- and row-sets. (A) Fold difference of total mRNA amount in HeLa-shRHAU cells between dox- and dox+ ($P < 0.05$). $N=30,599$. Up, up-regulated in dox+; down, down-regulated in dox+. (B) Starvation-sensitive genes. Probe sets showing more than 2-fold difference ($P < 0.05$) in both HeLa-shLuc and HeLa-shRHAU cells between FCS-containing culture and serum-starved condition. $N=30,599$, $n=593$. (C) Probe sets showing 1.5 fold or 2-fold difference in starved HeLa-shRHAU cells between dox+ and dox-. $N=30,599$, $n^{1.5\text{fold-up}}=153$, $n^{1.5\text{fold-down}}=1,685$, $n^{2\text{fold-up}}=38$, $n^{2\text{fold-down}}=256$.

SECTION 4 - DISCUSSIONS

4.01. RHAU is a nuclear-enriched protein.

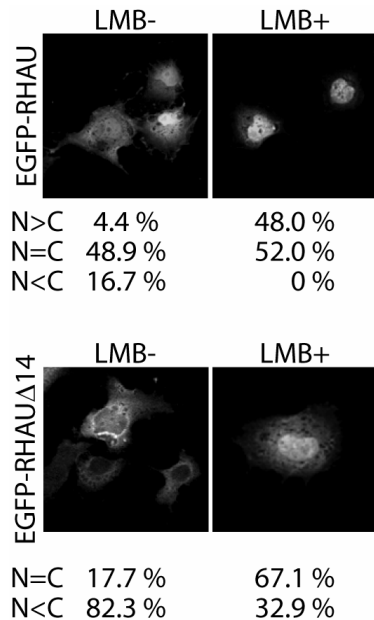


Figure 19. Leptomycin B inhibits nuclear export of RHAU and RHAU isoform. COS7 cells were transfected with EGFP-RHAU or EGFP-RHAUΔ14. Leptomycin B (10 ng/ml) or its solvent (ethanol) was added to the medium 8 h prior to fixation. Cellular localization of EGFP-proteins was observed in greater than 200 cells under microscope. N: Nucleus, C:cytoplasm.

Previous studies and the current work have shown that RHAU is localized predominantly in the nucleus, but with significant expression in the cytoplasm. Cell fractionation has also shown RHAU abundance in the nucleus and, furthermore, in the nuclear-insoluble fraction, suggesting that RHAU is tightly associated with the nuclear structure where it has a role. Since RHAU is a large nuclear protein with a molecular weight of 110 kDa, it is likely to be transported through the nuclear pore complex by an active transport mechanism requiring a nuclear localization signal (NLS) (Stewart 2007). Deletion experiments have shown that the N-terminal region of RHAU, containing a glycine-rich motif, is required for its nuclear localization. In addition, an EGFP-tagged N-terminal domain (of about 50 kDa) resulted in perfect nuclear localization and higher accumulation

than with the full-length RHAU, suggesting that this region contains the NLS. This was supported by observations in GST pull-down experiments where the N-terminal domain of RHAU was co-precipitated with the general nuclear import factors importin- α and importin- β (Figure 21). The nuclear-cytoplasmic transportation of RHAU may also be regulated by an active nuclear export mechanism involving a putative leucine-rich nuclear export signal (NES) located at the end of the helicase domain (see Figure 9). We observed that RHAU and a cytoplasmic isoform, RHAUΔ14, that lacks 14 amino acids in the helicase domain but still possesses the putative NES, were totally confined to the nucleus when cells were treated with leptomycin B, an inhibitor of the nuclear export factor CRM1 (Kudo et al. 1998). This suggests that RHAU is a nuclear shuttling protein (Figure 19). However, it is currently unclear whether RHAU is carried directly by CRM1 or in association with other molecules, including mRNA and mRNA-binding proteins. It seems that RHAU tightly associates with RNA in cells: [1] In situ nuclear extraction experiments showed that RHAU was completely released from the nucleus by treatment of cells with RNase but not DNase; [2] During

immunoprecipitation, RHAU is much more accessible to antibody in lysates treated with RNases than without (Figure 8A, compare lanes 2 and 3 or 5 and 6 in IP; also observed in the previous report (Tran et al. 2004)); [3] RHAU interacts with various proteins including RNA-binding proteins only in the presence of RNA. Messenger RNAs are always associated with RNA-binding proteins from sites of transcription in the nucleus to the cytoplasm (Dreyfuss et al. 2002). Although the major mRNA export pathway in mammalian cells is that via the TAP/p15 complex, which is a CRM1-independent pathway, it has been reported that CRM1 is specifically involved in nuclear export of ARE-containing mRNAs (Gallouzi and Steitz 2001). It is, therefore, reasonable to assume that RHAU is exported as a part of RNP complexes containing AREs via CRM1. Further investigation is required to determine which factors and mechanisms are involved in the nuclear export of RHAU.

The regulation of cellular traffic is important for RHAU function, since RHAU probably has different roles in different cellular compartments. Therefore, it is interesting to understand when and how its transport is regulated. To determine whether RHAU cellular transport is regulated in response to extracellular signals, we subjected cells to various stimuli. There was a significant difference in EGFP-RHAU localization when cells were serum starved (Figure 20) but not after treatment with insulin, EGF, or hydrogen peroxide (data not shown). RHAU tended to localize in the cytoplasm rather than the nucleus in serum-starved COS7 cells. Since this effect was not observed in HeLa cells, it may be cell- or cellular condition-specific but it is an interesting observation since we have shown that RHAU plays an anti-apoptotic role in cells cultured in serum-free medium. In this scenario, RHAU may have a cytoplasmic role, such as regulating mRNA decay during stress. It will be interesting to know whether RHAU localization varies with cell type. If the function of RHAU is correlated with its cellular localization, different localization patterns may be observed depending on cell function.

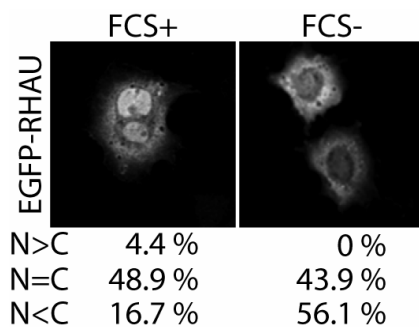


Figure 20. Serum-starvation causes cytoplasmic localization of EGFP-RHAU. COS7 cells were transfected with EGFP-RHAU. Cells were cultured in serum-free medium for 24 hours prior to fixation. Cellular localization of EGFP-proteins was observed in greater than 200 cells under microscope. N: Nucleus, C:cytoplasm.

4.02. ATPase activity and localization.

The regulation of the nuclear-cytoplasmic shuttling of RHAU is more complex than just a simple balance between nuclear import and export, since its ATPase activity and ongoing RNA synthesis are also involved. We observed that the ATPase-deficient mutant RHAU-E335A is completely excluded from the nucleus. Therefore, it is possible that movement of RHAU is tightly linked to its enzymatic activity; for example, its interactions with other proteins or RNAs important for nuclear import and/or export may be regulated by RHAU ATPase activity. The cytoplasmic localization of the RHAU mutant may be explained either by the acceleration of nuclear export or the inhibition of nuclear import. It is possible that RHAU nuclear activity depending on ATPase activity retains RHAU in the nucleus. However, RHAU hydrolyzes ATP more rapidly than other RNA helicases (V_{\max} : 77nmol/min/ μ g, Akimitsu unpublished) and, therefore, it is likely that the turnover of RHAU association with other proteins is also rapid if the interaction requires ATPase activity. RHAU ATPase activity destabilizes ARE-mRNA (Tran et al. 2004). Thus, if ATP-hydrolysis is required for the release of ARE-mRNAs from the degradation complex containing RHAU, an ATPase-deficient RHAU mutant would be unable to dissociate from RNA, which would inhibit further import of the protein into the nucleus. Alternatively, RHAU may have different conformations depending on whether it is bound by ATP or ADP, thus affecting its interaction with regulatory proteins that influence RHAU movement across the nuclear membrane. In accordance with this, several RNA helicases have been reported to exhibit different conformations upon ATP and/or nucleic acid binding (Jankowsky and Fairman 2007).

4.03. Transcriptional arrest-dependent localization of RHAU to nucleolar caps.

In the nucleus, RHAU was distributed throughout the nucleoplasm but especially concentrated in the nuclear speckles. Nuclear speckles are irregular forms of subnuclear structure located in interchromatin regions of the nucleoplasm in mammalian cells. A speckle is a site at which actively transcribed mRNAs and RNA-processing factors are concentrated and, therefore, where efficient recycling of RNA-metabolic proteins, such as splicing factors, transcription factors, and nuclear export factors, is managed (Lamond and Spector 2003), (Hall et al. 2006). According to a proteomic analysis of biochemically isolated speckles from mouse liver nuclei, the components of nuclear speckles include not only splicing factors but also various RNA-related proteins, such as transcription factors and mRNA transport factors. Several DEAD/DExH RNA helicases, which might play a role in modifying or maintaining RNA-RNA and RNA-protein interactions in the speckles, were also identified (Saitoh et al. 2004). Since RHAU itself was not detected in this analysis and the RHAU signal in the speckles was not as prominent as that of SC35 in our localization study, RHAU may not be confined to the speckles but rather shuttles between these structures and other parts of the nucleus.

Dynamic movement of RHAU was indeed observed in transcriptionally arrested cells. Unexpectedly, we found that RHAU is localized in the cap-like structures around nucleoli in ActD-treated cells, which were located close to heterochromatin and contained the RNA helicases p68 and p72. The nucleolus is a highly dynamic organelle, disassembling and reforming during the cell cycle (Shaw and Jordan 1995; Raska et al. 2006). In quiescent cells or cells subjected to transcriptional arrest, the nucleolus segregates and a cap-like structure, the nucleolar cap, appears on its surface (Malatesta et al. 2000; Shav-Tal et al. 2005). During this event, protein and RNA components of other nuclear bodies such as Cajal-, SMN-, and PML bodies, as well as some nucleoplasmic RNA-binding proteins including the RNA helicases p68 and p72, are sorted into the nucleolar caps, whereas conversely some nucleolar proteins are dispersed into the nucleoplasm (Shav-Tal et al. 2005). Similarly, proteomic analysis has shown that the protein composition of isolated nucleoli alters significantly upon inhibition of transcription by ActD (Andersen et al. 2002; Andersen et al. 2005). This indicates that nucleolar components can be dynamically reorganized in response to the metabolic state of the cell. Transcription is the major energy-consuming process in the active nucleus and is functionally and physically coupled to other RNA metabolism steps. Thus, once transcription is arrested by ActD, this orchestration of the RNA metabolic process is broken down and nuclear morphology is significantly altered. ActD blocks RNA polymerase II complexes in their elongation process, by which part of the transcriptional machinery may be left sitting on the DNA template. On the other hand, an excessive pool of free post-transcriptional factors released from the transcription machinery may be sorted into the segregated nucleolus where pre-rRNAs accumulate, because many of those proteins possess RNA-binding activity. Therefore, proteins sorted to nucleolar caps upon transcriptional arrest are considered to be proteins dynamically moving in the nucleus and associated with various RNA metabolic processes. The RNA helicase RHAU may be one such regulatory protein shuttling between splicing speckles and other compartments in the nucleus, with the consequence that it changes its nuclear localization when transcription is arrested.

4.04. Microarray to determine the RHAU target gene and RNA.

The finding that RHAU is actively and dynamically translocated in the nucleus prompted an investigation of its function there. A DNA microarray approach was taken using the ActD-chase method to identify genes or mRNAs misregulated by knockdown of RHAU. Based on the data collected at five time points after the addition of ActD, exponential decay of mRNAs was recorded and 5,613 mRNA half-lives were compared in cells expressing or not expressing RHAU. Although it has been reported that transfection of siRNAs as well as transient expression of shRNA expressed from both plasmid and lentiviral DNA vectors can trigger an

interferon response (Bridge et al. 2003; Sledz et al. 2003), activation of PKR that upregulates interferon- β in response to dsRNAs (Kumar et al. 1994) was not detected in our system (data not shown). The expression of shLuc affected the expression of only two genes, which also suggests that inducible expression of shRNA provides little non-specific up- or downregulation of cellular transcription. Furthermore, changes in expression of many RHAU targets was reversed when a silent-mutant of RHAU was exogenously expressed, indicating that the genes tested were indeed targets of RHAU. Taken together, intrinsic and inducible expression of shRNA using stably transfected cells is an efficient tool to downregulate mammalian mRNAs, causing fewer side effects than other methods using RNA interference.

4.05. RHAU changes gene expression through a mechanism not involved in mRNA degradation.

Of the 125 gene sets showing at least a twofold change in steady-state expression relative to RHAU-expressing cells, only two had correlating alterations in mRNA half-life and steady-state level, suggesting that RHAU influence on gene expression is mostly not through regulation of mRNA decay. It is possible that RHAU is involved in transcriptional regulation in the nucleus, as transcription of DAPK1 was seen to be altered by RHAU knockdown in nuclear run-on assays. We also showed that RHAU interacts with the transcriptional regulators p68, p72, and HDACs, and that RHAU, p68 and p72 are closely localized in nuclear speckles as well as around the nucleolar caps in transcription-arrested cells. Since these interactions were RNA-dependent, it is likely that RHAU resides in a part of the large transcription-related complex including RNA. RHAU is concentrated in nuclear speckles in normal culture conditions, where it may associate with pre-mRNA, splicing factors and transcription factors. Thus, we also do not rule out the possibility that RHAU influences other RNA metabolic steps in the nucleus, such as splicing and mRNA export. Further studies are required to test how many RHAU-influenced genes are regulated by transcription or by other steps of RNA metabolism.

In addition, RHAU may regulate gene expression via direct binding to DNA. One possibility related to the G4 resolvase activity of RHAU. Single point mutation analysis and compounds stabilizing the G4 structure indicate that the structure formed in the *c-myc* promoter acts as an inhibitory *cis*-element of its transcription (Siddiqui-Jain et al. 2002). At least in this example, the G4 structure functions as a transcriptional repressing element and, thus, resolving this structure is expected to activate transcription. Indeed, there was a slight enrichment of genes containing putative G4 sequences in their promoters amongst the genes downregulated after RHAU knockdown, indicating that these genes may be activated by RHAU through its resolvase activity. However, despite the high frequency of genes containing putative G4 sequences (42.7% of the total

human genome (Huppert and Balasubramanian 2007)), so far only the *c-myc* gene has been shown experimentally to be regulated by a G4-forming sequence in the promoter. Thus, we need to further investigate whether the existence of the G4 structure in RHAU target genes in fact affects their transcription. G4-forming sequences are also found in telomeric repeats, which are considered important for the maintenance of telomeric structures and, consequently, for genome stability. It is unlikely, however, that RHAU is engaged in the maintenance of telomeric structures, since we did not observe RHAU co-localization with TRF2, a telomere-binding protein, in the HeLa cell nucleus (Figure 21).

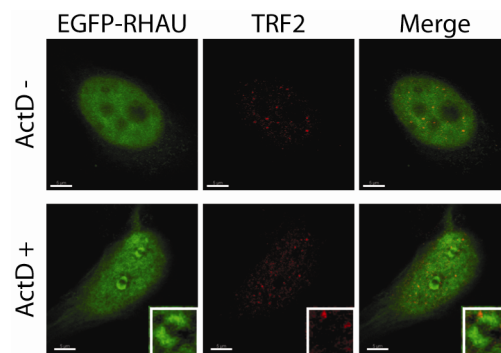


Figure 21. EGFP-RHAU is not co-localized with telomeric structures. HeLa cells were transfected with EGFP-RHAU. For ActD treatment, the drug (5 $\mu\text{g/ml}$) was added to the culture 2 h prior to fixation. Cells were immunostained with anti-TRF2 antibody (in red). The merging of two colors for EGFP and TRF2 is shown. Scale bar: 5 μm .

4.06. Involvement of RHAU in mRNA degradation.

In the analysis of mRNA decay rate, 99 mRNAs were significantly stabilized and 200 mRNAs were destabilized after RHAU knockdown, although surprisingly the steady-state levels of the majority of these mRNAs were not significantly affected. A similar phenomenon was, in fact, observed in our original study of RHAU (Tran et al. 2004), where it was shown that overexpression of RHAU accelerated the decay of uPA mRNA despite the absence of changes in its steady-state levels, suggesting that RHAU increased transcriptional activity of the same gene under these conditions. Since many mRNAs were not only stabilized but also destabilized after RHAU knockdown, including both ARE and non-ARE mRNAs, the effect of RHAU on mRNA decay may not necessarily be restricted to ARE-containing mRNAs. At the moment, however, we are unable to distinguish between direct and indirect targets of RHAU in this study. It is also possible that some of the alterations in mRNA decay were caused by changes in the expression

of other mRNAs. Thus, further approaches, such as *in vitro* mRNA decay assays, will be required to determine the direct mRNA targets of RHAU.

4.07. Relationship of regulations by transcription and mRNA stability.

Of the steady-state upregulated mRNAs, 78% showed no changes (Group1 in Figure 13) in half-life and the remaining 22% showed decreased half-lives (Group2), which was a statistically significant enrichment. mRNAs in Group2 with both increased steady-state levels and shorter half-lives after RHAU knockdown appear contradictory but this might be explained by homeostatic regulation between transcription and mRNA decay. When transcription is activated, the stabilities of mRNAs coded by a given gene might be regulated in the opposite direction in preparation for imminent suppression of transcription. The activation of both transcription and mRNA decay at the same time is an energy-consuming process, but this response will ensure rapid restoration of the initial conditions once the signal for transcriptional activation has declined. In support of this hypothesis, half-life differences were observed for mRNAs whose steady-state levels were upregulated but not those downregulated, possibly because change in mRNA stability to prepare approaching upregulation of transcription is not necessary in the latter case. This observation implies some type of communication between mechanisms regulating transcription and mRNA degradation. RHAU may be a protein that is involved in two different regulatory pathways and that transfers feedback about gene expression to both mechanisms. It would be interesting to know at the molecular level how the two processes are functionally coordinated by RHAU.

4.08. RHAU in tumor cell growth.

RHAU knockdown in HeLa cells partially reversed the characteristics of cancer cells, which ceased growth in serum-starved conditions as a consequence of decreased viability. RHAU-expressing cells divided further for a few days under the same conditions. Preliminary experiments in nude mice inoculating HeLa-shRHAU cells targeting two different sequences of RHAU mRNA showed that RHAU knockdown slowed the growth of HeLa cell-derived tumors, suggesting that RHAU has a role in tumor progression (Figure 22). Several genes encoding potential tumor-suppressors were indeed upregulated in RHAU knockdown cells. For example, in RHAU knockdown cells the steady-state levels of DAPK1 (death-associated protein kinase1: 2.1-fold), SPRED1 (Sprouty-related protein with EVH-1 domain: 2.3-fold), and an MAP-kinase inhibitor, DUSP6 (dual-specificity phosphatase 6: 2.8-fold) were all upregulated. DAPK1 is a positive mediator of apoptosis (Bialik and Kimchi 2006). Cancer development and metastasis stemming from Lewis carcinoma cells, which do not express DAPK1, are

suppressed when DAPK1 expression is restored (Inbal et al. 1997). It has been shown also that SPRED1 inactivates the Ras-dependent MAP kinase signalling pathway (Wakioka et al. 2001), and that its overexpression inhibits cancer cell motility, leading to the suppression of metastasis (Miyoshi et al. 2004). Furthermore, hypermethylation in the promoter regions and, consequently, transcriptional suppression of DUSP6 (Jeffrey et al. 2007) has been reported in pancreatic cancer cells (Xu et al. 2005) and also for DAPK1 in various cancer cells (Tang et al. 2000; Tozawa et al. 2004; Chan et al. 2005; Kuester et al. 2007). According to the tumor database Oncomine 3.0 (<http://www.oncomine.org/main/index.jsp>), expression of RHAU is significantly increased in hepatocellular carcinoma, squamous cell carcinoma, and pancreatic adenocarcinoma, suggesting a proto-oncogenic property of RHAU in these cancers. Thus, examination of the role of RHAU in tumor model systems will be of great interest.

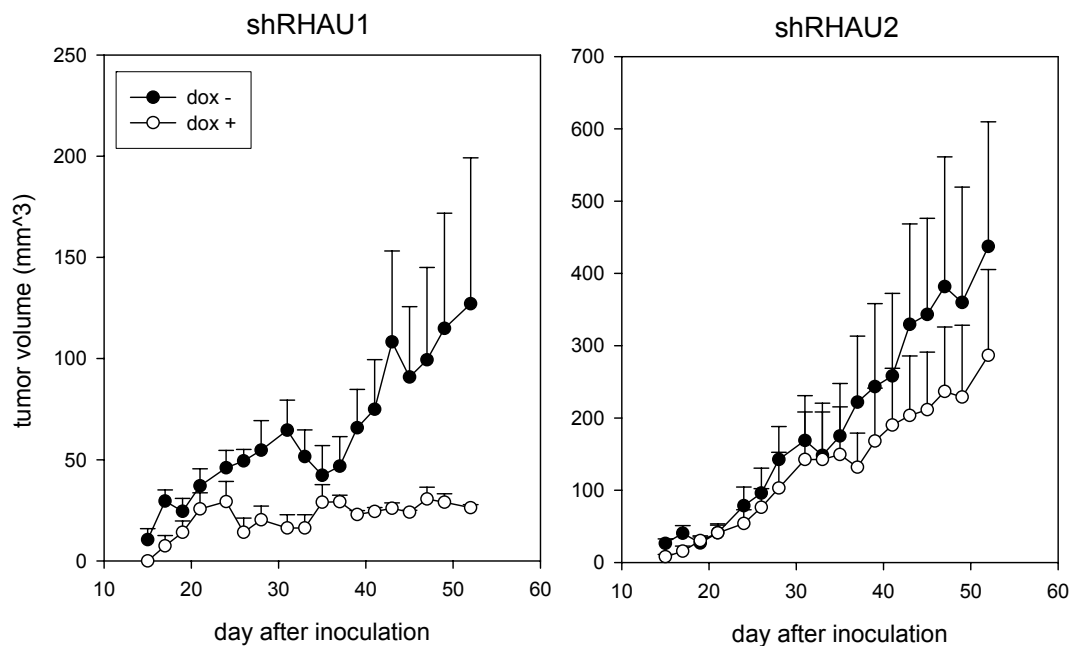


Figure 22. Knockdown of RHAU in HeLa cells retards tumor growth in nude mice. HeLa-shRHAU1 or HeLa-shRHAU2 were subcutaneously injected into the right and left flanks of CD1 female nude mice (two million cells per injection). Mice were fed with or without 1mg/ml doxycycline to induce shRNA expression in the injected cells and tumor diameter was measured constantly to estimate tumor volume. N=6 (3 mice per condition).

4.09. RHAU as a multi-functional RNA helicase.

Results from the current study infer that RHAU has at least two functions in mammalian cells, regulating gene expression through both mRNA degradation and transcription (or another gene expression-regulatory pathway in the nucleus).

So far, several RNA helicases have been shown to be multi-functional proteins, many of them involved in transcriptional regulation and other RNA-metabolism pathways (Fuller-Pace 2006). Examples include DEAD-box proteins p68 and p72, which are involved in the transcription regulation of various genes as well as in pre-mRNA processing and in alternative splicing. It is suggested that these RNA helicases play different cellular roles through interactions with various proteins. For instance, p68 can act as both a transcription activator and a repressor depending on whether it binds to co-activators like p300/CBP (Rossow and Janknecht 2003) or co-repressors like HDAC1 (Wilson et al. 2004) in different cellular contexts. It is possible that RHAU fulfils different functions in a similar way, through different molecular associations. We found that RHAU interacts with p68, p72 and HDACs in a fashion dependent on RNA (Figure 8). In addition, GST-pull-down assays using the GST-tagged RHAU N-terminal domain has identified many other RNA helicases, hnRNPs and factors involved in DNA repair or DNA replication both in the nucleus and in cytoplasm (Figure 23). Thus, RHAU seems to preferentially interact with RNA-related rather than DNA-related proteins. These results suggest that RHAU functions as part of various RNP complexes and is involved in different processes of RNA metabolism through interactions with other molecules.

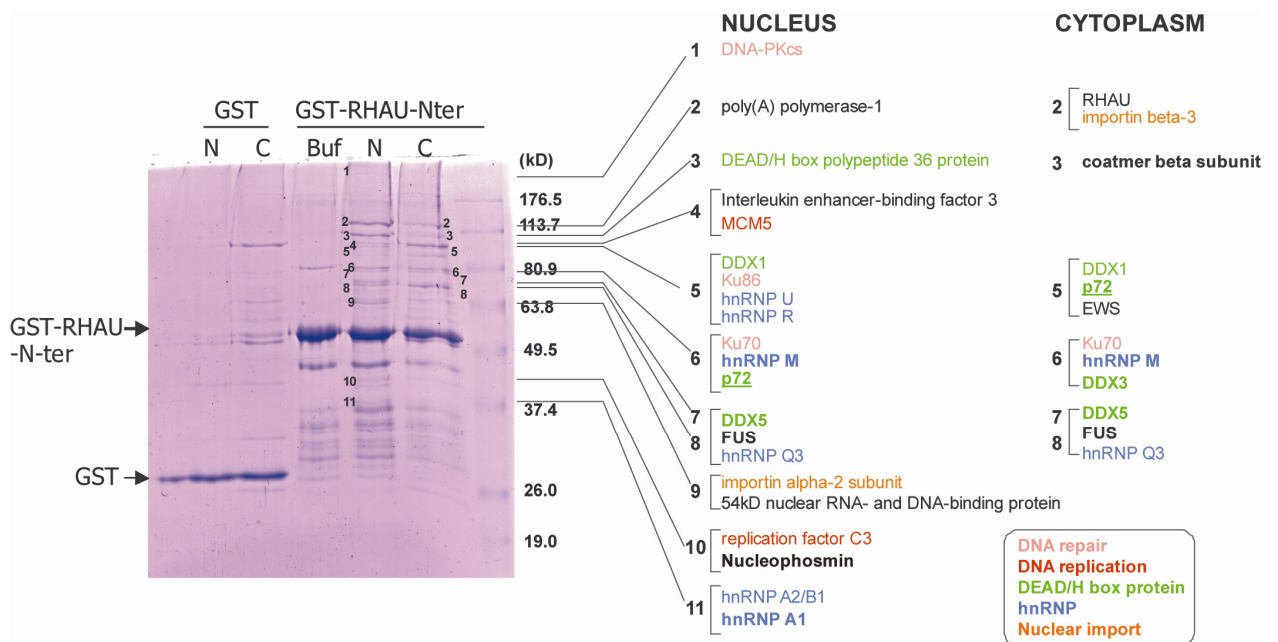


Figure 23. GST-RHAU Nter pull-down using HeLa nuclear and cytoplasmic extracts. Bacterial purified GST or GST-RHAU-Nterminus (1-200aa) were incubated with HeLa nuclear extract (N), Cytoplasmic S100 extract (C), or binding buffer (Buf). GST proteins were collected with Glutathione sepharose, loaded in 10% SDS-PAGE and stained with Coomassie Blue. Proteins specifically interacting with GST-RHAU N-ter were identified by LC-MS/MS.

PERSPECTIVES

Overall, the results indicate that RHAU is a protein involved in various processes of RNA metabolism but probably in no case as a principal factor. In mRNA degradation, RHAU only weakly interacts with ARE-RNA compared with other AUBPs and affects only limited numbers of ARE-RNA. In fact, depletion of RHAU had only a minor effect on the degradation of many mRNAs. In transcriptional regulation, it is unlikely that RHAU acts as a transcription factor binding directly to DNA and changing promoter activities since it seems to have a higher affinity for RNA than DNA. Furthermore, the threshold of impact on steady-state levels after depletion of RHAU was limited to about twofold in most genes. So, the question remains of what is the actual role of RHAU in mammalian cells.

I view RHAU as a more general and basic factor in RNA-protein complexes. The basic function of RHAU could be the maintenance or rearrangement of secondary structures of RNA and RNA-protein complexes in a process with low specificity. RHAU has no RNA-binding domain apart from the NTP-binding motifs in the helicase core domain; thus, it is unlikely that RHAU finds its specific targets itself. DExH-box proteins generally do not show so much specificity for their substrates in duplex unwinding. Yeast DEAH-box splicing factor Prp22p unwinds not only RNA-RNA but also RNA-DNA duplexes of various length (Tanaka and Schwer 2005). Human RNA helicase A also unwinds both dsDNA and dsRNA (Zhang and Grosse 1994). These *in vitro* experiments suggest that DExH-box helicases recognize structures of nucleotides such as the length of single and double strands rather than specific sequences. Furthermore, RHAU ATP-hydrolysis activity was activated by a wide range of polynucleotides as well as dsRNA, dsDNA and ssDNA ((Tran et al. 2004) and unpublished data from Akimitsu), suggesting that RHAU has low specificity for stimulation of enzymatic activity.

RHAU is presumably a protein passively used by other molecules in different contexts, rather than having an active function by itself. It gains specificity only through interactions with other proteins that bind to specific RNAs. For RHAU, NF90 is required for the interaction with ARE^{uPA} and ARE^{uPA} is required for the interaction with NF90. RHAU affects the decay of ARE^{uPA} only in the context of these two molecules. Proportionally, only a small number of RHAU molecules (a few percent of total RHAU expression) are found in such a complex in whole cell lysates, suggesting that other populations of RHAU are involved in different cellular processes through interactions with different molecules. If RHAU has a broad capacity for molecular interactions, there must be a way to increase its specificity. One possibility is by cellular compartmentalization. RHAU may be

restricted to particular cell compartments where it selectively associates with other molecules. In mammalian cells, RHAU is detected both in the nucleus and the cytoplasm, particularly in places where RNA exists at high concentrations. RHAU may affect transcriptional activity of some genes only when located at sites enriched with other transcription-related factors with which it interacts.

Thus, to further understand this molecule, more detailed information on cellular transportation is required. One problem in measuring RHAU activity in whole cell extracts is that the activity may be diluted below detection since RHAU is involved in many processes at the same time. Where RHAU movement can be restricted to one cellular compartment, its single function should be more prominent. The isolation of RHAU mutants with different cellular localizations would facilitate such an approach. It is also important to investigate interactions between RHAU and other molecules *in situ*. For this thesis, I have carried out immunoprecipitation experiments using whole cell lysates treated with RNases to examine protein-protein interactions and their RNA dependency. However, this approach does not necessarily reflect the *in vivo* situation. It lacks information on cellular compartments and, thus, molecular interactions occurring only in a specific cellular compartment would be lost in the lysates. Furthermore, treatment with RNases would destroy the structures of proteins associating with RNAs, so RHAU probably loses even direct protein-protein interactions in which RHAU recognizes particular protein structures. Therefore, the visualization of protein-protein or protein-RNA interactions *in situ* will be advantageous for understanding molecular interactions by RHAU. Fluorescence resonance energy transfer (FRET) using fluorescent proteins could be one method to provide such information. Furthermore, live-cell imaging should also provide important information, such as the velocity of molecular movements in different cellular conditions or the relationship between enzymatic activity and RHAU movement.

More important, the definition of the basic functions of RHAU is necessary in order to fully understand this molecule. Since RHAU activity exhibits low specificity, it is probably difficult to determine its RNA or protein substrates in crude whole cell extracts. An important issue then is how RHAU affects RNA-protein complexes, which could be answered by *in vitro* experiments, rather than to determine in which pathway RHAU is involved. Does it use the unwinding activity of duplex RNAs or RNPase activity to dissociate proteins from RNAs, or has it other as yet unknown activities? Answers to these basic questions will reveal the general function of RHAU and, thus, its involvement in various cellular processes.

ACKNOWLEDGEMENTS

First of all, I would like to express my deep gratitude to my supervisor, Dr. Yoshikuni Nagamine. I thank him for giving me the opportunity to pursue my studies in such a great environment. His educational philosophy “let students think by themselves” gave me many precious experiences in challenging experiments and, more important, valuable time to think deeply about my work. It has been really worthwhile training for me to learn how to pursue studies with my own ideas. I am certain that all the experiences I have encountered during my PhD work have provided me with wealth for my further life.

I would like to thank all the members of the Nagamine laboratory, past and present, for their wonderful support and for creating a pleasant working atmosphere. I thank Kateřina Chalupníková for sharing discussions and materials, as well as for her good friendship right from the start of my PhD studies. I am grateful to Stéphane Thiry for his help with many experiments as well as for providing a practical research environment. I thank Sandra Pauli and Janice Lai for purification of RHAU-antibodies and Simon Lattmann for providing me with knowledge of bioinformatics and for various discussions. I am grateful to Hoanh Tran, from whom I inherited his discovery of RHAU, for supporting me in the early stages of my project. I thank Nobuyoshi Akimitsu for giving much valuable advice.

I would like to thank all the people in the FMI facilities from various scientific fields who have helped me: Michael Stadler for statistical analysis of microarray data, especially for obtaining half-lives for tens of thousands of mRNAs, Ed Oakeley for helping me analyze microarray data, Herbert Angliker for processing samples for the microarray, Patrick Schwarb, Jens Rietdorf, and Aaron Ponti for their kind support in taking and assigning microscopic images, Daniel Hess for help with mass spectrometry, Hubertus Kohler for FACS analysis, Maciej Pietrzak for providing DNA sequences for my plasmid constructs, and Birgit Heller-Stilb and all the people in the mouse facility for helping maintain the mice.

I thank the many investigators around the world who were generous in their gifts of protocols, antibodies and plasmids: H. Clevers, S. Zhang, W. Filipowicz, A. Hergovich, A. Peters, B. Hemmings, P. Mathias, T. Yamaguchi, and K. Shimada. Patrick King is acknowledged for critically reading a manuscript and the thesis before submission.

And finally, I would like to thank Yutaka Matsuda for his advice and directions to many scientific works, as well as beyond.

APPENDIX - I : *Oligonucleotides used in this study*

Primers used for cDNA cloning	5' - 3'
shRHAU1-s	GATCCCGGGA <u>ACTGCGAAGAAGGTATTCAAGAGATACCTTCTTCG</u> CAGTTCCCTTTTTGGAAA
shRHAU1-as	AGCTTTTCCAAAAAGGGA <u>ACTGCGAAGAAGGTATCTCTTGAATAC</u> CTTCTTCGCAGTTCCCGG
shRHAU2-s	GATCCCGCTGTCATCTGTGCTGGTTTTCAAGAGAA <u>ACCAGCACAG</u> ATGACAGCTTTTTGGAAA
shRHAU2-as	AGCTTTTCCAAAAAGCTGTCATCTGTGCTGGTTTTCTCTTGA <u>AAAC</u> CAGCACAGATGACAGCGG
RHAUsm-s	GATTATGTAAGGGA <u>ACTACGGAGAAGGTATTCTGC</u>
RHAUsm-as	GCAGAATACCTTCT <u>CCGTAGTTCCCTTACATAATC</u>
E335A-s	GTTAGTCATATCGTACTTGATG <u>CAATCCATGAAAGAAATCTGCAG</u>
E335A-as	CTGCAGATTTCTTTTCATGGATT <u>GCATCAAGTACGATATGACTAAC</u>
RHAU 2 fw BamHI	GATTA <i>GGATCC</i> CATGAGTTATGACTACCATCAG
RHAU 201 fw BamHI	CG <i>GGATCC</i> CAGCATTTTCAGAGAAAAGCTG
RHAU 379 fw BamHI	CG <i>GGATCC</i> GGTA <u>ACTGTCCAATGATACAT</u>
RHAU 483 fw BamHI	CG <i>GGATCC</i> GTTTTGGAAGAAGAGGATGGT
RHAU 651 fw BamHI	CG <i>GGATCC</i> ATTGCTTATTTTTCTGAGTAGA
RHAU 200 rv EcoRI	G <i>GAATTC</i> C CATTTCATATACCGAAGGTC
RHAU 378 rv EcoRI	G <i>GAATTC</i> C AAAATATTCTGAAA <u>ACTTTTC</u>
RHAU 482 rv EcoRI	G <i>GAATTC</i> C AATGTATCGGATGAGGGCAAC
RHAU 650 rv EcoRI	G <i>GAATTC</i> C TCCACCTAGCCTTAAAATCTT
RHAU1008 rv EcoRI	G <i>GAATTC</i> C GCTGTAATATCCATCCTGGAA
Flag-s	AGCTTGCCGCCATGGACTACAAGGACGACGACGACAAGG
Flag-as	GATCCCTTGTCGTCGTCGTCCTTGTAGTCCATGGCGGCA
HA-s	AGCTTGCCGCCATGGCTTACCCATACGATGTTCCAGATTACGCTG
HA-as	GATCCAGCGTAATCTGGAACATCGTATGGGTAAGCCATGGCGGCA
p68-fw-BamHI	AT <i>GGATCC</i> ATGTCGGGTTATTCGAGT
p68-rv-XhoI	C <i>CTCGAG</i> TTATTGGGAATATCCTGTTG
p72-fw-BamHI	AT <i>GGATCC</i> ATGCGCGGAGGAGGCTT
p72-rv-XhoI	C <i>CTCGAG</i> TCATTTACGTGAAGGAGGAGGA

Primers used for real-time PCR 5' - 3'

NDUFA12-fw	ATGGCATCGTTGGCTTCAC
NDUFA12-rv	GCCAGTCACGTTGAATTTATGG
MARK1-fw	TGTATTCTGGAGGTAGCATGGC
MARK1-rv	CGTAAGGCTGCTGTCTTTTCC
DUSP6-fw	CTGAGGCCATTTCTTTCATAGATG
DUSP6-rv	CACAGTCACAGTGACTGAGCG
THBS1-fw	TCCGCAAAGTGACTGAAGAGA
THBS1-rv	GCAGCTATCAACAGTCCATTCC
NTN4-fw	AACTGCTCCGCTACATTTGG
NTN4-rv	TAACCTCTCCTCCAGTGCATG
HMGA2-fw	AGCAAGAACCAACCGGTGA
HMGA2-rv	TTCTCCAGTGGCTTCTGCTTTC
CDKN1C-fw	TGAGCCAAAGCCCAAAGA
CDKN1C-rv	TGCTACATGAACGGTCCCA
CXorf12-fw	CGCCAATACTGAAAAAGGCA
CXorf12-rv	ATTTCCGAGGCAGATGCTG
TERF2-fw	AAGGACCCCACTCAGAA
TERF2-rv	TCTGCTGGAAGGTCTCATATGA
MCP-fw	GCCCCAATATGTGAAAAGG
MCP-rv	GAAAATGGATCTGGTCCAGG
TMF1-fw	CAAAGGATAGTGAGGCACAGG
TMF1-rv	AAGGTCCCCCACTTGAATG
SNCA-fw	ACAGTGGCTGAGAAGACCAAAG
SNCA-rv	TTGACAAAGCCAGTGGCTG
DAPK1	QuantiTect Primer Assays (QIAGEN), Hs_DAPK1_SG_1

Oligonucleotides used in this thesis are shown.

Underline: sequence generating RHAU-specific shRNA (shRHAU1-s and -as, shRHAU2-s and -as) and mutation sites (RHAUsm-s and -as, E335A-s and -as). Italic: restriction sites.

Primers for real-time PCR were designed using Primer ExpressTM (Applied Biosystems, version 2.0.0). Primers' T_m values are set about 60 °C.

APPENDIX - II : *RHAU*-target mRNAs (on steady-state mRNA level)
 Probe sets showing up-regulation of steady-state mRNA in shRHAU dox+ cells.

	Affymetrix ID	Gene Symbol	ARE	fold change		fold in STV		decay-shLuc						decay-shRHAU					
				shLuc	shRHAU1	shLuc	shRHAU1	dox+		dox-		sig.change		dox+		dox-		sig.change	
								t1/2	SE	t1/2	SE	dec	inc	t1/2	SE	t1/2	SE	dec	inc
1	222940_at	SULT1E1		0.92	6.31	1.10	1.43	>600	>600	>600	NA	no	no	382	>600	>600	NA	no	no
2	208025_s_at	HMGA2		0.93	5.06	0.93	1.88	61	6	54	9	no	no	187	69	89	7	no	no
	219934_s_at	SULT1E1		0.87	4.42	1.00	1.48	289	71	>600	NA	no	no	>600	NA	>600	NA	no	no
3	221911_at	ETV1		1.17	3.26	1.05	1.61	442	417	>600	NA	no	no	364	323	>600	NA	no	no
4	223772_s_at	DKFZP564G2022	II-3	1.27	2.86	1.66	3.09	>600	NA	>600	NA	no	no	95	38	>600	NA	no	no
5	208892_s_at	DUSP6		1.44	2.82	1.11	1.22	27	4	35	7	no	no	27	6	45	9	no	no
6	238462_at	STS-1		0.88	2.75	1.01	0.87	198	79	402	348	no	no	>600	NA	>600	NA	no	no
7	203603_s_at	ZFHX1B	I-5	1.28	2.61	1.46	2.27	60	15	93	32	no	no	41	8	264	174	no	no
8	201110_s_at	THBS1	I-5	1.53	2.56	1.82	1.85	308	169	>600	NA	no	no	72	15	>600	NA	no	no
9	215150_at	YOD1		1.11	2.56	1.42	1.57	20	3	17	2	no	no	18	4	56	9	no	no
	208891_at	DUSP6		1.17	2.49	1.22	1.32	36	6	32	7	no	no	30	6	36	4	no	no
10	211959_at	IGFBP5		1.75	2.46	1.66	1.48	>600	NA	>600	>600	no	no	>600	NA	>600	NA	no	no
11	206953_s_at	LPHN2	I-5	1.19	2.46	1.16	2.37	85	20	>600	NA	no	no	107	37	221	62	no	no
12	207717_s_at	PKP2		1.04	2.35	1.21	1.91	493	375	>600	NA	no	no	128	44	533	363	no	no
13	218668_s_at	RAP2C		1.28	2.33	1.38	2.32	221	96	>600	NA	no	no	85	21	>600	NA	no	no
14	226837_at	SPRED1		1.10	2.30	1.23	1.48	69	9	64	13	no	no	51	8	119	24	no	no
15	209909_s_at	TGFB2		1.13	2.28	1.39	1.04	202	131	>600	NA	yes	no	>600	NA	245	76	no	no
16	1554576_a_at	ETV4		0.89	2.26	1.03	1.49	>600	>600	>600	NA	no	no	>600	NA	>600	NA	no	no
17	240432_x_at			1.06	2.25	1.32	1.86	84	27	76	25	no	no	35	6	121	24	no	no
18	210002_at	GATA6		1.03	2.25	1.33	1.38	49	10	51	6	no	no	40	5	45	4	no	no
19	230559_x_at	FGD4		1.29	2.23	1.13	1.56	80	14	102	25	no	no	38	11	144	33	no	no
20	204120_s_at	ADK	I-5	1.14	2.23	1.56	2.40	>600	NA	>600	NA	no	no	79	35	>600	NA	no	no
21	1553995_a_at	NT5E		0.80	2.23	1.03	1.03	>600	>600	>600	173	no	no	187	86	302	203	no	no
22	220038_at	SGK3	I-5	1.06	2.21	1.02	2.08	169	84	>600	NA	no	no	167	72	>600	>600	no	no
23	228128_x_at	PAPPA		1.21	2.21	1.72	1.50	79	16	54	10	no	no	67	17	222	116	no	no
24	213506_at	F2RL1		1.12	2.19	0.97	0.76	139	35	140	55	no	no	82	15	153	71	no	no
25	201889_at	FAM3C		1.16	2.17	1.20	1.99	220	81	381	323	no	no	208	57	>600	NA	no	no
26	222765_x_at	C20orf6	I-5	1.19	2.15	1.36	2.27	205	94	>600	NA	no	no	72	18	>600	NA	no	no
27	219312_s_at	ZBTB10		1.14	2.14	1.08	2.24	58	15	>600	NA	no	no	36	6	59	11	no	no
28	242828_at	FIGN		1.24	2.13	1.08	1.27	59	8	64	13	no	no	57	12	119	30	no	no
29	204388_s_at	MAOA		0.91	2.13	0.87	1.33	>600	NA	>600	NA	no	no	>600	NA	>600	NA	no	no
30	203139_at	DAPK1		1.16	2.13	0.98	2.11	108	19	132	19	no	no	221	80	161	38	no	no
31	235230_at			1.33	2.12	1.27	1.53	45	15	>600	NA	no	no	28	5	60	12	no	no
	233899_x_at	ZBTB10		0.91	2.12	1.35	1.34	55	9	62	20	no	no	36	6	91	18	no	no
32	237737_at	LOC375010		1.03	2.12	0.97	1.95	149	30	415	368	no	no	>600	NA	>600	>600	no	no
33	232020_at	SMURF2		1.27	2.11	1.40	2.05	68	16	129	82	no	no	81	29	203	102	no	no
34	217556_at	CLCN4		1.12	2.11	0.97	1.11	181	61	>600	NA	no	no	321	271	>600	>600	no	no
35	235521_at	HOXA3	II-4	0.97	2.11	0.85	3.33	149	23	115	30	no	no	89	20	172	48	no	no
36	209101_at	CTGF		1.08	2.10	1.39	1.09	72	9	77	8	no	no	60	13	63	8	no	no
37	209098_s_at	JAG1	II-3	0.98	2.10	1.21	0.90	95	12	82	14	no	no	62	9	116	13	no	no
	1553994_at	NT5E		0.79	2.10	1.07	0.86	>600	>600	242	70	no	no	202	69	308	207	no	no
38	225589_at	SH3MD2	I-5	1.18	2.09	1.50	1.50	77	16	85	24	no	no	55	12	276	121	no	no
39	221510_s_at	GLS		1.17	2.08	1.73	1.91	>600	NA	>600	NA	no	no	134	51	>600	NA	no	no
40	203989_x_at	F2R		1.06	2.08	0.98	1.48	390	329	>600	NA	no	no	207	131	>600	NA	no	no
41	218513_at	FLJ11184	I-5	1.26	2.06	1.28	1.83	293	217	>600	NA	no	no	63	18	>600	NA	no	no
42	228850_s_at			0.87	2.06	1.24	1.49	>600	NA	269	235	no	no	>600	NA	>600	NA	no	no
	203939_at	NT5E		1.07	2.04	1.10	1.15	372	165	>600	NA	no	no	>600	NA	>600	NA	no	no
43	210868_s_at	ELOVL6		0.87	2.04	1.06	1.76	>600	>600	>600	>600	no	no	443	319	>600	NA	no	no
44	235848_x_at	ARL6IP2		1.37	2.02	1.30	2.04	104	31	>600	NA	no	no	52	8	233	100	no	no
45	206020_at	SOCS6	I-5	0.92	2.02	1.18	1.65	59	8	46	7	no	no	33	4	64	12	no	no
46	243916_x_at	UBLC1		1.12	2.02	1.30	2.16	>600	NA	>600	NA	no	no	107	41	>600	NA	no	no
47	228324_at	C9orf41		1.08	2.02	1.36	1.92	>600	NA	>600	NA	no	no	121	35	>600	NA	no	no
48	239710_at			0.89	2.02	1.32	1.61	51	9	39	10	no	no	29	4	59	8	no	no
49	225290_at	ETNK1	I-5	1.08	2.01	1.34	2.08	>600	NA	>600	NA	no	no	122	37	>600	NA	no	no
50	228603_at	ACTR3		1.09	2.01	1.46	1.05	289	174	NA	NA	no	no	>600	>600	600	NA	no	no
51	230127_at			1.05	2.01	1.42	1.94	26	5	24	3	no	no	18	3	21	6	no	no
52	227314_at	ITGA2		1.05	2.01	1.25	1.33	213	55	>600	>600	no	no	575	447	>600	>600	no	no
53	227399_at	VGL-3		1.33	2.00	1.56	1.91	>600	NA	>600	NA	no	no	120	34	>600	NA	no	no
	223315_at	NTN4	I-5	1.18	1.64	1.12	0.94	134	53	>600	NA	no	no	181	45	>600	>600	no	no
	226653_at	MARK1		0.96	1.52	1.10	1.31	115	23	77	16	no	no	81	22	283	109	yes	no

Up- and down-regulated probe sets in shRHAU cells or shLuc cells after doxycycline-treatment (dox+) are shown. ARE, clusters of ARE set in the ARED (<http://rc.kfshrc.edu.sa/ARED/>) are shown if gene contains an ARE sequence; Fold change, fold change between dox- and dox+ derived by expression value in dox+ divided by dox-; t1/2, half-life in each sample; SE, standard error of half-life; sig-change, whether there is a significant changes of half-life between dox- and dox+ (P<0.05); dec, decreased half-life in dox+, inc, increased half-life in dox+; NA, not available.

Probe sets showing down-regulation of steady-state mRNA in shRHAU dox+ cells.

Affymetrix ID	Gene Symbol	ARE	fold change		fold in STV		decay-shLuc						decay-shRHAU							
			shLuc	shRHAU1	shLuc	shRHAU1	dox+		dox-		sig.change		dox+		dox-		sig.change			
							t1/2	SE	t1/2	SE	dec	inc	t1/2	SE	t1/2	SE	dec	inc		
1	213131_at	OLFM1			1.42	0.13	1.27	0.08	177	46	253	58	no	no	>600	>600	>600	NA	no	no
2	223140_s_at	DHX36			1.00	0.17	0.94	0.18	155	18	>600	NA	no	no	46	9	166	21	yes	no
3	227180_at	ELOVL7			0.98	0.20	0.84	0.18	466	169	>600	>600	no	no	>600	NA	>600	NA	no	no
4	204576_s_at	CLUAP1	I-5		1.00	0.21	0.83	0.17	391	139	231	53	no	no	280	147	306	136	no	no
	223139_s_at	DHX36			1.19	0.22	1.14	0.22	158	34	213	40	no	no	78	11	215	63	yes	no
5	221541_at	CRISPLD2			1.01	0.26	0.93	0.92	320	150	>600	>600	no	no	>600	NA	>600	NA	no	no
	223138_s_at	DHX36			1.15	0.27	1.05	0.19	138	37	180	42	no	no	81	15	210	81	no	no
6	226925_at	ACPL2			1.11	0.28	1.33	0.47	221	48	183	86	no	no	124	41	488	247	no	no
7	213182_x_at	CDKN1C			0.85	0.30	0.82	0.17	127	43	105	25	no	no	82	21	195	83	no	no
8	221008_s_at	AGXT2L1			0.95	0.30	0.96	0.56	270	110	>600	NA	no	no	>600	NA	>600	NA	no	no
	219534_x_at	CDKN1C			0.96	0.30	0.86	0.28	125	40	127	24	no	no	99	22	210	87	no	no
9	211368_s_at	CASP1			1.14	0.31	1.12	0.35	>600	>600	>600	NA	no	no	>600	NA	>600	NA	no	no
10	220794_at	GREM2			1.26	0.31	1.06	0.37	187	73	NA	NA	no	no	>600	>600	148	85	no	no
	211366_x_at	CASP1			0.94	0.32	1.08	0.39	>600	>600	>600	>600	no	no	>600	NA	>600	NA	no	no
11	236081_at				1.43	0.33	1.09	0.52	170	50	>600	NA	no	no	>600	NA	>600	NA	no	no
	216894_x_at	CDKN1C			0.89	0.33	0.87	0.28	133	45	108	22	no	no	103	22	235	113	no	no
12	229152_at	C4orf7			1.21	0.34	1.27	0.51	>600	NA	>600	NA	no	no	>600	NA	>600	NA	no	no
	213348_at	CDKN1C			0.96	0.35	0.88	0.33	247	57	214	59	no	no	113	14	339	111	yes	no
13	204637_at	COG4			1.02	0.38	1.00	0.52	174	24	179	31	no	no	>600	NA	386	129	no	no
	209970_x_at	CASP1			1.03	0.38	1.00	0.46	>600	>600	>600	NA	no	no	>600	NA	>600	NA	no	no
14	243426_at	LOC339290			1.04	0.39	1.04	0.34	>600	NA	357	259	no	no	111	26	140	31	no	no
15	227761_at	MYO5A			1.12	0.40	1.36	0.28	>600	NA	>600	NA	no	no	189	84	>600	NA	no	no
16	226839_at	TRA16			0.97	0.40	1.08	0.53	105	17	92	13	no	no	217	109	120	15	no	no
17	207501_s_at	FGF12			0.77	0.40	0.86	0.32	286	110	154	54	no	no	>600	NA	>600	NA	no	no
18	1554696_s_at	TYMS			0.96	0.40	0.90	0.34	192	31	187	44	no	no	>600	>600	325	213	no	no
19	210046_s_at	IDH2			0.93	0.40	0.86	0.52	>600	NA	>600	>600	no	no	>600	NA	>600	>600	no	no
20	218966_at	MYO5C	I-5		1.00	0.41	0.96	0.40	>600	>600	>600	NA	no	no	>600	NA	>600	>600	no	no
21	220588_at	BCAS4			0.95	0.41	0.88	0.38	>600	>600	378	160	no	no	>600	NA	>600	>600	no	no
22	240180_at				1.20	0.41	0.99	0.29	165	48	543	595	no	no	>600	NA	>600	NA	no	no
23	230251_at	C6orf176			1.20	0.42	0.95	0.45	65	3	67	9	no	no	167	61	89	10	no	no
24	202728_s_at	LTBP1			1.16	0.42	1.03	0.47	108	32	>600	NA	no	no	>600	NA	>600	>600	no	no
25	233340_at	SPINK5L3			1.27	0.42	1.17	0.44	>600	>600	>600	NA	no	no	>600	NA	>600	NA	no	no
26	241759_at	ADA			1.04	0.43	0.95	0.42	388	214	>600	>600	no	no	>600	NA	>600	NA	no	no
27	239169_at	RDM1			0.90	0.44	0.80	0.39	>600	NA	>600	NA	no	no	>600	NA	>600	NA	no	no
28	210756_s_at	NOTCH2	II-4		1.05	0.44	1.08	0.34	188	49	213	60	no	no	>600	>600	401	177	no	no
29	225234_at	CBL			1.26	0.44	1.24	0.41	147	44	267	144	no	no	564	506	435	304	no	no
30	207038_at	SLC16A6			1.38	0.45	1.21	0.37	91	12	170	51	no	no	162	67	115	19	no	no
31	230788_at	GCNT2	II-4		1.06	0.45	1.00	0.40	35	2	34	3	no	no	34	5	49	2	yes	no
32	202687_s_at	TNFSF10			1.32	0.45	0.85	0.77	124	25	169	78	no	no	500	>600	122	41	no	no
33	224893_at	DKFZP564J0863			0.71	0.45	0.70	0.35	117	16	174	32	no	no	510	212	314	72	no	no
34	219326_s_at	B3GNT1	I-5		0.95	0.46	0.93	0.48	63	5	48	4	no	no	72	15	60	6	no	no
35	204440_at	CD83			0.96	0.46	1.16	0.31	139	36	107	21	no	no	>600	NA	146	54	no	no
36	217867_x_at	BACE2			1.08	0.46	0.81	0.47	208	129	187	66	no	no	>600	NA	493	275	no	no
37	224957_at	LOC497661			0.98	0.46	1.02	0.47	284	72	228	83	no	no	>600	NA	>600	369	no	no
	211367_s_at	CASP1			0.98	0.47	1.07	0.28	>600	NA	>600	>600	no	no	>600	NA	>600	NA	no	no
38	228262_at	FLJ14503			0.94	0.47	0.90	0.36	>600	NA	>600	NA	no	no	>600	NA	>600	NA	no	no
39	225458_at	DKFZP564H1171			0.96	0.47	0.88	0.47	68	8	66	10	no	no	49	6	70	11	no	no
40	217506_at	LOC400642			0.97	0.47	0.80	0.57	147	59	172	43	no	no	>600	NA	384	249	no	no
41	209340_at	UAP1			1.10	0.47	1.01	0.39	174	16	187	43	no	no	202	42	226	26	no	no
42	219255_x_at	IL17RB			1.03	0.47	1.05	0.40	>600	>600	>600	NA	no	no	>600	NA	515	376	no	no
43	219562_at	RAB26			0.94	0.48	0.83	0.58	>600	NA	>600	NA	no	no	>600	NA	>600	NA	no	no
44	204467_s_at	SNCA			1.18	0.48	1.06	0.46	224	36	349	137	no	no	>600	NA	>600	338	no	no
45	220479_at	PROO132			0.93	0.48	1.60	0.64	63	18	56	15	no	no	150	46	67	15	no	no
46	227452_at	LOC440462			0.97	0.48	0.97	0.61	57	8	53	4	no	no	117	22	45	6	no	yes
47	229189_s_at				0.84	0.48	0.82	0.46	>600	NA	>600	>600	no	no	>600	NA	>600	NA	no	no
48	224909_s_at	PREX1			0.89	0.48	0.97	0.40	165	43	128	31	no	no	>600	>600	>600	>600	no	no
49	241765_at	CPM			1.01	0.48	1.12	0.62	362	256	350	330	no	no	>600	NA	>600	NA	no	no
50	214869_x_at	GAPVD1			1.09	0.48	0.93	0.38	114	16	139	27	no	no	276	186	286	141	no	no
51	224970_at	NFIA			1.08	0.49	1.06	0.44	159	39	161	34	no	no	>600	NA	271	91	no	yes
	235706_at	CPM			1.05	0.49	0.87	0.36	364	163	550	347	no	no	>600	NA	>600	>600	no	no
	224156_x_at	IL17RB			0.84	0.49	1.09	0.44	>600	NA	>600	>600	no	no	>600	NA	>600	NA	no	no
52	206037_at	CCBL1			0.93	0.49	0.79	0.49	>600	NA	>600	NA	no	no	>600	NA	>600	NA	no	no
53	205952_at	KCNK3			0.94	0.49	0.82	0.62	105	15	91	18	no	no	>600	NA	287	145	no	no
54	238577_s_at				1.20	0.49	1.00	0.80	116	38	>600	NA	no	no	>600	>600	>600	NA	no	no
55	1568592_at	LOC400368			1.05	0.50	0.90	0.68	211	35	253	80	no	no	>600	NA	>600	NA	no	no
56	212977_at	CMKOR1			1.16	0.50	1.10	0.43	92	17	105	30	no	no	109	25	134	19	no	no
57	215215_s_at	LOC81691			0.93	0.50	0.91	0.41	349	182	547	229	no	no	>600	NA	547	499	no	no
58	227747_at				0.89	0.50	0.99	0.59	192	131	>600	NA	no	no	>600	NA	>600	NA	no	no
59	207174_at	GPC5			1.04	0.50	1.15	0.46	>600	>600	>600	NA	no	no	>600	NA	>600	NA	no	no
60	219874_at	SLC12A8			1.02	0.50	0.95	0.72	>600	>600	>600	355	no	no	>600	NA	>600	NA	no	no
	211574_s_at	MCP			1.12	0.50	0.92	0.45	336	144	246	42	no	no	>600	NA	531	490	no	no
	204340_at	CXorf12			1.18	0.50	0.77	0.67	278	115	187	52	no	no	>600	NA	>600	>600	no	no
	214948_s_at	LOC441347, TMF1			1.24	0.50	1.05	0.57	134	17	200	35	no							

APPENDIX - III : *RHAU-target mRNAs (on mRNA stability)*

Probe sets showing significantly decreased half-life in shRHAU dox+ cells.

Affymetrix ID	Description	ARE	shRHAU						shLuc					
			Fold change		half-life (min)				Fold change		half-life (min)			
			Steady-state	t/2	dox+		dox-		Steady-state	t/2	dox+		dox-	
1	213150_at	Similar to LOC166075	1.48	0.11	71.1	12.5	634.5	300.4	91.3	6.5	71.1	11.2		
2	228189_at	FYVE, RhoGEF and PH domain containing 4	2.55	0.19	36.3	9.9	187.3	63.6	82.3	10.8	97.7	21.6		
3	212670_at	amyotrophic lateral sclerosis 2 (juvenile) chromosome region, candidate 3	0.66	0.20	150.0	16.2	733.4	306.1	89.5	23.8	157.5	51.0		
4	225916_at	cyclin E2	1.05	0.21	109.4	20.7	524.6	215.7	NA	NA	NA	NA		
5	223618_at	baculoviral IAP repeat-containing 4	1.57	0.22	97.9	20.3	440.7	195.6	106.8	14.8	96.8	24.7		
6	205289_at	casein kinase 1, gamma 3	1.11	0.23	112.2	17.7	426.0	215.9	47.2	4.8	40.7	6.1		
7	217196_s_at	THAP domain containing 5	1.36	0.23	70.7	11.7	301.4	132.4	141.2	21.1	123.8	28.8		
8	239007_at	CCR4-NOT transcription complex, subunit 8	1.40	0.24	104.2	17.5	437.2	181.8	71.4	10.3	65.6	5.6		
9	212804_s_at	Iron-responsive element binding protein 2	0.99	0.24	100.0	14.2	417.2	170.2	191.2	27.8	238.1	63.2		
10	226341_at	CDNA clone IMAGE:4807381	1.82	0.25	62.0	10.3	247.6	88.8	NA	NA	NA	NA		
11	205034_at	DEAH (Asp-Glu-Ala-His) box polypeptide 36	0.24	0.26	79.6	10.9	310.6	122.4	101.7	16.1	113.8	34.8		
12	218490_s_at	Zinc finger, MYM-type 5	2.09	0.26	38.4	9.5	148.8	24.9	146.0	25.0	129.4	25.9		
13	227004_at	DEAH (Asp-Glu-Ala-His) box polypeptide 36	0.18	0.26	46.0	8.1	175.7	24.9	76.1	13.8	84.5	25.3		
14	214678_x_at	hypothetical protein MGC17943	1.12	0.26	171.7	27.0	655.7	228.6	92.7	19.9	102.1	27.7		
15	225698_s_at	ADP-ribosylation factor-like 6 interacting protein 2	1.91	0.27	55.8	10.6	206.8	71.3	150.3	24.2	144.1	42.3		
16	221918_at	Salvador homolog 1 (Drosophila)	0.88	0.28	76.8	9.2	276.3	76.6	78.1	6.1	74.9	12.8		
17	209271_at	GTPase activating protein and VPS9 domains 1	0.65	0.28	118.7	15.2	426.0	109.6	125.5	17.7	155.2	36.0		
18	236599_at	zinc finger protein 131 (clone pHZ-10)	1.47	0.28	72.1	11.9	255.6	98.1	154.4	25.8	129.8	37.8		
19	220180_at	zinc finger protein, X-linked	1.36	0.28	76.6	13.5	269.6	79.6	100.1	15.6	NA	NA		
20	228181_at	chromosome 17 open reading frame 39	1.26	0.28	119.6	28.6	420.6	132.0	94.0	11.3	77.5	12.8		
21	203543_s_at	hypothetical protein FLJ10560	1.17	0.28	84.8	15.8	298.2	96.3	46.2	8.1	44.5	5.6		
22	227034_at	decay accelerating factor for complement (CD55, Cromer blood group system)	1.11	0.29	167.0	39.2	667.7	183.9	78.4	4.5	69.3	4.8		
23	227636_at	CTCL tumor antigen se57-1	1.5	0.30	62.9	9.8	212.7	59.9	NA	NA	NA	NA		
24	241993_x_at	hypothetical protein LOC339745	1.1	0.30	47.2	10.2	159.3	42.5	NA	NA	NA	NA		
25	238808_at	MAP/microtubule affinity-regulating kinase 1	1.46	0.30	75.1	19.5	252.3	79.7	43.6	2.9	31.4	1.3		
26	227539_at	similar to RIKEN cDNA 4921524J17	1.24	0.30	62.5	7.4	209.0	63.0	67.2	7.0	87.7	11.9		
27	238729_x_at	toll-like receptor 4, toll-like receptor 4	1.47	0.30	51.3	5.9	168.6	47.7	171.6	33.1	195.0	40.1		
28	1553111_a_at	ring finger and KH domain containing 2	1.73	0.31	81.9	12.3	267.0	102.3	70.9	15.9	85.3	30.1		
29	230559_x_at	Forkhead box P1	1.28	0.31	82.7	13.4	264.5	71.7	79.5	14.1	101.5	25.5		
30	224657_at	poliovirus receptor-related 3	1.86	0.31	93.8	16.0	298.5	96.1	73.4	3.0	69.1	6.3		
31	217812_at	kelch repeat and BTB (POZ) domain containing 6	0.72	0.31	35.9	6.9	113.9	34.1	102.2	7.0	105.8	16.3		
32	238634_x_at	CDNA FLJ25301 fis, clone STM07812	1.91	0.32	64.7	9.4	205.4	60.8	125.1	23.7	132.7	31.1		
33	218541_s_at	spindle assembly 6 homolog (C. elegans)	1.09	0.32	151.3	27.9	475.3	137.7	51.7	5.0	43.4	4.9		
34	229970_at	MAP3K12 binding inhibitory protein 1	1.53	0.32	79.8	14.0	249.5	69.6	53.5	6.4	50.6	5.5		
35	225022_at	ligase IV, DNA, ATP-dependent	1.45	0.32	107.5	19.0	332.6	110.4	89.1	7.8	91.8	16.2		
36	227973_at	heat shock transcription factor 2	1.30	0.33	65.5	10.6	198.3	70.0	49.9	7.5	47.2	8.3		
37	38892_at	RAB23, member RAS oncogene family	0.94	0.34	96.3	11.7	284.5	99.9	69.7	12.5	59.4	9.3		
38	228050_at	mitogen-activated protein kinase kinase kinase 3	1.81	0.34	81.5	12.8	236.5	71.0	163.5	23.3	181.8	51.4		
39	233127_at	CDNA FLJ12412 fis, clone MAMMA1003004	1.45	0.35	193.0	53.1	647.2	116.7	114.0	27.9	124.3	33.6		
40	238122_at	Sp3 transcription factor	1.45	0.35	79.0	11.7	222.8	58.3	53.5	8.4	60.6	7.4		
41	204709_s_at	ubiquitin specific peptidase 53	1.50	0.36	83.8	14.8	235.7	45.4	106.4	11.1	139.4	30.5		
42	240432_x_at	Transcribed locus	2.12	0.36	38.5	6.7	108.2	22.8	NA	NA	NA	NA		
43	226317_at	hypothetical protein FLJ21657	1.22	0.36	159.2	26.6	445.8	118.5	67.2	11.6	64.5	13.1		
44	231869_at	Serpin peptidase inhibitor, clade E (plasminogen activator inhibitor type 1)	1.65	0.36	71.0	16.9	197.0	45.9	75.9	7.3	77.5	9.6		
45	226608_at	kinesin family member 21A	1.29	0.36	174.2	42.7	480.6	134.1	118.1	20.5	79.0	17.4		
46	225735_at	RAB23, member RAS oncogene family	0.98	0.37	79.9	6.2	215.7	58.1	55.9	6.1	45.3	5.4		
47	203544_s_at	ADP-ribosylation factor 7	1.85	0.37	105.7	19.3	283.4	87.6	105.8	14.7	101.8	22.3		
48	218411_s_at	golgi associated PDZ and coiled-coil motif containing	1.54	0.38	118.0	25.1	313.5	89.4	145.6	39.1	157.9	48.1		
49	204032_at	AE binding protein 2	1.32	0.38	109.0	17.9	286.4	54.1	54.1	2.6	54.9	4.1		
50	236128_at	BCL2-associated atrophogene 4	1.39	0.38	147.1	29.3	362.9	76.5	16.5	3.6	16.8	3.5		
51	226100_at	CSRP2 binding protein	1.00	0.39	69.7	6.7	179.7	32.6	44.7	5.2	45.0	6.1		
52	236526_x_at	CDNA FLJ26957 fis, clone SLV00486	1.14	0.40	17.9	2.8	45.1	6.2	29.1	6.8	34.9	9.4		
53	1555803_a_at	hypothetical protein FLJ31139	1.54	0.40	58.4	15.1	146.6	22.7	143.7	16.8	122.1	22.7		
54	224597_at	CDNA clone IMAGE:5270680	1.32	0.40	213.3	60.2	632.4	126.2	147.6	18.0	NA	NA		
55	1556821_x_at	gb:H48516	1.44	0.41	76.7	22.4	189.3	47.5	43.8	9.2	43.8	9.0		
56	226479_at	zinc finger protein 588	1.30	0.41	56.7	11.7	138.9	40.9	45.7	5.9	51.1	8.6		
57	201210_at	YTH domain family, member 3	1.30	0.41	126.7	25.9	307.5	87.8	117.4	14.1	136.2	27.9		
58	203837_at	hypothetical protein FLJ11171	1.47	0.42	45.1	5.8	108.6	14.1	153.1	30.4	123.1	37.8		
59	201362_at	debranching enzyme homolog 1 (S. cerevisiae)	1.21	0.42	82.2	11.3	197.8	45.4	172.4	16.3	154.9	30.8		
60	224341_x_at	DEAD (Asp-Glu-Ala-Asp) box polypeptide 59	1.10	0.42	114.8	16.6	276.0	74.3	NA	NA	NA	NA		
61	223463_at	Ras association (RalGDS/AF-6) and pleckstrin homology domains 1	1.14	0.42	92.2	11.4	221.3	32.0	92.0	10.9	95.3	16.5		
62	209120_at	SH3 multiple domains 2	1.66	0.42	64.2	14.0	154.1	42.6	97.4	10.0	83.9	15.1		
63	210260_s_at	kelch repeat and BTB (POZ) domain containing 7	0.84	0.42	34.7	4.4	83.3	6.9	94.9	7.9	91.6	16.0		
64	225658_at	YOD1 OTU deubiquitinating enzyme 1 homolog (yeast)	2.25	0.42	22.5	5.1	53.9	9.5	99.3	25.5	88.5	21.9		
65	225457_s_at	DkFZP564I171 protein	0.73	0.42	38.5	5.1	91.7	12.1	69.2	10.9	62.3	9.8		
66	223288_at	par-6 partitioning defective 6 homolog beta (C. elegans)	1.28	0.43	23.9	4.7	56.0	13.8	85.3	7.9	82.9	16.1		
67	202653_s_at	zinc finger protein 302	1.06	0.43	152.0	24.3	355.7	60.3	104.5	9.7	92.8	14.6		
68	235165_at	Rab geranyltransferase, beta subunit	1.41	0.44	75.8	13.8	173.5	38.0	35.0	8.3	37.7	7.9		
69	1558700_s_at	zinc finger protein ZNF466	1.71	0.44	50.0	6.2	114.5	26.3	62.9	6.9	NA	NA		
70	202798_at	Zinc finger protein 91 (HPF7, HTF10)	1.29	0.44	17.8	4.6	40.7	8.2	88.6	9.8	79.3	12.9		
71	200670_at	runt-related transcription factor 2	1.69	0.44	54.9	6.0	124.9	18.2	88.3	6.4	100.0	11.1		
72	217996_at	transcription factor B2, mitochondrial	0.93	0.44	121.7	19.5	276.8	74.0	27.8	2.4	20.0	3.5		
73	239768_x_at	CDNA FLJ41751 fis, clone HSYRA2008154	1.45	0.44	72.1	13.0	163.5	44.0	108.2	24.7	81.6	18.1		
74	227766_at	hypothetical protein FLJ10726	0.90	0.44	164.7	26.7	372.9	71.4	NA	NA	NA	NA		
75	225186_at	Zinc finger and BTB domain containing 10	2.05	0.44	40.8	7.8	92.2	17.4	73.9	12.2	NA	NA		
76	219990_at	transmembrane protein 23	1.48	0.45	64.6	9.1	145.1	27.8	44.8	6.4	38.0	5.6		
77	227767_at	cytoplasmic polyadenylation element binding protein 3	1.57	0.45	44.9	8.3	100.6	26.0	139.6	19.8	151.6	55.9		
78	233899_x_at	pleckstrin homology-like domain, family B, member 2	1.31	0.45	153.8	29.3	342.6	89.5	54.6	9.4	61.6	19.8		
79	241348_at	kinesin family member 23	1.25	0.45	111.9	20.0	247.9	66.8	43.4	8.7	44.3	5.8		
80	218940_at	catenin (cadherin-associated protein), beta 1, 88kDa	1.76	0.45	53.8	13.2	118.9	17.1	89.4	16.2	62.4	14.5		
81	202163_s_at	hypothetical protein LOC201725	1.43	0.46	88.7	11.3	194.1	35.3	150.1	39.5	179.5	55.9		
82	231786_at	SMAD, mothers against DPP homolog 1 (Drosophila)	1.56	0.46	91.8	12.5	200.9	42.4	65.5	5.6	87.5	14.4		
83	213168_at	centrosome and spindle pole associated protein 1	1.61	0.46	65.3	10.2	142.6</							

Affymetrix ID	Description	ARE	shRNA						shLuc			
			Fold change		half-life (min)		half-life (min)		half-life (min)		half-life (min)	
			Steady-state	t/2	dox+	dox-	dox+	dox-	dox+	dox-	dox+	dox-
101	221596_s_at		0.82	0.49	78.2	11.3	160.1	34.5	60.9	10.5	54.4	16.3
102	206451_at		1.33	0.50	102.3	13.1	205.2	39.2	168.3	41.9	289.0	180.5
103	208296_x_at		1.49	0.50	41.7	6.2	83.4	15.5	119.2	9.1	114.6	22.9
104	223412_at	I - 5	1.23	0.50	98.2	9.0	194.8	34.3	64.6	7.3	57.0	11.1
105	220235_s_at		1.77	0.50	68.1	10.9	135.0	30.4	68.6	5.0	66.4	10.6
106	228468_at	II - 4	1.19	0.51	115.2	13.7	227.4	50.9	143.8	22.7	98.5	20.4
107	206307_s_at		1.33	0.51	73.2	12.1	143.1	26.1	69.8	8.3	61.7	7.5
108	226337_at		1.24	0.51	91.7	8.0	178.6	34.8	72.0	10.4	53.9	10.4
109	209112_at		2.19	0.51	68.5	8.2	133.1	17.8	35.9	3.5	31.8	2.7
110	206020_at	II - 3	1.16	0.52	109.9	13.3	212.1	43.3	58.8	8.1	45.9	7.3
111	238562_at		1.18	0.52	173.3	29.0	334.3	60.5	48.5	4.4	58.4	9.7
112	211220_s_at	I - 5	1.18	0.52	168.2	26.7	324.1	60.1	124.3	49.2	120.5	30.1
113	32723_at		1.32	0.52	122.5	17.2	233.4	32.3	80.9	7.8	70.4	10.8
114	205773_at	I - 5	1.33	0.53	27.3	2.4	51.8	6.0	72.8	12.6	69.0	15.7
115	235230_at		1.96	0.53	32.0	5.6	60.6	12.6	44.6	14.8	NA	NA
116	219149_x_at		1.24	0.53	56.2	5.9	105.9	17.6	NA	NA	NA	NA
117	201363_s_at		1.23	0.53	62.6	7.9	118.0	19.6	123.1	15.7	110.4	27.5
118	244487_at		1.50	0.53	62.1	11.8	116.7	21.5	59.8	13.3	57.1	26.1
119	228385_at		1.06	0.53	44.1	6.3	82.7	9.3	125.1	20.5	193.2	58.3
120	221803_s_at	I - 5	1.11	0.53	56.8	10.2	106.5	18.2	73.6	6.6	76.0	9.8
121	1568943_x_at	II - 3	1.42	0.54	98.7	19.7	183.4	31.7	72.9	6.0	66.6	9.6
122	231895_at	I - 5	1.41	0.54	69.4	7.8	127.3	20.7	341.3	105.1	213.0	42.7
123	226003_at		0.85	0.55	46.9	7.7	85.6	6.9	136.2	20.9	130.3	44.0
124	221749_at		0.64	0.55	41.5	3.9	75.6	8.3	122.3	23.6	141.4	47.2
125	212989_at		1.27	0.55	159.2	19.7	288.8	33.0	87.1	15.3	NA	NA
126	205281_s_at		1.41	0.55	75.9	12.3	137.5	23.1	123.4	9.8	107.7	22.0
127	227162_at		1.22	0.55	76.1	10.8	137.5	22.9	56.5	6.1	56.6	7.7
128	1554176_a_at		1.36	0.55	92.2	13.1	166.4	18.1	88.9	20.3	NA	NA
129	214751_at	I - 5	2.01	0.55	32.2	4.0	58.0	8.9	71.2	12.0	76.5	12.3
130	225689_at		1.55	0.56	29.5	5.8	53.0	9.2	76.7	16.4	84.5	23.8
131	226649_at		1.22	0.56	64.3	4.5	115.4	19.7	89.1	5.7	80.4	18.0
132	225486_at		0.76	0.56	117.6	22.1	210.3	29.2	76.5	13.1	84.6	15.7
133	231817_at		1.25	0.56	93.2	11.1	166.1	20.9	95.0	23.3	NA	NA
134	222630_at		1.00	0.56	78.4	10.6	139.4	21.1	77.8	7.1	69.1	11.9
135	224759_s_at		1.24	0.56	112.7	16.2	199.8	25.0	167.3	33.3	137.9	33.3
136	230788_at		0.88	0.56	94.2	10.7	166.9	28.3	35.4	2.3	33.7	3.3
137	228543_at	I - 5	1.43	0.57	40.3	5.0	71.2	12.9	108.8	11.5	119.1	17.4
138	52731_at		1.49	0.57	102.2	11.8	180.3	29.1	98.0	23.7	NA	NA
139	220468_at		0.64	0.57	150.4	20.8	264.3	50.2	94.8	12.1	104.8	14.9
140	225688_at		1.10	0.57	139.7	11.1	245.2	42.7	148.0	16.0	140.7	33.4
141	227798_at		1.04	0.57	73.6	9.9	128.5	20.0	125.7	25.1	108.2	28.7
142	229886_at		0.74	0.57	41.1	4.7	71.8	11.3	98.9	5.9	86.4	14.5
143	228452_at		1.09	0.58	65.9	10.2	114.0	10.3	127.4	28.4	NA	NA
144	206613_s_at		1.30	0.58	58.4	6.1	100.9	12.1	74.7	9.3	65.1	14.9
145	225512_at		1.49	0.58	55.2	9.5	95.1	15.2	116.0	18.3	123.2	32.6
146	236738_at		1.22	0.58	86.5	13.2	152.1	24.1	97.5	14.0	119.1	30.0
147	227105_at		1.07	0.59	51.3	4.8	87.6	9.9	89.2	15.8	83.4	21.1
148	202180_at	II - 4	0.92	0.59	120.8	19.1	205.7	25.4	141.2	20.6	130.2	27.7
149	220195_at	I - 5	1.18	0.59	53.7	6.0	91.3	11.1	57.3	7.9	77.9	17.3
150	203487_s_at	I - 5	0.76	0.59	46.8	4.0	79.4	11.3	136.3	27.1	84.9	17.5
151	240592_at		1.71	0.59	23.3	2.7	39.3	4.4	40.7	6.6	32.6	6.0
152	212615_at	I - 5	1.04	0.59	65.5	7.3	110.3	15.6	60.5	6.7	56.4	6.9
153	213325_at		1.30	0.59	92.1	9.9	154.9	13.6	NA	NA	NA	NA
154	205263_at		0.99	0.60	177.8	36.1	297.0	36.6	87.5	8.0	74.0	10.6
155	203232_s_at	II - 3	1.21	0.61	59.6	4.4	98.3	10.3	122.2	22.8	137.9	34.6
156	219178_at		1.03	0.61	78.9	7.7	128.8	15.3	102.3	10.5	125.9	28.5
157	228069_at	I - 5	1.03	0.61	66.3	8.1	108.2	13.1	87.6	11.9	84.1	11.6
158	222472_at		1.44	0.62	49.1	4.4	79.5	8.1	149.7	27.5	NA	NA
159	225884_s_at	I - 5	1.23	0.62	60.1	6.1	97.2	8.3	55.0	3.4	57.7	3.0
160	235088_at		1.63	0.62	37.3	5.2	60.2	8.8	79.1	6.8	87.0	20.5
161	225889_at		1.17	0.62	60.0	5.6	96.8	8.1	147.2	23.2	149.2	49.7
162	1570507_at		1.14	0.62	72.7	8.4	117.2	14.5	54.0	11.1	40.9	6.9
163	227525_at		1.37	0.62	69.8	6.3	112.0	18.0	67.2	6.5	66.8	11.0
164	218311_at		1.18	0.63	81.8	6.3	130.6	19.6	97.9	14.4	NA	NA
165	231902_at		1.22	0.63	44.8	5.2	71.2	9.7	95.1	15.4	82.2	16.5
166	217954_s_at		1.62	0.63	97.5	13.5	155.0	21.9	87.1	8.9	94.3	18.2
167	235848_x_at		1.11	0.63	69.8	6.0	110.7	16.5	NA	NA	NA	NA
168	213704_at		1.07	0.63	63.5	12.6	100.4	10.6	96.4	20.5	72.9	23.6
169	205990_s_at	I - 5	1.09	0.64	105.5	12.8	165.7	25.5	124.7	14.0	118.1	25.6
170	209211_at		1.08	0.64	136.6	15.4	214.1	27.6	66.9	7.3	62.1	8.8
171	203312_x_at		1.31	0.64	91.4	16.3	142.5	13.0	98.0	6.0	NA	NA
172	222794_x_at		1.14	0.64	98.4	10.9	152.5	17.0	146.8	19.8	139.6	28.1
173	215150_at		1.39	0.65	70.6	6.3	109.5	7.1	19.6	3.1	17.2	2.3
174	229337_at		1.31	0.65	49.6	7.7	76.3	8.5	124.8	14.9	95.4	22.2
175	212366_at		1.25	0.65	63.3	7.5	96.7	9.4	52.7	4.5	54.8	7.6
176	223139_s_at		1.03	0.66	105.5	11.2	160.3	16.3	157.9	34.4	213.0	39.7
177	207125_at	II - 4	1.18	0.66	38.7	3.5	58.5	8.1	34.7	5.7	32.2	5.2
178	218875_s_at	II - 4	0.48	0.67	35.0	4.7	52.5	2.7	34.2	2.1	34.2	6.0
179	223140_s_at		1.05	0.67	102.1	10.7	152.7	16.0	154.9	18.1	NA	NA
180	228812_at		1.20	0.67	45.0	4.2	67.1	7.0	54.6	5.6	41.7	5.7
181	225210_s_at	II - 4	1.02	0.67	51.0	3.6	75.7	8.5	166.0	24.9	119.4	29.0
182	218640_s_at		0.82	0.67	52.8	3.5	78.2	8.2	37.9	1.6	32.3	2.8
183	229504_at		0.97	0.68	38.4	2.6	56.8	7.4	110.7	13.5	97.1	21.5
184	218878_s_at		1.21	0.68	82.6	9.0	121.6	13.3	82.6	6.6	84.0	9.7
185	201925_s_at		1.20	0.68	93.7	10.6	137.7	11.0	117.7	17.3	128.4	33.1
186	222870_s_at		0.95	0.68	85.8	9.8	125.9	15.7	59.8	3.5	64.0	6.6
187	222815_at		1.13	0.68	39.5	1.6	57.9	6.8	69.9	10.0	66.5	10.2
188	225892_at		1.36	0.69	69.3	6.6	86.3	9.0	130.9	21.3	125.2	36.2
189	209005_at		1.14	0.69	23.5	0.9	34.0	2.0	77.8	3.7	87.0	11.5
190	226680_at		1.32	0.70	80.4	7.9	115.0	10.5	74.3	14.0	73.1	18.4

Probe sets showing significantly increased half-life in shRHAU dox+ cells.

Affymetrix ID	Description	ARE	shRHAU						shLuc					
			Fold change		half-life (min)				Fold change		half-life (min)			
			Steady-state	t1/2	dox+		dox-		dox+		dox-			
1	206495_s_at	MBD2 (methyl-CpG-binding protein)-interacting zinc finger protein	0.73	3.59	338.0	136.9	94.1	10.7	89.9	9.2	65.2	6.6		
2	213844_at	homeo box A5	0.80	3.06	139.2	34.2	45.5	3.4	53.8	7.1	32.7	6.7		
3	228445_at	apoptosis-inducing factor (AIF)-like mitochondrion-associated inducer of death	I - 5	0.81	2.81	592.2	170.7	210.5	50.9	130.6	24.1	103.4	20.8	
4	244049_at	RAB13, member RAS oncogene family		0.64	2.77	205.8	64.4	74.3	12.8	53.3	8.7	65.1	7.3	
5	226044_at	tyrosyl-DNA phosphodiesterase 1		0.76	2.66	236.3	71.2	88.7	18.6	87.7	16.1	61.4	10.7	
6	226130_at	ribosomal protein S16, similar to 40S ribosomal protein S16		0.69	2.55	123.6	37.2	48.4	9.5	71.0	10.3	50.6	11.4	
7	227452_at	CDNA FLJ26252 fis		0.48	2.50	107.6	19.7	43.1	4.7	57.2	8.1	53.4	4.5	
8	235355_at	CDNA FLJ30740 fis, clone FEBRA2000319		0.83	2.46	358.0	105.9	145.3	26.3	194.3	40.1	189.7	33.4	
9	240258_at	enolase 1, (alpha)		0.62	2.43	57.0	14.5	23.4	6.1	26.1	4.4	15.9	5.8	
10	203482_at	chromosome 10 open reading frame 6		0.84	2.41	301.8	99.2	125.1	12.8	141.6	26.8	120.0	16.9	
11	233369_at	gb:AU146027		0.70	2.34	180.5	41.7	77.0	20.5	88.5	15.8	116.7	31.0	
12	204780_s_at	Fas (TNF receptor superfamily, member 6)	I - 5	1.46	2.33	260.9	66.4	112.1	17.4	144.3	22.4	121.2	29.7	
13	237116_at	Profilin 2	I - 5	0.67	2.32	212.5	57.9	91.7	19.2	66.7	8.2	74.7	16.0	
14	205171_at	protein tyrosine phosphatase, non-receptor type 4 (megakaryocyte)		0.75	2.28	293.4	63.9	128.8	16.7	99.1	13.8	106.4	11.6	
15	203318_s_at	zinc finger protein 148 (pHZ52)		0.94	2.28	259.6	65.4	114.1	20.2	83.0	16.8	103.3	16.5	
16	218246_at	chromosome 1 open reading frame 166		0.78	2.24	162.1	45.9	72.3	9.7	91.6	9.2	75.8	6.3	
17	227124_at	MRNA full length insert cDNA clone EUROIMAGE 966164		1.09	2.22	329.3	61.4	148.5	16.6	63.9	6.9	56.1	6.4	
18	225204_at	T-cell activation protein phosphatase 2C	I - 5	0.98	2.16	367.5	91.4	170.2	13.9	99.2	15.2	131.2	22.0	
19	222732_at	tripartite motif-containing 39		0.78	2.15	224.8	50.8	104.6	13.9	103.0	22.0	142.2	43.1	
20	228676_at	oral cancer overexpressed 1		0.71	2.14	256.2	26.5	119.5	32.9	145.3	26.1	152.8	40.2	
21	235796_at	Exportin 7		0.74	2.13	136.1	28.1	63.9	13.3	56.9	5.6	45.1	8.9	
22	221660_at	gb:AL044078		0.84	2.13	148.1	36.1	69.7	11.1	106.9	27.0	70.0	16.9	
23	230738_at	Histone H4/e		0.80	2.12	185.9	33.0	87.8	10.7	83.9	20.6	88.7	22.6	
24	224458_at	chromosome 9 open reading frame 125		0.99	2.10	294.4	83.8	140.5	11.3	128.6	8.4	93.7	16.2	
25	238880_at	general transcription factor IIIA		0.81	2.09	134.0	33.1	64.0	8.8	60.1	15.4	44.6	6.2	
26	210239_at	iroquois homeobox protein 5	I - 5	0.66	2.08	94.3	17.7	45.3	6.7	38.4	6.8	46.3	8.4	
27	1557954_at	Retinoblastoma binding protein 7		1.06	2.05	309.0	82.9	150.5	11.3	113.1	14.2	102.7	17.1	
28	1568111_at	SRV (sex determining region Y)-box 13		0.88	2.05	224.7	50.9	109.6	20.9	84.0	15.7	89.2	15.8	
29	219595_at	zinc finger protein 26 (KOX 20)		1.05	2.05	187.2	35.0	91.5	12.4	60.6	7.6	54.6	6.3	
30	213654_at	TAFs-like RNA polymerase II, p300/CBP-associated factor (PCAF)-associated factor		1.02	2.05	199.2	44.8	97.4	18.2	116.1	26.1	73.9	12.6	
31	227606_s_at	associated molecule with the SH3 domain of STAM (AMSH) like protein		0.99	2.01	202.7	48.5	101.0	11.2	77.7	9.2	76.1	10.0	
32	224046_s_at	phosphodiesterase 7A	I - 5	1.04	2.00	168.9	32.0	84.4	12.2	88.3	15.0	82.6	11.1	
33	219906_at	hypothetical protein FLJ10213		0.72	1.98	106.4	24.3	53.8	6.0	50.1	5.9	48.6	7.6	
34	225920_at	hypothetical protein LOC148413		0.80	1.97	300.4	60.8	152.4	26.7	93.5	9.8	107.7	13.9	
35	226625_at	Transforming growth factor, beta receptor III (betaglycan, 300kDa)		1.18	1.97	142.3	19.1	72.4	8.6	60.9	8.0	NA	NA	
36	220770_s_at	transposon-derived Buster3 transposase-like		0.49	1.94	90.3	18.2	46.5	4.2	37.3	2.3	34.4	2.6	
37	213555_at	RWD domain containing 2		0.73	1.94	158.1	38.6	81.5	9.6	63.8	11.1	61.2	5.8	
38	37586_at	zinc finger protein 142 (clone pHZ-49)		0.94	1.94	165.9	34.8	85.5	12.2	111.3	8.1	NA	NA	
39	212153_at	pogo transposable element with ZNF domain		0.88	1.93	149.4	33.8	77.4	7.8	91.3	9.7	86.8	15.6	
40	218641_at	hypothetical protein MGC3032		0.94	1.92	162.2	22.4	84.3	6.5	50.5	6.7	44.7	6.4	
41	225998_at	GRB2-associated binding protein 1		1.01	1.92	114.2	14.8	59.5	7.6	55.0	3.3	52.9	8.7	
42	201834_at	protein kinase, AMP-activated, beta 1 non-catalytic subunit		0.80	1.89	136.7	17.8	72.2	11.8	53.7	6.8	56.0	7.8	
43	229793_at	CDNA FLJ27121 fis, clone SPL06753		0.92	1.89	169.4	36.0	89.8	9.8	68.2	10.6	79.4	17.3	
44	201236_s_at	BTC family, member 2		0.80	1.87	124.4	23.5	66.4	13.2	45.4	6.4	71.9	13.8	
45	206261_at	zinc finger protein 239	I - 5	0.75	1.86	155.8	27.2	83.7	12.6	87.3	15.9	94.4	20.2	
46	227072_at	rotatin		1.08	1.86	326.7	47.8	176.0	19.5	135.2	26.3	157.0	30.4	
47	230330_at	Protein phosphatase 1D magnesium-dependent, delta isoform		0.74	1.85	123.6	23.4	67.0	7.1	48.7	5.1	50.6	6.4	
48	219810_at	valosin containing protein (p97)/p47 complex interacting protein 1		0.87	1.82	160.6	28.0	88.3	10.1	80.4	9.0	85.9	12.7	
49	213198_at	activin A receptor, type IB		1.24	1.82	163.4	32.6	89.9	9.7	112.8	15.1	114.6	16.7	
50	212978_at	Hypothetical gene supported by AK130864		0.98	1.78	168.9	27.7	94.8	14.4	54.1	4.4	48.1	5.1	
51	213407_at	PH domain and leucine rich repeat protein phosphatase-like	I - 5	0.99	1.78	94.0	18.1	52.8	7.5	42.8	4.0	40.6	5.4	
52	223023_at	blocked early in transport 1 homolog (S. cerevisiae)-like		0.77	1.77	135.0	23.3	76.1	4.7	68.4	10.1	60.6	7.5	
53	202924_s_at	pleiomorphic adenoma gene-like 2	I - 5	0.82	1.77	59.1	9.9	33.4	4.3	43.4	3.9	30.4	4.6	
54	202743_at	phosphoinositide-3-kinase, regulatory subunit 3 (p55, gamma)		0.86	1.77	93.7	13.5	53.0	3.5	45.0	3.7	40.1	4.6	
55	227825_at	chromosome 9 open reading frame 90		0.87	1.76	92.6	13.6	52.6	5.0	53.1	4.1	52.2	5.8	
56	225927_at	mitogen-activated protein kinase kinase kinase 1		1.18	1.76	108.4	13.3	61.7	10.1	64.6	11.0	67.2	8.6	
57	229518_at	family with sequence similarity 46, member B		0.79	1.75	68.8	13.7	39.4	4.0	40.4	6.9	41.1	4.7	
58	223424_s_at	zinc finger protein 38		0.73	1.73	76.2	12.8	43.9	3.9	55.6	5.9	59.0	9.4	
59	214438_at	H2.D-like homeo box 1 (Drosophila)		0.84	1.73	100.4	10.7	58.2	8.0	57.4	5.6	53.1	7.9	
60	228536_at	hypothetical protein BC004337		0.92	1.71	175.7	25.0	102.7	10.8	92.1	8.1	90.8	8.0	
61	244407_at	cytochrome P450, family 39, subfamily A, polypeptide 1		0.80	1.69	133.5	22.9	79.0	8.8	89.4	12.9	101.8	17.3	
62	233461_x_at	zinc finger protein 226		0.90	1.67	130.6	20.6	78.2	11.0	76.9	9.3	90.7	12.8	
63	226155_at	KJAA1600		1.10	1.65	148.2	28.9	89.6	6.9	60.9	5.3	61.1	6.4	
64	227339_at	RGM domain family, member B		0.84	1.64	92.1	13.3	56.3	6.6	49.2	5.2	51.3	7.7	
65	221135_s_at	HTDD1 protein		0.81	1.63	79.4	11.6	48.8	5.0	51.5	5.3	54.2	7.8	
66	214805_at	Eukaryotic translation initiation factor 4A, isoform 1		0.81	1.62	62.7	12.0	38.8	3.2	42.2	2.6	30.8	3.4	
67	218399_s_at	cell division cycle associated 4		0.94	1.62	118.6	20.4	73.3	8.1	65.3	9.0	57.5	8.4	
68	226866_at	establishment of cohesion 1 homolog 1 (S. cerevisiae)		0.82	1.62	166.8	17.9	103.3	7.4	75.9	7.2	70.2	8.4	
69	220444_at	zinc finger protein 557		0.97	1.61	67.4	11.4	41.8	4.1	37.6	6.5	23.3	3.9	
70	208686_s_at	bromodomain containing 2		0.86	1.59	101.8	17.8	64.1	4.4	55.4	10.0	50.3	7.8	
71	212447_at	kelch repeat and BTB (POZ) domain containing 2	I - 5	1.00	1.57	95.8	12.9	60.9	6.1	42.3	4.6	43.8	3.5	
72	204695_at	cell division cycle 25A		0.78	1.56	85.5	10.1	54.8	3.1	53.4	3.4	48.0	4.0	
73	201010_s_at	thioredoxin interacting protein		1.11	1.55	33.2	4.5	21.3	2.5	27.6	2.6	22.8	2.6	
74	218528_s_at	ring finger protein 38		1.17	1.55	77.9	11.8	50.4	4.6	43.7	3.5	47.2	8.5	
75	224832_at	dual specificity phosphatase 16		0.87	1.54	69.4	9.4	45.0	2.7	41.1	6.9	42.9	8.3	
76	225033_at	hypothetical protein LOC286167	I - 5	0.92	1.54	49.5	7.7	32.1	1.7	27.1	5.9	33.7	5.6	
77	223689_at	zinc finger protein 416		0.93	1.52	27.7	2.7	18.2	2.6	20.9	1.6	23.1	2.0	
78	201008_s_at	thioredoxin interacting protein		1.01	1.52	46.8	5.6	30.9	4.2	40.4	4.9	38.0	4.6	
79	225077_at	hypothetical protein LOC283680		0.99	1.50	67.8	9.2	45.1	3.4	43.4	8.2	46.8	6.4	
80	204433_s_at	spermatogenesis associated 2		1.01	1.50	74.6	10.3	49.8	4.7	36.8	5.5	39.7	8.4	
81	202301_s_at	similar to splicing factor, arginine/serine-rich 4		0.86	1.49	140.0	1							

APPENDIX - IV : Starvation-sensitive genes

Probe sets showing up-regulation in starving culture condition.

Affymetrix ID	Description	Gene Symbol	fold - normal / stv		SE		
			shLuc	shRHAU	shLuc	shRHAU	
1	206893_s_at	dual specificity phosphatase 6	DUSP6	8.23	19.58	0.84	2.92
2	206892_s_at	dual specificity phosphatase 6	DUSP6	10.31	18.31	1.13	1.99
3	202688_at	tumor necrosis factor (ligand) superfamily, member 10	TNFSF10	7.80	16.62	1.51	2.49
4	206891_at	dual specificity phosphatase 6	DUSP6	9.10	14.79	1.86	1.16
5	202687_s_at	tumor necrosis factor (ligand) superfamily, member 10	TNFSF10	7.67	14.58	1.23	3.25
6	214329_x_at	tumor necrosis factor (ligand) superfamily, member 10	TNFSF10	4.49	10.14	1.60	3.21
7	204036_at	lysophosphatic acid G-protein-coupled receptor, 2	EDG2	4.19	6.98	0.37	0.96
8	203914_x_at	hydroxyprostaglandin dehydrogenase 15-(NAD)	HPGD	5.88	6.57	1.08	0.56
9	229242_at	Transcribed locus		5.53	6.53	1.28	1.02
10	211548_s_at	hydroxyprostaglandin dehydrogenase 15-(NAD)	HPGD	5.10	6.27	0.49	1.86
11	202859_x_at	interleukin 8	IL8	6.55	6.27	1.37	1.35
12	203349_s_at	ets variant gene 5 (ets-related molecule)	ETV5	3.59	6.00	1.07	0.93
13	219914_at	endothelin converting enzyme-like 1	ECEL1	3.85	5.97	0.45	0.86
14	1564511_a_at	folistatin-like 4	FSTL4	4.60	5.86	0.91	1.73
15	225762_x_at	hypothetical protein LOC284801	LOC284801	3.47	5.84	0.58	1.43
16	209189_at	v-fos FBJ murine osteosarcoma viral oncogene homolog	FOS	3.98	5.75	0.59	0.90
17	232898_at	disabled homolog 2, mitogen-responsive phosphoprotein (Drosophila)	DAB2	3.45	5.58	1.06	2.23
18	229674_at	SERTA domain containing 4	SERTAD4	2.47	5.38	0.39	0.98
19	221911_at	ets variant gene 1	ETV1	5.51	5.10	1.70	1.00
20	243586_at	Phosphodiesterase 4D, cAMP-specific	PDE4D	3.12	5.09	0.79	1.60
21	228918_at	Solute carrier family 43, member 2	SLC43A2	3.42	5.04	0.74	1.43
22	207214_at	serine peptidase inhibitor, Kazal type 4	SPINK4	5.62	4.97	0.95	0.65
23	202566_s_at	supervillin	SVIL	3.27	4.95	0.70	0.32
24	205654_at	complement component 4 binding protein, alpha	C4BPA	2.63	4.89	0.30	0.61
25	230012_at	hypothetical protein FLJ34790	FLJ34790	2.45	4.82	0.24	0.97
26	225767_at	hypothetical protein LOC284801	LOC284801	3.19	4.70	0.96	1.04
27	244387_at	Transcribed locus		3.46	4.65	0.84	1.70
28	204072_s_at	hypothetical protein CG003	13CDNA73	5.85	4.62	0.52	0.70
29	203913_s_at	hydroxyprostaglandin dehydrogenase 15-(NAD)	HPGD	3.52	4.53	0.55	1.36
30	232867_at	Hypothetical protein LOC285513	LOC285513	2.03	4.51	0.15	0.91
31	204664_at	alkaline phosphatase, placental (Regan isozyme)	ALPP	4.41	4.36	0.64	0.77
32	1554576_a_at	ets variant gene 4 (E1A enhancer binding protein, E1AF)	ETV4	2.43	4.31	0.50	0.84
33	229569_at	CDNA FLJ32413 fis, clone SKMUS2000705		6.59	4.31	1.05	0.50
34	204595_s_at	stanniocalcin 1	STC1	2.34	4.29	0.43	0.83
35	229178_at	hypothetical protein LOC145786	LOC145786	2.26	4.27	0.24	0.30
36	207723_s_at	killer cell lectin-like receptor subfamily C, member 3	KLRC3	3.82	4.18	0.23	0.57
37	225166_at	Rho GTPase activating protein 18	ARHGAP18	4.92	4.17	0.48	0.77
38	229073_at	Protogenin homolog (Gallus gallus)	PRTG	2.78	4.09	0.51	0.66
39	235099_at	chemokine-like factor superfamily 8	CKLFSF8	3.09	3.93	0.42	0.67
40	204622_x_at	nuclear receptor subfamily 4, group A, member 2	NR4A2	3.86	3.82	0.56	0.62
41	221060_s_at	toll-like receptor 4, toll-like receptor 4	TLR4	2.39	3.81	0.11	0.21
42	231136_at	gb:AJ087792.DB		3.27	3.79	0.63	0.86
43	203414_at	monocyte to macrophage differentiation-associated	MMD	2.95	3.76	0.29	0.38
44	219764_at	frizzled homolog 10 (Drosophila)	FZD10	4.49	3.73	0.38	0.42
45	204037_at	lysophosphatic acid G-protein-coupled receptor, 2	EDG2	2.25	3.72	0.35	0.69
46	218858_at	DEP domain containing 6	DEPDC6	2.88	3.71	0.48	0.60
47	239270_at	phosphatidylinositol-specific phospholipase C, X domain containing 3	PLCXD3	4.33	3.69	0.79	0.54
48	233547_x_at	phosphodiesterase 1A, calmodulin-dependent	PDE1A	2.78	3.67	0.34	0.38
49	230081_at	phosphatidylinositol-specific phospholipase C, X domain containing 3	PLCXD3	5.30	3.62	0.67	0.51
50	203474_at	IG motif containing GTPase activating protein 2	IGGAP2	3.91	3.60	0.46	0.23
51	208396_s_at	phosphodiesterase 1A, calmodulin-dependent	PDE1A	3.02	3.54	0.34	0.46
52	225173_at	Rho GTPase activating protein 18	ARHGAP18	3.71	3.54	0.73	0.77
53	213222_at	phospholipase C, beta 1 (phosphoinositide-specific)	PLCB1	2.50	3.51	0.21	0.41
54	223075_s_at	chromosome 9 open reading frame 58	C9orf58	3.45	3.51	0.34	0.28
55	202761_s_at	spectrin repeat containing, nuclear envelope 2	SYNE2	2.05	3.50	0.33	0.43
56	225171_at	Rho GTPase activating protein 18	ARHGAP18	3.03	3.48	0.32	0.34
57	238751_at	Sorbin and SH3 domain containing 2	SORBS2	2.38	3.48	0.51	1.18
58	230102_at	Ets variant gene 5 (ets-related molecule)	ETV5	2.46	3.42	0.36	1.32
59	204798_at	v-myb myeloblastosis viral oncogene homolog (avian)	MYB	3.54	3.39	0.66	0.18
60	204519_s_at	plasma membrane proteolipid (plasmalipin)	PLLP	3.09	3.36	0.23	0.61
61	212646_at	raft-linking protein	RAFTLIN	2.58	3.33	0.11	0.24
62	216248_s_at	nuclear receptor subfamily 4, group A, member 2	NR4A2	3.39	3.32	0.33	0.43
63	202565_s_at	supervillin	SVIL	2.66	3.28	0.22	0.35
64	212942_s_at	KIAA1199	KIAA1199	2.31	3.27	0.23	0.19
65	1552695_a_at	solute carrier family 2 (facilitated glucose transporter), member 13	SLC2A13	2.16	3.27	0.38	0.63
66	238441_at	Protein kinase, AMP-activated, alpha 2 catalytic subunit	PRKAA2	2.70	3.22	0.56	0.56
67	235592_at	CDNA clone IMAGE:4903593		2.90	3.20	0.44	0.45
68	230746_s_at	Stanniocalcin 1	STC1	6.38	3.20	1.95	1.44
69	225123_at	Sestrin 3	SESN3	2.97	3.18	0.45	0.77
70	215811_at	Synuclein, alpha (non A4 component of amyloid precursor)	SNCA	2.64	3.16	0.42	1.01
71	226884_at	leucine rich repeat neuronal 1	LRRN1	3.90	3.15	0.61	0.29
72	204440_at	CD83 antigen (activated B lymphocytes, immunoglobulin superfamily)	CD83	3.49	3.14	0.59	0.31
73	227819_at	leucine-rich repeat-containing G protein-coupled receptor 6	LGR6	2.78	3.14	0.44	0.59
74	204476_s_at	pyruvate carboxylase	PC	3.00	3.12	0.35	0.44
75	236610_at	Phosphodiesterase 4D, cAMP-specific	PDE4D	3.00	3.10	0.65	0.73
76	201852_x_at	collagen, type III, alpha 1	COL3A1	2.10	3.06	0.20	0.23
77	215076_s_at	collagen, type III, alpha 1	COL3A1	2.24	3.05	0.17	0.31
78	224341_x_at	toll-like receptor 4, toll-like receptor 4	TLR4	2.71	3.04	0.54	0.58
79	241681_at	Muscleblind-like (Drosophila)	MBNL1	2.41	3.04	0.21	0.74
80	227176_at	Solute carrier family 2 (facilitated glucose transporter), member 13	SLC2A13	2.38	3.04	0.38	0.43
81	201280_s_at	disabled homolog 2, mitogen-responsive phosphoprotein (Drosophila)	DAB2	2.70	3.02	0.29	0.38
82	230518_at	epithelial V-like antigen 1	EVA1	3.53	3.01	0.49	0.38

Probe sets showing down-regulation in starving culture condition.

Affymetrix ID	Description	Gene Symbol	fold - normal / stv		SE	
			shLuc	shRHAU	shLuc	shRHAU
1	1555724_s_at	transgelin	0.057	0.042	0.009	0.008
2	205547_s_at	transgelin	0.063	0.044	0.007	0.005
3	205132_at	actin, alpha, cardiac muscle	0.137	0.062	0.027	0.008
4	229339_at	Transcribed locus	0.166	0.094	0.007	0.003
5	237206_at	myocardin	0.202	0.096	0.037	0.024
6	205798_at	interleukin 7 receptor, interleukin 7 receptor	0.270	0.097	0.029	0.016
7	229125_at	ankyrin repeat domain 38	0.090	0.099	0.010	0.012
8	221541_at	cysteine-rich secretory protein LCCL domain containing 2	0.130	0.104	0.018	0.012
9	226218_at	Interleukin 7 receptor	0.326	0.113	0.036	0.011
10	204368_at	solute carrier organic anion transporter family, member 2A1	0.144	0.118	0.012	0.016
11	209230_s_at	p8 protein (candidate of metastasis 1)	0.179	0.146	0.033	0.011
12	220191_at	gastrokine 1	0.212	0.152	0.045	0.018
13	202628_s_at	serpin peptidase inhibitor, clade E	0.227	0.186	0.027	0.012
14	201565_s_at	inhibitor of DNA binding 2, dominant negative helix-loop-helix protein	0.376	0.184	0.088	0.048
15	219874_at	solute carrier family 12 (potassium/chloride transporters), member 8	0.437	0.189	0.075	0.040
16	209758_s_at	microfibrillar associated protein 5	0.159	0.194	0.028	0.029
17	204222_s_at	GLI pathogenesis-related 1 (glioma)	0.181	0.200	0.028	0.031
18	239370_at	gb:AV081982	0.281	0.217	0.056	0.036
19	202627_s_at	serpin peptidase inhibitor, clade E	0.283	0.224	0.030	0.023
20	209016_s_at	keratin 7	0.317	0.231	0.037	0.024
21	226136_at	gb:N32834 /DB_XREF=gi:1153233	0.226	0.242	0.019	0.018
22	201566_x_at	inhibitor of DNA binding 2	0.413	0.244	0.042	0.066
23	203828_s_at	interleukin 32, interleukin 32	0.467	0.245	0.087	0.021
24	220266_s_at	Kruppel-like factor 4 (gut)	0.261	0.250	0.054	0.033
25	219529_at	chloride intracellular channel 3	0.445	0.253	0.091	0.053
26	218559_s_at	v-maf musculoaponeurotic fibrosarcoma oncogene homolog B (avian)	0.430	0.253	0.021	0.018
27	205157_s_at	keratin 17	0.462	0.255	0.051	0.035
28	226142_at	GLI pathogenesis-related 1 (glioma)	0.225	0.256	0.027	0.027
29	1560477_a_at	sterile alpha motif domain containing 11	0.391	0.259	0.064	0.061
30	205047_s_at	asparagine synthetase	0.249	0.260	0.022	0.025
31	201506_at	transforming growth factor, beta-induced, 68kDa	0.314	0.268	0.017	0.017
32	202434_s_at	cytochrome P450, family 1, subfamily B, polypeptide 1	0.184	0.268	0.061	0.102
33	212236_x_at	keratin 17	0.480	0.268	0.039	0.030
34	214085_x_at	GLI pathogenesis-related 1 (glioma)	0.277	0.272	0.051	0.038
35	227919_at	UCA1 protein	0.380	0.283	0.049	0.029
36	1569765_at	CDNA clone IMAGE:4812570	0.324	0.284	0.010	0.021
37	1559433_at	CDNA FLJ34385 fis, clone HCHON1000142	0.387	0.285	0.049	0.030
38	1556200_a_at	chromosome 10 open reading frame 90	0.496	0.287	0.054	0.053
39	208937_s_at	inhibitor of DNA binding 1, dominant negative helix-loop-helix protein	0.348	0.290	0.025	0.025
40	229518_at	family with sequence similarity 46, member B	0.387	0.296	0.031	0.018
41	209949_at	neutrophil cytosolic factor 2 (65kDa, chronic granulomatous disease, autosomal 2)	0.239	0.297	0.074	0.071
42	226876_at	hypothetical protein MGC45871	0.306	0.301	0.031	0.043
43	206582_s_at	G protein-coupled receptor 56	0.437	0.312	0.097	0.082
44	204221_x_at	GLI pathogenesis-related 1 (glioma)	0.273	0.313	0.031	0.043
45	211981_at	collagen, type IV, alpha 1	0.476	0.318	0.031	0.046
46	221841_s_at	Kruppel-like factor 4 (gut)	0.458	0.320	0.019	0.025
47	206101_at	extracellular matrix protein 2, female organ and adipocyte specific	0.297	0.329	0.035	0.047
48	226905_at	hypothetical protein MGC45871	0.283	0.331	0.010	0.017
49	207147_at	distal-less homeo box 2	0.302	0.336	0.032	0.035
50	206117_at	tropomyosin 1 (alpha)	0.472	0.337	0.039	0.031
51	213711_at	keratin, hair, basic, 1	0.302	0.341	0.041	0.034
52	203665_at	heme oxygenase (decycling) 1	0.454	0.342	0.042	0.058
53	203058_s_at	3'-phosphoadenosine 5'-phosphosulfate synthase 2	0.459	0.346	0.026	0.056
54	1555355_a_at	v-ets erythroblastosis virus E26 oncogene homolog 1 (avian)	0.450	0.353	0.066	0.039
55	226248_s_at	KIAA1324	0.394	0.354	0.097	0.084
56	201194_at	selenoprotein W, 1	0.362	0.355	0.027	0.025
57	201108_s_at	thrombospondin 1	0.331	0.359	0.035	0.036
58	235236_at	Dedicator of cytokinesis 2	0.302	0.365	0.023	0.048
59	208782_at	folliculin-like 1	0.414	0.374	0.030	0.034
60	228158_at	PREDICTED: Homo sapiens similar to D(1B) dopamine receptor	0.454	0.385	0.085	0.080
61	229004_at	CDNA FLJ26557 fis, clone LNF01992	0.458	0.391	0.027	0.056
62	209010_s_at	triple functional domain (PTPRF interacting)	0.443	0.400	0.106	0.111
63	235367_at	myopalladin	0.385	0.401	0.065	0.034
64	213764_s_at	microfibrillar associated protein 5	0.425	0.403	0.061	0.073
65	207528_s_at	solute carrier family 7, (cationic amino acid transporter, y+ system) member 11	0.331	0.409	0.041	0.086
66	1555851_s_at	selenoprotein W, 1	0.423	0.410	0.028	0.036
67	213880_at	leucine-rich repeat-containing G protein-coupled receptor 5	0.459	0.410	0.063	0.019
68	207826_s_at	inhibitor of DNA binding 3, dominant negative helix-loop-helix protein	0.492	0.411	0.045	0.048
69	204794_at	dual specificity phosphatase 2	0.368	0.413	0.037	0.034
70	202435_s_at	cytochrome P450, family 1, subfamily B, polypeptide 1	0.254	0.418	0.059	0.053
71	203592_s_at	folliculin-like 3 (secreted glycoprotein)	0.456	0.421	0.008	0.049
72	219702_at	placenta-specific 1	0.501	0.424	0.090	0.048
73	1569555_at	guanine deaminase	0.501	0.431	0.037	0.066
74	209800_at	keratin 16 (focal non-epidermolytic palmoplantar keratoderma)	0.324	0.434	0.024	0.047
75	201058_s_at	myosin, light polypeptide 9, regulatory	0.425	0.439	0.054	0.077
76	221276_s_at	syncollin, intermediate filament 1, syncollin, intermediate filament 1	0.483	0.439	0.035	0.049
77	220333_at	progesterin and adipoQ receptor family member V	0.478	0.440	0.081	0.027
78	235350_at	Transcribed locus	0.468	0.442	0.079	0.045
79	233737_s_at	hypothetical protein LOC284561	0.228	0.444	0.024	0.055
80	209588_at	EPH receptor B2	0.482	0.449	0.106	0.083
81	209383_at	DNA-damage-inducible transcript 3	0.438	0.450	0.076	0.038
82	202847_at	phosphoenolpyruvate carboxykinase 2 (mitochondrial)	0.448	0.450	0.025	0.035
83	201466_s_at	v-jun sarcoma virus 17 oncogene homolog (avian)	0.468	0.452	0.045	0.034
84	241759_at	Adenosine deaminase	0.484	0.453	0.062	0.071
85	202437_s_at	cytochrome P450, family 1, subfamily B, polypeptide 1	0.301	0.458	0.031	0.068
86	238462_at	Cbl-interacting protein Sts-1	0.447	0.463	0.073	0.063
87	202436_s_at	cytochrome P450, family 1, subfamily B, polypeptide 1	0.270	0.464	0.032	0.043
88	211527_x_at	vascular endothelial growth factor	0.436	0.467	0.046	0.060
89	205207_at	interleukin 6 (interferon, beta 2)	0.282	0.475	0.027	0.048
90	205194_at	phosphoserine phosphatase	0.427	0.481	0.087	0.110
91	219014_at	placenta-specific 8	0.463	0.481	0.037	0.038
92	204797_s_at	echinoderm microtubule associated protein like 1	0.502	0.488	0.067	0.055
93	228923_at	S100 calcium binding protein A6 (calycylin)	0.474	0.495	0.037	0.113
94	226516_at	chromosome 19 open reading frame 26	0.464	0.502	0.039	0.095
95	225867_at	slit-like 2 (Drosophila)	0.435	0.513	0.042	0.116

Up- and down-regulated probe sets in both HeLa-shLuc and HeLa-shRHAU cells (dox-) in serum-starved (STV) condition compared to not-starved condition. fold change, between not-starved (cells cultured with FCS) and starved cells derived by expression value in FCS- divided by FCS+ ;SE,, standard error of the fold-differences.

REFERENCES

- Abdelhaleem, M., Maltais, L., and Wain, H. 2003. The human DDX and DHX gene families of putative RNA helicases. *Genomics* **81**(6): 618-622.
- Abovich, N. and Rosbash, M. 1997. Cross-intron bridging interactions in the yeast commitment complex are conserved in mammals. *Cell* **89**(3): 403-412.
- Anantharaman, V., Koonin, E.V., and Aravind, L. 2002. Comparative genomics and evolution of proteins involved in RNA metabolism. *Nucleic Acids Res* **30**(7): 1427-1464.
- Andersen, C.B., Ballut, L., Johansen, J.S., Chamieh, H., Nielsen, K.H., Oliveira, C.L., Pedersen, J.S., Seraphin, B., Le Hir, H., and Andersen, G.R. 2006. Structure of the exon junction core complex with a trapped DEAD-box ATPase bound to RNA. *Science* **313**(5795): 1968-1972.
- Andersen, J.S., Lam, Y.W., Leung, A.K., Ong, S.E., Lyon, C.E., Lamond, A.I., and Mann, M. 2005. Nucleolar proteome dynamics. *Nature* **433**(7021): 77-83.
- Andersen, J.S., Lyon, C.E., Fox, A.H., Leung, A.K., Lam, Y.W., Steen, H., Mann, M., and Lamond, A.I. 2002. Directed proteomic analysis of the human nucleolus. *Curr Biol* **12**(1): 1-11.
- Anderson, P. and Kedersha, N. 2002. Visibly stressed: the role of eIF2, TIA-1, and stress granules in protein translation. *Cell stress & chaperones* **7**(2): 213-221.
- Anderson, S.F., Schlegel, B.P., Nakajima, T., Wolpin, E.S., and Parvin, J.D. 1998. BRCA1 protein is linked to the RNA polymerase II holoenzyme complex via RNA helicase A. *Nature genetics* **19**(3): 254-256.
- Bakheet, T., Williams, B.R., and Khabar, K.S. 2006. ARED 3.0: the large and diverse AU-rich transcriptome. *Nucleic Acids Res* **34**(Database issue): D111-114.
- Bates, G.J., Nicol, S.M., Wilson, B.J., Jacobs, A.M., Bourdon, J.C., Wardrop, J., Gregory, D.J., Lane, D.P., Perkins, N.D., and Fuller-Pace, F.V. 2005. The DEAD box protein p68: a novel transcriptional coactivator of the p53 tumour suppressor. *Embo J* **24**(3): 543-553.
- Bernstein, P.L., Herrick, D.J., Prokipcak, R.D., and Ross, J. 1992. Control of c-myc mRNA half-life in vitro by a protein capable of binding to a coding region stability determinant. *Genes Dev* **6**(4): 642-654.
- Bhattacharyya, S.N., Habermacher, R., Martine, U., Closs, E.I., and Filipowicz, W. 2006. Relief of microRNA-mediated translational repression in human cells subjected to stress. *Cell* **125**(6): 1111-1124.
- Bialik, S. and Kimchi, A. 2006. The Death-Associated Protein Kinases: Structure, Function, and Beyond. *Annu Rev Biochem*.
- Binder, R., Horowitz, J.A., Basilion, J.P., Koeller, D.M., Klausner, R.D., and Harford, J.B. 1994. Evidence that the pathway of transferrin receptor mRNA degradation involves an endonucleolytic cleavage within the 3' UTR and does not involve poly(A) tail shortening. *Embo J* **13**(8): 1969-1980.
- Bolinger, C., Yilmaz, A., Hartman, T.R., Kovacic, M.B., Fernandez, S., Ye, J., Forget, M., Green, P.L., and Boris-Lawrie, K. 2007. RNA helicase A interacts with divergent lymphotropic retroviruses and promotes translation of human T-cell leukemia virus type 1. *Nucleic Acids Res* **35**(8): 2629-2642.
- Bono, F., Ebert, J., Lorentzen, E., and Conti, E. 2006. The crystal structure of the exon junction complex reveals how it maintains a stable grip on mRNA. *Cell* **126**(4): 713-725.
- Bowers, H.A., Maroney, P.A., Fairman, M.E., Kastner, B., Luhrmann, R., Nilsen, T.W., and Jankowsky, E. 2006. Discriminatory RNP remodeling by the DEAD-box protein DED1. *Rna* **12**(5): 903-912.
- Bridge, A.J., Pebernard, S., Ducraux, A., Nicoulaz, A.L., and Iggo, R. 2003. Induction of an interferon response by RNAi vectors in mammalian cells. *Nature genetics* **34**(3): 263-264.
- Caput, D., Beutler, B., Hartog, K., Thayer, R., Brown-Shimer, S., and Cerami, A. 1986. Identification of a common nucleotide sequence in the 3'-untranslated region of mRNA molecules specifying inflammatory mediators. *Proc Natl Acad Sci U S A* **83**(6): 1670-1674.

- Caretti, G., Schiltz, R.L., Dilworth, F.J., Di Padova, M., Zhao, P., Ogryzko, V., Fuller-Pace, F.V., Hoffman, E.P., Tapscott, S.J., and Sartorelli, V. 2006. The RNA helicases p68/p72 and the noncoding RNA SRA are coregulators of MyoD and skeletal muscle differentiation. *Dev Cell* **11**(4): 547-560.
- Chan, A.W., Chan, M.W., Lee, T.L., Ng, E.K., Leung, W.K., Lau, J.Y., Tong, J.H., Chan, F.K., and To, K.F. 2005. Promoter hypermethylation of Death-associated protein-kinase gene associated with advance stage gastric cancer. *Oncol Rep* **13**(5): 937-941.
- Cheadle, C., Fan, J., Cho-Chung, Y.S., Werner, T., Ray, J., Do, L., Gorospe, M., and Becker, K.G. 2005. Control of gene expression during T cell activation: alternate regulation of mRNA transcription and mRNA stability. *BMC Genomics* **6**(1): 75.
- Chen, C.Y., Del Gatto-Konczak, F., Wu, Z., and Karin, M. 1998. Stabilization of interleukin-2 mRNA by the c-Jun NH2-terminal kinase pathway. *Science* **280**(5371): 1945-1949.
- Chen, C.Y., Gherzi, R., Ong, S.E., Chan, E.L., Raijmakers, R., Pruijn, G.J., Stoecklin, G., Moroni, C., Mann, M., and Karin, M. 2001. AU binding proteins recruit the exosome to degrade ARE-containing mRNAs. *Cell* **107**(4): 451-464.
- Chen, C.Y. and Shyu, A.B. 1995. AU-rich elements: characterization and importance in mRNA degradation. *Trends Biochem Sci* **20**(11): 465-470.
- Colley, A., Beggs, J.D., Tollervey, D., and Lafontaine, D.L. 2000. Dhr1p, a putative DEAH-box RNA helicase, is associated with the box C+D snoRNP U3. *Mol Cell Biol* **20**(19): 7238-7246.
- Cordin, O., Banroques, J., Tanner, N.K., and Linder, P. 2006. The DEAD-box protein family of RNA helicases. *Gene* **367**: 17-37.
- Curwen, V., Eyraes, E., Andrews, T.D., Clarke, L., Mongin, E., Searle, S.M., and Clamp, M. 2004. The Ensembl automatic gene annotation system. *Genome Res* **14**(5): 942-950.
- de la Cruz, J., Kressler, D., and Linder, P. 1999. Unwinding RNA in *Saccharomyces cerevisiae*: DEAD-box proteins and related families. *Trends Biochem Sci* **24**(5): 192-198.
- Dreyfuss, G., Kim, V.N., and Kataoka, N. 2002. Messenger-RNA-binding proteins and the messages they carry. *Nature reviews* **3**(3): 195-205.
- Dumont, S., Cheng, W., Serebrov, V., Beran, R.K., Tinoco, I., Jr., Pyle, A.M., and Bustamante, C. 2006. RNA translocation and unwinding mechanism of HCV NS3 helicase and its coordination by ATP. *Nature* **439**(7072): 105-108.
- Enukashvily, N., Donev, R., Sheer, D., and Podgornaya, O. 2005. Satellite DNA binding and cellular localisation of RNA helicase P68. *J Cell Sci* **118**(Pt 3): 611-622.
- Eulalio, A., Behm-Ansmant, I., and Izaurralde, E. 2007. P bodies: at the crossroads of post-transcriptional pathways. *Nature reviews* **8**(1): 9-22.
- Fairman, M.E., Maroney, P.A., Wang, W., Bowers, H.A., Gollnick, P., Nilsen, T.W., and Jankowsky, E. 2004. Protein displacement by DExH/D "RNA helicases" without duplex unwinding. *Science* **304**(5671): 730-734.
- Fan, J., Yang, X., Wang, W., Wood, W.H., 3rd, Becker, K.G., and Gorospe, M. 2002. Global analysis of stress-regulated mRNA turnover by using cDNA arrays. *Proc Natl Acad Sci U S A* **99**(16): 10611-10616.
- Fey, E.G., Krochmalnic, G., and Penman, S. 1986. The nonchromatin substructures of the nucleus: the ribonucleoprotein (RNP)-containing and RNP-depleted matrices analyzed by sequential fractionation and resinless section electron microscopy. *J Cell Biol* **102**(5): 1654-1665.
- Fong, Y.W. and Zhou, Q. 2001. Stimulatory effect of splicing factors on transcriptional elongation. *Nature* **414**(6866): 929-933.
- Franks, T.M. and Lykke-Andersen, J. 2007. TTP and BRF proteins nucleate processing body formation to silence mRNAs with AU-rich elements. *Genes Dev* **21**(6): 719-735.

- Fukuda, T., Yamagata, K., Fujiyama, S., Matsumoto, T., Koshida, I., Yoshimura, K., Mihara, M., Naitou, M., Endoh, H., Nakamura, T., Akimoto, C., Yamamoto, Y., Katagiri, T., Foulds, C., Takezawa, S., Kitagawa, H., Takeyama, K.I., O'Malley B, W., and Kato, S. 2007. DEAD-box RNA helicase subunits of the Drosha complex are required for processing of rRNA and a subset of microRNAs. *Nat Cell Biol*.
- Fuller-Pace, F.V. 2006. DExD/H box RNA helicases: multifunctional proteins with important roles in transcriptional regulation. *Nucleic Acids Res* **34**(15): 4206-4215.
- Gallouzi, I.E. and Steitz, J.A. 2001. Delineation of mRNA export pathways by the use of cell-permeable peptides. *Science* **294**(5548): 1895-1901.
- Gao, M., Wilusz, C.J., Peltz, S.W., and Wilusz, J. 2001. A novel mRNA-decapping activity in HeLa cytoplasmic extracts is regulated by AU-rich elements. *Embo J* **20**(5): 1134-1143.
- Gouka, R.J., Stam, H., Fellingner, A.J., Muijsenberg, R.J., van de Wijngaard, A., Punt, P.J., Musters, W., and van den Hondel, C.A. 1996. Kinetics of mRNA and protein synthesis of genes controlled by the 1,4-beta-endoxylanase A promoter in controlled fermentations of *Aspergillus awamori*. *Appl Environ Microbiol* **62**(10): 3646-3649.
- Guhaniyogi, J. and Brewer, G. 2001. Regulation of mRNA stability in mammalian cells. *Gene* **265**(1-2): 11-23.
- Guil, S., Gattoni, R., Carrascal, M., Abian, J., Stevenin, J., and Bach-Elias, M. 2003. Roles of hnRNP A1, SR proteins, and p68 helicase in c-H-ras alternative splicing regulation. *Mol Cell Biol* **23**(8): 2927-2941.
- Hall, L.L., Smith, K.P., Byron, M., and Lawrence, J.B. 2006. Molecular anatomy of a speckle. *Anat Rec A Discov Mol Cell Evol Biol* **288**(7): 664-675.
- Haraguchi, T., Holaska, J.M., Yamane, M., Koujin, T., Hashiguchi, N., Mori, C., Wilson, K.L., and Hiraoka, Y. 2004. Emerin binding to Btf, a death-promoting transcriptional repressor, is disrupted by a missense mutation that causes Emery-Dreifuss muscular dystrophy. *European journal of biochemistry / FEBS* **271**(5): 1035-1045.
- Hartman, T.R., Qian, S., Bolinger, C., Fernandez, S., Schoenberg, D.R., and Boris-Lawrie, K. 2006. RNA helicase A is necessary for translation of selected messenger RNAs. *Nat Struct Mol Biol* **13**(6): 509-516.
- Hergovich, A., Lamla, S., Nigg, E.A., and Hemmings, B.A. 2007. Centrosome-Associated NDR Kinase Regulates Centrosome Duplication. *Molecular cell* **25**(4): 625-634.
- Huppert, J.L. and Balasubramanian, S. 2005. Prevalence of quadruplexes in the human genome. *Nucleic Acids Res* **33**(9): 2908-2916.
- . 2007. G-quadruplexes in promoters throughout the human genome. *Nucleic Acids Res* **35**(2): 406-413.
- Inbal, B., Cohen, O., Polak-Charcon, S., Kopolovic, J., Vadai, E., Eisenbach, L., and Kimchi, A. 1997. DAP kinase links the control of apoptosis to metastasis. *Nature* **390**(6656): 180-184.
- Iost, I., Dreyfus, M., and Linder, P. 1999. Ded1p, a DEAD-box protein required for translation initiation in *Saccharomyces cerevisiae*, is an RNA helicase. *J Biol Chem* **274**(25): 17677-17683.
- Jankowsky, E. and Bowers, H. 2006. Remodeling of ribonucleoprotein complexes with DExH/D RNA helicases. *Nucleic Acids Res* **34**(15): 4181-4188.
- Jankowsky, E. and Fairman, M.E. 2007. RNA helicases - one fold for many functions. *Curr Opin Struct Biol*.
- Jankowsky, E., Gross, C.H., Shuman, S., and Pyle, A.M. 2000. The DExH protein NPH-II is a processive and directional motor for unwinding RNA. *Nature* **403**(6768): 447-451.
- . 2001. Active disruption of an RNA-protein interaction by a DExH/D RNA helicase. *Science* **291**(5501): 121-125.
- Jeffrey, K.L., Camps, M., Rommel, C., and Mackay, C.R. 2007. Targeting dual-specificity phosphatases: manipulating MAP kinase signalling and immune responses. *Nat Rev Drug Discov* **6**(5): 391-403.

- Jing, Q., Huang, S., Guth, S., Zarubin, T., Motoyama, A., Chen, J., Di Padova, F., Lin, S.C., Gram, H., and Han, J. 2005. Involvement of microRNA in AU-rich element-mediated mRNA instability. *Cell* **120**(5): 623-634.
- Kedersha, N., Stoecklin, G., Ayodele, M., Yacono, P., Lykke-Andersen, J., Fritzler, M.J., Scheuner, D., Kaufman, R.J., Golan, D.E., and Anderson, P. 2005. Stress granules and processing bodies are dynamically linked sites of mRNP remodeling. *J Cell Biol* **169**(6): 871-884.
- Khabar, K.S. 2005. The AU-rich transcriptome: more than interferons and cytokines, and its role in disease. *J Interferon Cytokine Res* **25**(1): 1-10.
- Kiledjian, M., Wang, X., and Liebhaber, S.A. 1995. Identification of two KH domain proteins in the alpha-globin mRNP stability complex. *Embo J* **14**(17): 4357-4364.
- Kim, J.L., Morgenstern, K.A., Griffith, J.P., Dwyer, M.D., Thomson, J.A., Murcko, M.A., Lin, C., and Caron, P.R. 1998. Hepatitis C virus NS3 RNA helicase domain with a bound oligonucleotide: the crystal structure provides insights into the mode of unwinding. *Structure* **6**(1): 89-100.
- Kohler, A. and Hurt, E. 2007. Exporting RNA from the nucleus to the cytoplasm. *Nature reviews* **8**(10): 761-773.
- Kos, M. and Tollervey, D. 2005. The Putative RNA Helicase Dbp4p Is Required for Release of the U14 snoRNA from Preribosomes in *Saccharomyces cerevisiae*. *Molecular cell* **20**(1): 53-64.
- Kudo, N., Wolff, B., Sekimoto, T., Schreiner, E.P., Yoneda, Y., Yanagida, M., Horinouchi, S., and Yoshida, M. 1998. Leptomycin B inhibition of signal-mediated nuclear export by direct binding to CRM1. *Exp Cell Res* **242**(2): 540-547.
- Kuester, D., Dar, A.A., Moskaluk, C.C., Krueger, S., Meyer, F., Hartig, R., Stolte, M., Malferteiner, P., Lippert, H., Roessner, A., El-Rifai, W., and Schneider-Stock, R. 2007. Early involvement of death-associated protein kinase promoter hypermethylation in the carcinogenesis of Barrett's esophageal adenocarcinoma and its association with clinical progression. *Neoplasia* **9**(3): 236-245.
- Kumar, A., Haque, J., Lacoste, J., Hiscott, J., and Williams, B.R. 1994. Double-stranded RNA-dependent protein kinase activates transcription factor NF-kappa B by phosphorylating I kappa B. *Proc Natl Acad Sci U S A* **91**(14): 6288-6292.
- Lai, W.S., Kennington, E.A., and Blackshear, P.J. 2003. Tristetraprolin and its family members can promote the cell-free deadenylation of AU-rich element-containing mRNAs by poly(A) ribonuclease. *Mol Cell Biol* **23**(11): 3798-3812.
- Lamond, A.I. and Sleeman, J.E. 2003. Nuclear substructure and dynamics. *Curr Biol* **13**(21): R825-828.
- Lamond, A.I. and Spector, D.L. 2003. Nuclear speckles: a model for nuclear organelles. *Nature reviews* **4**(8): 605-612.
- Lee, C.G., da Costa Soares, V., Newberger, C., Manova, K., Lacy, E., and Hurwitz, J. 1998. RNA helicase A is essential for normal gastrulation. *Proc Natl Acad Sci U S A* **95**(23): 13709-13713.
- Li, X.L., Blackford, J.A., and Hassel, B.A. 1998. RNase L mediates the antiviral effect of interferon through a selective reduction in viral RNA during encephalomyocarditis virus infection. *J Virol* **72**(4): 2752-2759.
- Li, X.L., Blackford, J.A., Judge, C.S., Liu, M., Xiao, W., Kalvakolanu, D.V., and Hassel, B.A. 2000. RNase-L-dependent destabilization of interferon-induced mRNAs. A role for the 2-5A system in attenuation of the interferon response. *J Biol Chem* **275**(12): 8880-8888.
- Lin, C., Yang, L., Yang, J.J., Huang, Y., and Liu, Z.R. 2005. ATPase/helicase activities of p68 RNA helicase are required for pre-mRNA splicing but not for assembly of the spliceosome. *Mol Cell Biol* **25**(17): 7484-7493.
- Lin, W.J., Duffy, A., and Chen, C.Y. 2007. Localization of AU-rich element-containing mRNA in cytoplasmic granules containing exosome subunits. *J Biol Chem* **282**(27): 19958-19968.
- Linder, P. 2006. Dead-box proteins: a family affair--active and passive players in RNP-remodeling. *Nucleic Acids Res* **34**(15): 4168-4180.

- Lindquist, J.N., Parsons, C.J., Stefanovic, B., and Brenner, D.A. 2004. Regulation of alpha1(I) collagen messenger RNA decay by interactions with alphaCP at the 3'-untranslated region. *J Biol Chem* **279**(22): 23822-23829.
- Lindstein, T., June, C.H., Ledbetter, J.A., Stella, G., and Thompson, C.B. 1989. Regulation of lymphokine messenger RNA stability by a surface-mediated T cell activation pathway. *Science* **244**(4902): 339-343.
- Liu, J., Valencia-Sanchez, M.A., Hannon, G.J., and Parker, R. 2005. MicroRNA-dependent localization of targeted mRNAs to mammalian P-bodies. *Nat Cell Biol* **7**(7): 719-723.
- Liu, Q., Greimann, J.C., and Lima, C.D. 2006. Reconstitution, activities, and structure of the eukaryotic RNA exosome. *Cell* **127**(6): 1223-1237.
- Liu, Z.R. 2002. p68 RNA helicase is an essential human splicing factor that acts at the U1 snRNA-5' splice site duplex. *Mol Cell Biol* **22**(15): 5443-5450.
- Lorsch, J.R. and Herschlag, D. 1998. The DEAD box protein eIF4A. 1. A minimal kinetic and thermodynamic framework reveals coupled binding of RNA and nucleotide. *Biochemistry* **37**(8): 2180-2193.
- Lykke-Andersen, J. and Wagner, E. 2005. Recruitment and activation of mRNA decay enzymes by two ARE-mediated decay activation domains in the proteins TTP and BRF-1. *Genes Dev* **19**(3): 351-361.
- Mackintosh, S.G., Lu, J.Z., Jordan, J.B., Harrison, M.K., Sikora, B., Sharma, S.D., Cameron, C.E., Raney, K.D., and Sakon, J. 2006. Structural and biological identification of residues on the surface of NS3 helicase required for optimal replication of the hepatitis C virus. *J Biol Chem* **281**(6): 3528-3535.
- Maizels, N. 2006. Dynamic roles for G4 DNA in the biology of eukaryotic cells. *Nat Struct Mol Biol* **13**(12): 1055-1059.
- Malatesta, M., Gazzanelli, G., Battistelli, S., Martin, T.E., Amalric, F., and Fakan, S. 2000. Nucleoli undergo structural and molecular modifications during hibernation. *Chromosoma* **109**(7): 506-513.
- Matera, A.G. 1999. Nuclear bodies: multifaceted subdomains of the interchromatin space. *Trends in cell biology* **9**(8): 302-309.
- Matera, A.G. and Shpargel, K.B. 2006. Pumping RNA: nuclear bodybuilding along the RNP pipeline. *Current opinion in cell biology* **18**(3): 317-324.
- Medcalf, R.L., Van den Berg, E., and Schleuning, W.D. 1988. Glucocorticoid-modulated gene expression of tissue- and urinary-type plasminogen activator and plasminogen activator inhibitor 1 and 2. *J Cell Biol* **106**(3): 971-978.
- Meyer, S., Temme, C., and Wahle, E. 2004. Messenger RNA turnover in eukaryotes: pathways and enzymes. *Crit Rev Biochem Mol Biol* **39**(4): 197-216.
- Miyoshi, K., Wakioka, T., Nishinakamura, H., Kamio, M., Yang, L., Inoue, M., Hasegawa, M., Yonemitsu, Y., Komiya, S., and Yoshimura, A. 2004. The Sprouty-related protein, Spred, inhibits cell motility, metastasis, and Rho-mediated actin reorganization. *Oncogene* **23**(33): 5567-5576.
- Morris, D.P. and Greenleaf, A.L. 2000. The splicing factor, Prp40, binds the phosphorylated carboxyl-terminal domain of RNA polymerase II. *J Biol Chem* **275**(51): 39935-39943.
- Mukherjee, D., Gao, M., O'Connor, J.P., Raijmakers, R., Pruijn, G., Lutz, C.S., and Wilusz, J. 2002. The mammalian exosome mediates the efficient degradation of mRNAs that contain AU-rich elements. *Embo J* **21**(1-2): 165-174.
- Myohanen, S. and Baylin, S.B. 2001. Sequence-specific DNA binding activity of RNA helicase A to the p16INK4a promoter. *J Biol Chem* **276**(2): 1634-1642.
- Nakajima, T., Uchida, C., Anderson, S.F., Lee, C.G., Hurwitz, J., Parvin, J.D., and Montminy, M. 1997. RNA helicase A mediates association of CBP with RNA polymerase II. *Cell* **90**(6): 1107-1112.
- Parker, R. and Sheth, U. 2007. P bodies and the control of mRNA translation and degradation. *Molecular cell* **25**(5): 635-646.

- Payton, M.E., Greenstone, M.H., and Schenker, N. 2003. Overlapping confidence intervals or standard error intervals: what do they mean in terms of statistical significance? *J Insect Sci* **3**: 34.
- Peng, S.S., Chen, C.Y., and Shyu, A.B. 1996. Functional characterization of a non-AUUUA AU-rich element from the c-jun proto-oncogene mRNA: evidence for a novel class of AU-rich elements. *Mol Cell Biol* **16**(4): 1490-1499.
- Perez-Ortin, J.E., Alepuz, P.M., and Moreno, J. 2007. Genomics and gene transcription kinetics in yeast. *Trends Genet.*
- Peters, A.H., Kubicek, S., Mechtler, K., O'Sullivan, R.J., Derijck, A.A., Perez-Burgos, L., Kohlmaier, A., Opravil, S., Tachibana, M., Shinkai, Y., Martens, J.H., and Jenuwein, T. 2003. Partitioning and plasticity of repressive histone methylation states in mammalian chromatin. *Molecular cell* **12**(6): 1577-1589.
- Polach, K.J. and Uhlenbeck, O.C. 2002. Cooperative binding of ATP and RNA substrates to the DEAD/H protein DbpA. *Biochemistry* **41**(11): 3693-3702.
- Raska, I., Shaw, P.J., and Cmarko, D. 2006. Structure and function of the nucleolus in the spotlight. *Current opinion in cell biology* **18**(3): 325-334.
- Reed, R. 2003. Coupling transcription, splicing and mRNA export. *Current opinion in cell biology* **15**(3): 326-331.
- Robb, G.B. and Rana, T.M. 2007. RNA Helicase A Interacts with RISC in Human Cells and Functions in RISC Loading. *Molecular cell* **26**(4): 523-537.
- Ross, J. 1995. mRNA stability in mammalian cells. *Microbiol Rev* **59**(3): 423-450.
- Rossow, K.L. and Janknecht, R. 2003. Synergism between p68 RNA helicase and the transcriptional coactivators CBP and p300. *Oncogene* **22**(1): 151-156.
- Saitoh, N., Spahr, C.S., Patterson, S.D., Bubulya, P., Neuwald, A.F., and Spector, D.L. 2004. Proteomic analysis of interchromatin granule clusters. *Mol Biol Cell* **15**(8): 3876-3890.
- Scheper, W., Holthuisen, P.E., and Sussenbach, J.S. 1996. The cis-acting elements involved in endonucleolytic cleavage of the 3' UTR of human IGF-II mRNAs bind a 50 kDa protein. *Nucleic Acids Res* **24**(6): 1000-1007.
- Scheper, W., Meinsma, D., Holthuisen, P.E., and Sussenbach, J.S. 1995. Long-range RNA interaction of two sequence elements required for endonucleolytic cleavage of human insulin-like growth factor II mRNAs. *Mol Cell Biol* **15**(1): 235-245.
- Sengoku, T., Nureki, O., Nakamura, A., Kobayashi, S., and Yokoyama, S. 2006. Structural basis for RNA unwinding by the DEAD-box protein Drosophila Vasa. *Cell* **125**(2): 287-300.
- Shav-Tal, Y., Blechman, J., Darzacq, X., Montagna, C., Dye, B.T., Patton, J.G., Singer, R.H., and Zipori, D. 2005. Dynamic sorting of nuclear components into distinct nucleolar caps during transcriptional inhibition. *Mol Biol Cell* **16**(5): 2395-2413.
- Shaw, G. and Kamen, R. 1986. A conserved AU sequence from the 3' untranslated region of GM-CSF mRNA mediates selective mRNA degradation. *Cell* **46**(5): 659-667.
- Shaw, P.J. and Jordan, E.G. 1995. The nucleolus. *Annu Rev Cell Dev Biol* **11**: 93-121.
- Shirude, P.S., Okumus, B., Ying, L., Ha, T., and Balasubramanian, S. 2007. Single-Molecule Conformational Analysis of G-Quadruplex Formation in the Promoter DNA Duplex of the Proto-Oncogene C-Kit. *J Am Chem Soc.*
- Shuman, S. 1992. Vaccinia virus RNA helicase: an essential enzyme related to the DE-H family of RNA-dependent NTPases. *Proc Natl Acad Sci U S A* **89**(22): 10935-10939.
- Siddiqui-Jain, A., Grand, C.L., Bearss, D.J., and Hurley, L.H. 2002. Direct evidence for a G-quadruplex in a promoter region and its targeting with a small molecule to repress c-MYC transcription. *Proc Natl Acad Sci U S A* **99**(18): 11593-11598.

- Silverman, R.H. 1994. Fascination with 2-5A-dependent RNase: a unique enzyme that functions in interferon action. *J Interferon Res* **14**(3): 101-104.
- Sledz, C.A., Holko, M., de Veer, M.J., Silverman, R.H., and Williams, B.R. 2003. Activation of the interferon system by short-interfering RNAs. *Nat Cell Biol* **5**(9): 834-839.
- St Johnston, D. 2005. Moving messages: the intracellular localization of mRNAs. *Nature reviews* **6**(5): 363-375.
- Stewart, M. 2007. Molecular mechanism of the nuclear protein import cycle. *Nature reviews* **8**(3): 195-208.
- Stoecklin, G., Lu, M., Rattenbacher, B., and Moroni, C. 2003. A constitutive decay element promotes tumor necrosis factor alpha mRNA degradation via an AU-rich element-independent pathway. *Mol Cell Biol* **23**(10): 3506-3515.
- Stoecklin, G., Mayo, T., and Anderson, P. 2006. ARE-mRNA degradation requires the 5'-3' decay pathway. *EMBO Rep* **7**(1): 72-77.
- Stolle, C.A. and Benz, E.J., Jr. 1988. Cellular factor affecting the stability of beta-globin mRNA. *Gene* **62**(1): 65-74.
- Strasser, K., Masuda, S., Mason, P., Pfannstiel, J., Oppizzi, M., Rodriguez-Navarro, S., Rondon, A.G., Aguilera, A., Struhl, K., Reed, R., and Hurt, E. 2002. TREX is a conserved complex coupling transcription with messenger RNA export. *Nature* **417**(6886): 304-308.
- Talavera, M.A. and De La Cruz, E.M. 2005. Equilibrium and kinetic analysis of nucleotide binding to the DEAD-box RNA helicase DbpA. *Biochemistry* **44**(3): 959-970.
- Tanaka, N. and Schwer, B. 2005. Characterization of the NTPase, RNA-binding, and RNA helicase activities of the DEAH-box splicing factor Prp22. *Biochemistry* **44**(28): 9795-9803.
- . 2006. Mutations in PRP43 that uncouple RNA-dependent NTPase activity and pre-mRNA splicing function. *Biochemistry* **45**(20): 6510-6521.
- Tang, H., Gaietta, G.M., Fischer, W.H., Ellisman, M.H., and Wong-Staal, F. 1997. A cellular cofactor for the constitutive transport element of type D retrovirus. *Science* **276**(5317): 1412-1415.
- Tang, H., McDonald, D., Middlesworth, T., Hope, T.J., and Wong-Staal, F. 1999. The carboxyl terminus of RNA helicase A contains a bidirectional nuclear transport domain. *Mol Cell Biol* **19**(5): 3540-3550.
- Tang, X., Khuri, F.R., Lee, J.J., Kemp, B.L., Liu, D., Hong, W.K., and Mao, L. 2000. Hypermethylation of the death-associated protein (DAP) kinase promoter and aggressiveness in stage I non-small-cell lung cancer. *J Natl Cancer Inst* **92**(18): 1511-1516.
- Tanner, N.K. and Linder, P. 2001. DExD/H box RNA helicases: from generic motors to specific dissociation functions. *Molecular cell* **8**(2): 251-262.
- Tetsuka, T., Uranishi, H., Sanda, T., Asamitsu, K., Yang, J.P., Wong-Staal, F., and Okamoto, T. 2004. RNA helicase A interacts with nuclear factor kappaB p65 and functions as a transcriptional coactivator. *European journal of biochemistry / FEBS* **271**(18): 3741-3751.
- Thomson, A.M., Rogers, J.T., and Leedman, P.J. 1999. Iron-regulatory proteins, iron-responsive elements and ferritin mRNA translation. *Int J Biochem Cell Biol* **31**(10): 1139-1152.
- Tozawa, T., Tamura, G., Honda, T., Nawata, S., Kimura, W., Makino, N., Kawata, S., Sugai, T., Suto, T., and Motoyama, T. 2004. Promoter hypermethylation of DAP-kinase is associated with poor survival in primary biliary tract carcinoma patients. *Cancer Sci* **95**(9): 736-740.
- Tran, H., Schilling, M., Wirbelauer, C., Hess, D., and Nagamine, Y. 2004. Facilitation of mRNA deadenylation and decay by the exosome-bound, DExH protein RHAU. *Molecular cell* **13**(1): 101-111.
- van de Wetering, M., Oving, I., Muncan, V., Pon Fong, M.T., Brantjes, H., van Leenen, D., Holstege, F.C., Brummelkamp, T.R., Agami, R., and Clevers, H. 2003. Specific inhibition of gene expression using a stably integrated, inducible small-interfering-RNA vector. *EMBO Rep* **4**(6): 609-615.

- Vasudevan, S. and Steitz, J.A. 2007. AU-rich-element-mediated upregulation of translation by FXR1 and Argonaute 2. *Cell* **128**(6): 1105-1118.
- Vaughn, J.P., Creacy, S.D., Routh, E.D., Joyner-Butt, C., Jenkins, G.S., Pauli, S., Nagamine, Y., and Akman, S.A. 2005. The DEXH protein product of the DHX36 gene is the major source of tetramolecular quadruplex G4-DNA resolving activity in HeLa cell lysates. *J Biol Chem* **280**(46): 38117-38120.
- Vinciguerra, P. and Stutz, F. 2004. mRNA export: an assembly line from genes to nuclear pores. *Current opinion in cell biology* **16**(3): 285-292.
- Wakioka, T., Sasaki, A., Kato, R., Shouda, T., Matsumoto, A., Miyoshi, K., Tsuneoka, M., Komiya, S., Baron, R., and Yoshimura, A. 2001. Spred is a Sprouty-related suppressor of Ras signalling. *Nature* **412**(6847): 647-651.
- Warner, D.R., Bhattacharjee, V., Yin, X., Singh, S., Mukhopadhyay, P., Pisano, M.M., and Greene, R.M. 2004. Functional interaction between Smad, CREB binding protein, and p68 RNA helicase. *Biochem Biophys Res Commun* **324**(1): 70-76.
- Wilson, B.J., Bates, G.J., Nicol, S.M., Gregory, D.J., Perkins, N.D., and Fuller-Pace, F.V. 2004. The p68 and p72 DEAD box RNA helicases interact with HDAC1 and repress transcription in a promoter-specific manner. *BMC Mol Biol* **5**: 11.
- Wilusz, C.J., Wormington, M., and Peltz, S.W. 2001. The cap-to-tail guide to mRNA turnover. *Nature reviews* **2**(4): 237-246.
- Xu, S., Furukawa, T., Kanai, N., Sunamura, M., and Horii, A. 2005. Abrogation of DUSP6 by hypermethylation in human pancreatic cancer. *J Hum Genet* **50**(4): 159-167.
- Yamashita, A., Chang, T.C., Yamashita, Y., Zhu, W., Zhong, Z., Chen, C.Y., and Shyu, A.B. 2005. Concerted action of poly(A) nucleases and decapping enzyme in mammalian mRNA turnover. *Nat Struct Mol Biol* **12**(12): 1054-1063.
- Yang, L., Lin, C., and Liu, Z.R. 2006. P68 RNA helicase mediates PDGF-induced epithelial mesenchymal transition by displacing Axin from beta-catenin. *Cell* **127**(1): 139-155.
- Yang, Q. and Jankowsky, E. 2006. The DEAD-box protein Ded1 unwinds RNA duplexes by a mode distinct from translocating helicases. *Nat Struct Mol Biol* **13**(11): 981-986.
- Yeilding, N.M. and Lee, W.M. 1997. Coding elements in exons 2 and 3 target c-myc mRNA downregulation during myogenic differentiation. *Mol Cell Biol* **17**(5): 2698-2707.
- Yu, J. and Russell, J.E. 2001. Structural and functional analysis of an mRNP complex that mediates the high stability of human beta-globin mRNA. *Mol Cell Biol* **21**(17): 5879-5888.
- Zhang, S. and Grosse, F. 1994. Nuclear DNA helicase II unwinds both DNA and RNA. *Biochemistry* **33**(13): 3906-3912.
- Zhang, S., Maacke, H., and Grosse, F. 1995. Molecular cloning of the gene encoding nuclear DNA helicase II. A bovine homologue of human RNA helicase A and Drosophila Mle protein. *J Biol Chem* **270**(27): 16422-16427.
- Zhong, X. and Safa, A.R. 2004. RNA helicase A in the MEF1 transcription factor complex up-regulates the MDR1 gene in multidrug-resistant cancer cells. *J Biol Chem* **279**(17): 17134-17141.

FIGURE INDEX

Figure 1.	Six steps at which eukaryotic gene expression can be controlled.	9
Figure 2.	Human DExH proteins.	20
Figure 3.	Cell fractionation using HeLa cells.	33
Figure 4.	<i>In situ</i> extraction of EGFP-RHAU.	34
Figure 5.	RHAU is enriched in the nucleus.	36
Figure 6.	Nucleolar cap formation of EGFP-RHAU upon ActD treatment.	37
Figure 7.	RHAU is co-localized with p68 and p72 in nucleolar caps upon transcriptional inhibition.	38
Figure 8.	Interaction between RHAU and p68, p72, HDACs.	39
Figure 9.	N-terminal domain of RHAU is responsible for the nuclear and nucleolar caps localization.	40
Figure 10.	RHAU knockdown in HeLa cells by RHAU-specific shRNA expression.	41
Figure 11.	Microarray to measure both steady-state mRNA level and mRNA half-life.	42
Figure 12.	Box plots of mRNA levels at five time points.	43
Figure 13.	The relationship of steady-state difference and mRNA half-lives in RHAU-knock down cells.	46
Figure 14.	mRNAs regulated by RHAU.	47
Figure 15.	Distribution of RHAU-regulated mRNA half-lives.	49
Figure 16.	Rescue expression of RHAU by transient transfection of the silent RHAU mutant.	50
Figure 17.	Nuclear run-on assay using HeLa-shRHAU cells.	51
Figure 18.	RHAU-knockdown cells stop growing and show less viability upon serum-starvation.	52
Figure 19.	Leptomycin B inhibits nuclear export of RHAU and RHAU isoform.	55
Figure 20.	Serum-starvation causes cytoplasmic localization of EGFP-RHAU.	56
Figure 21.	EGFP-RHAU is not co-localized with telomeric structures.	60
Figure 22.	Knockdown of RHAU in HeLa cells retards tumor growth in nude mice.	62
Figure 23.	GST-RHAU(1-200aa) pull down using HeLa nuclear and cytoplasmic extracts.	63
TABLE 1.	Comparison of probe sets with significantly altered steady-state levels in HeLa-shRHAU cells and other specific probe sets.	44
TABLE 2.	Number of probe sets with significantly altered mRNA half-life in HeLa-shRHAU or HeLa-shLuc cells treated with dox.	48
TABLE 3.	Comparison of probe sets with significantly altered steady-state levels in HeLa-shRHAU cells and starvation-sensitive genes.	53

CURRICULUM VITAE

FUMIKO IWAMOTO

Date and Place of birth: 14.02.1979, Fukuoka, Japan
Nationality: Japanese
Private Address: Gartengasse25 4125 Riehen, Switzerland
Office Address: Friedrich Miescher Institute for Biomedical Research
Maulbeerstrasse 66, CH-4058 Basel, Switzerland
Email: fumiko@fmi.ch

EDUCATIONAL QUALIFICATION

04. 2003 to 12. 2007 Friedrich Miescher Institute for Biomedical Research,
University of Basel, Switzerland
International Ph.D. Program
Thesis: Biological roles of DExH RNA helicase, RHAU
Supervisor: Dr. Yoshikuni Nagamine
04. 2001 to 03. 2003 Kyushu University, Fukuoka, Japan
Graduate School of Sciences, Department of Biology
Master of Science
Thesis: Regulation of nuclear transport and protein
degradation of PPAR α and γ (mark A)
Supervisor: Prof. Yukio Fujiki
07. 1998 to 08. 1998 University of Winnipeg, Canada
English language course
04. 1997 to 03. 2001 Kyushu University, Fukuoka, Japan
School of Sciences, Department of Biology,
Bachelor of Science (mark A)

GRANTS AND FELLOWSHIPS

09. 2006 EC Marie Curie scholarship for traveling grant for
apoptosis meeting.
01. 2005 to 12. 2005 Research Grant from Swiss cancer league.
04. 2003 to 12. 2007 International Ph.D. Program Scholarship from
Friedrich Miescher Institute.
04. 2001 to 03. 2003 Scholarship from the Japan Scholarship Foundation.

RESEARCH EXPERIENCES

Ph.D study 04. 2003 to 12. 2007 Biological roles of DExH RNA helicase, RHAU	
Publication	Transcription-dependent nucleolar cap localization and possible nuclear function of DExH RNA helicase RHAU Fumiko Iwamoto, Michael Stadler, Kateřina Chalupníková, Edward Oakeley and Yoshikuni Nagamine, <i>Exp.Cell.Res (submitted)</i>
Technical expertise	RNA and DNA Northern blot, RNA degradation assay, Nuclear Run-on assay, in vitro ATPase assay, in vitro transcription, synthesis and transfection of dsRNA, siRNA, Chromatin immunoprecipitation (ChIP), cloning of cDNA, site-directed mutagenesis, methylation-specific PCR, DNA microarray (statistical analysis using Expressionist, Excel, Pathway, and R)
	Protein Purification of recombinant proteins (from E.Coli and insect cells), Pull down experiment using GST proteins, Immunoprecipitation, Western blot, Purification of antibodies and antigens (recombinant His-protein)
	Cell and Animal model Immunofluorescence, Confocal microscope (ZEISS LSM meta), Luciferase reporter assay, apoptosis assay using FACS, cell proliferation assay, Tumor development experiments in nude mice

Bachelor and Master's study 04. 2001 to 03. 2003 Regulation of nuclear transport and protein degradation of PPAR α and γ	
Summary	PPARs are ligand-induced transcription factors that have important roles on lipid metabolism and adipocyte differentiation. I have identified 50 amino acid-nuclear localization signals (NLS) of PPARs that were necessary and sufficient for their nuclear translocation. I found that ligands induce their nuclear translocation by live-cell imaging using confocal microscope. In addition to that, I discover ubiquitination of the NLS that were necessary for the protein degradation, thus I could show the important relationship between protein degradation and cellular compartmentalization.

TECHNICAL DIPLOMA

09.2003 Swiss animal course (module 1)

CONFERENCES ATTENDED

09.2006 14th Euroconference on Apoptosis, Chia, Italy
 10.2005 Novartis – FMI joint meeting on Epigenetics, Switzerland
 07.2005 International helicase meeting: Helicases and NTP driven nucleic acid machines, Arolla, Switzerland
 (selected as an oral presenter)
 10.2004 Novartis Corporate Research Conference, Boston, USA
 10.2003 Novartis – FMI joint meeting on Epigenetics, Emmetten, Switzerland
 06.2003 First International meeting on ARE's and AUBP's in mRNA stability and translational control, Florence, Italy
 2003 –2007 Annual meetings of Friedrich Miescher Institute, Switzerland.
 (selected as an oral presenter, 2006)
 10.2002 75th Annual meeting of Japanese Biochemical Society, Kyoto, Japan
 12.2001 24th Annual meeting of the Molecular Biology Society of Japan, Yokohama
 12.2000 23rd Annual meeting of the Molecular Biology Society of Japan, Kobe, Japan

